DESIGN OF AN ANNULAR CASCADE TUNNEL AND A CASCADE OF AIRFOILS

CONLEY C. LASTER, JR.
DONALD R. GEEHRING

Thesis
L28

Mont 151
8854

Copy No. 2

DESIGN OF

AN ANNULAR CASCADE TUNNEL

AND

A CASCADE OF AIRFOILS

by

Lt. Comdr. C. C. Laster, Jr. USN
B.S. U.S. Naval Academy
(1940)

Lieut. D. R. Geehring USN
B.S. University of Alabama
(1939)

Submitted in Partial Fulfillment of the
Requirements for the Degree of
Master of Science
at
Massachusetts Institute of Technology

20 May 1949

Thesis
L28

TABLE OF CONTENTS

	Page No.
Letter of Transmittal	
Acknowledgements	
Summary	1
Introduction	2
I The Low Speed Annular Cascade Tunnel	7
Description	7
Discussion of Design Details	9
Pressure Losses in Tunnel	12
Design Drawings	17
II The Annular Cascade of Airfoils	19
Two Dimensional Cascade Theory	19
Forces on an Airfoil in Cascade	25
Cascade A	27
Cascade B	28
III Experimental Investigation	36
Results	36
Suggestions for Further Work	38
Appendix A	40
References	50
Table I Ordinates of Mean Camber Line - Blade Sections - Cascade B	52
Table II Ordinates of Blade Sections - Cascade B	53

Figures:

1. MIT Annular Cascade Tunnel - General Arrangement and Dimensions .....
2. Cascade Nomenclature .....
3. Cascade A .....
4. Cascade B .....

13676

TABLE OF CONTENTS

	Page No.
Letter of Transmittal	
Acknowledgements	
Summary	1
Introduction	2
I The Low Speed Annular Cascade Tunnel	7
Description	7
Discussion of Design Details	9
Pressure Losses in Tunnel	12
Design Drawings	17
II The Annular Cascade of Airfoils	19
Two Dimensional Cascade Theory	19
Forces on an Airfoil in Cascade	23
Cascade A	27
Cascade B	28
III Experimental Investigation	36
Results	38
Suggestions for Further Work	38
Appendix A	40
References	50
Table I Ordinates of Mean Camber Line - Blade Sections - Cascade B	52
Table II Ordinates of Blade Sections - Cascade B	53
Figures:	
1. MIT Annular Cascade Tunnel - General Arrangement and Dimensions	
2. Cascade Nomenclature	
3. Cascade A	
4. Cascade B	

TABLE OF CONTENTS (continued)

Page No.

Figures (continued):

5. Determination of Fan Performance in MIT Annular Cascade Wind Tunnel .....

6. Velocity and Yaw Survey - Test Section - MIT Annular Cascade Wind Tunnel .....

7. Air Outflow Angles Determined by a Tangential Traverse of the Blade Wakes - Cascade A .....

8. Annular Cascade Tunnel - Overall View .....

9. Annular Cascade Tunnel - Test Section - Three-quarter Front View .....

10. Annular Cascade Tunnel - Test Section - Three-quarter Rear View .....

11. Traversing Mechanism - Showing Claw Type Yaw Head

Figure (Continued):

5. Variation of the Performance in MPH Another Engine Size Tested .....

6. Velocity and Tip Speed - Test Section - MPH Small Engine Size Tested .....

7. Tip Speed Ratio Determined by a Tachometer Reading of the Blade Tips - Figure 4 .....

8. Results - Test 1 Tested - Normal Flow .....

9. Results Data Is Tested - Test Section - Turbulent Flow Flow .....

10. Results Figure Tested - Test Section - Turbulent Flow Flow .....

11. Increasing Resistance - Testing Other Fan Not

MIT Gas Turbine Laboratory
Cambridge, Massachusetts

20 May 1949

Professor Joseph S. Newell
Secretary of the Faculty
Massachusetts Institute of Technology
Cambridge 39, Massachusetts

Dear Professor Newell:

A thesis entitled "Design of an Annular Cascade Tunnel and a Cascade of Airfoils" is submitted herewith, in partial fulfillment of the requirements for the Degree of Master of Science at the Massachusetts Institute of Technology.

Very truly yours,

Conley C. Laster, Jr.
Lt. Comdr. USN

Donald R. Geehring
Lieut. USN

ACKNOWLEDGEMENTS

The generous assistance, cooperation, and advice of the following are gratefully acknowledged:

Dr. W. R. Hawthorne

Mr. F. Lustwerk

The United States Naval Shipyard
Charlestown, Massachusetts

The General Electric Company
(Aircraft Gas Turbine Division)
Lynn, Massachusetts

ACKNOWLEDGEMENTS

The personal assistance, cooperation, and advice of the following are gratefully acknowledged:

Dr. [illegible]

Mr. [illegible]

The United States Naval Shipyard
Charlestown, Massachusetts

The General Electric Company
(Aircraft Gas Turbine Division)
Lynn, Massachusetts

SUMMARY

A low speed annular cascade wind tunnel was designed and constructed and is presently installed in the MIT Gas Turbine Laboratory. It is anticipated that this tunnel will be used to secure data for correlation with three dimensional theory of flow in an annular cascade, particularly applicable to the design of compressor inlet guide vanes.

An annular cascade of thirty-six airfoils having a cubic variation of circulation with radius was designed for use in the tunnel. Construction of this cascade is pending. Another annular cascade of fifty-four airfoils is installed in the tunnel awaiting test upon completion of instrumentation.

A three dimensional vortex theory of flow in an annular cascade, developed by Dr. W. R. Hawthorne, is presented. This theory was employed in the design of the thirty-six airfoil cascade.

PREFACE

A low speed annular cascade wind tunnel was designed and constructed and is presently installed in the MIT Gas Turbine Laboratory. It is anticipated that this tunnel will be used to gather data for correlation with three dimensional theory of flow in an annular cascade, particularly applicable to the design of compressor inlet guide vanes.

An annular cascade of thirty-six airfoils having a radial variation of circulation with radius was designed for use in the tunnel. Construction of this cascade is pending. Another annular cascade of fifty-four airfoils is installed in the tunnel awaiting first upon completion of instrumentation.

A three dimensional vortex theory of flow in an annular cascade, developed by Dr. R. Hawthorne, is presented. This theory was employed in the design of the thirty-six airfoil cascade.

INTRODUCTION

The ever increasing development and production of axial flow compressor components of gas generators and gas turbine power plants has clearly outlined the need for knowledge of airflow behavior in a cascade of airfoils. This problem has been the subject of considerable study during the past decade.

Compressor inlet guide vanes, in particular, have frequently been found to give considerably different turning angles under test from those for which the vanes had been designed by employment of two dimensional theory. A lack of adequate theoretical development, together with the increased difficulties involved in experimental determination of three dimensional flow characteristics, has limited many previous investigations to a two dimensional flow pattern (References (1), (2), (3)). Some work has been done on three dimensional rotating cascade blowers (References (2), (4)).

Additional investigations are currently in progress in the low speed, two dimensional cascade tunnel of the Gas Turbine Laboratory, MIT. It was felt that additional valuable information could be obtained from a companion three dimensional annular cascade tunnel to supplement a vortex theory of flow in an annular cascade being developed by Dr. W. R. Hawthorne.

This project, therefore, was undertaken in October 1948 and is the subject of this thesis. The project logically divided

INTRODUCTION

The more interesting development and production of social flow compressor components of gas turbines and gas turbine power plants are closely coalesced and meet for the purpose of airflow behavior in a cascade of airfoils. This problem has been the subject of a considerable study during the past decade.

Compressor joint guide vanes, in particular, have frequently been found to give considerably different bending angles under this from those for which the vanes had been designed by application of the dimensional theory. A lack of complete theoretical development, together with the increased difficulties involved in experimental determination of three dimensional flow characteristics, has limited many previous investigations to a two dimensional flow pattern (References (1), (2), (3)). Some work has been done on three dimensional rotating cascade blades (References (2), (4)).

Additional investigations are currently in progress in the low speed, two dimensional cascade tunnel of the Gas Turbine Laboratory, NYU. It was felt that additional valuable information could be obtained from a compatible three dimensional transfer cascade tunnel to represent a vortex theory of flow in an annular cascade being developed by Dr. H. G. Hornstein.

This project, therefore, was undertaken in October 1955 and is the subject of this thesis. The project logically divides

into three phases:

I Design and construction of the low speed annular cascade tunnel.

II Design and construction of the annular cascade of airfoils.

III Experimental investigation of the flow field about the annular cascade and correlation of test results with the theoretical development.

It was originally envisioned that only Phases I and II could be expected to have reached completion by May 1949 and this has been borne out by the results to date. Design of the tunnel was initiated in October 1948. Construction of the tunnel by the Naval Shipyard, Charlestown, Massachusetts, was begun in late December 1948. Design and construction proceeded simultaneously, and the tunnel and the traversing mechanism (minus the probes) were completed during the second week of April 1949. The claw type yaw-meter probes were received from the Airflo Instrument Company, Glastonbury, Connecticut, in April 1949, and the remaining instrumentation is currently in progress.

Design of the annular cascade of airfoils was begun in November 1948 and completed in March 1949. Construction of this cascade by the General Electric Company, Lynn, Massachusetts, is pending.

It is anticipated that future experimental results obtained in the tunnel will be directly applicable to the design of inlet guide vanes for axial compressors and will be suitable for comparison and correlation with predictions of the three dimensional theory presented in this thesis (Appendix A).

into three phases:

I Design and construction of the low speed annular cascade tunnel.

II Design and construction of the annular cascade of airfoils.

III Experimental investigation of the flow field about the annular cascade and correlation of test results with the theoretical development.

It was originally envisioned that only Phases I and II could be expected to have reached completion by May 1948 and this has been found out by the results to date. Design of the tunnel was initiated in October 1948. Construction of the tunnel by the Naval Laboratory, Washington, Massachusetts, was begun in late December 1948. Design and construction proceeded simultaneously, and the tunnel and the traversing mechanism (since the power) were completed during the second week of April 1949. The other type pre-meter tunnel were received from the Aerofin Instrument Company, Glastonbury, Connecticut, in April 1949, and the remaining instrumentation is currently in progress.

Design of the annular cascade of airfoils was begun in November 1948 and completed in March 1949. Construction of this cascade by the General Electric Company, Lynn, Massachusetts, is pending.

It is anticipated that future experimental results obtained in the tunnel will be distinctly additional to the design of inlet guide vanes for axial compressors and will be suitable for comparison and correlation with predictions of the vortex dissociated theory presented in this thesis (Appendix A).

SYMBOLS

A - cross-sectional area

a - distance, measured along chord line, from leading edge of airfoil to point of maximum camber

a_o - $dC_L/d\alpha$

C - velocity

C_D - drag coefficient

C_{D_p} - profile drag coefficient

C_L - lift coefficient

c - chord of airfoil

c_w - pressure loss coefficient through screen - $\dfrac{\phi^2}{(1-\phi)^2}$

D - drag force

F - screen area

F_r - projected wire area of screen

f - coefficient of friction

h - enthalpy per unit mass of gas

L - length (referring to cascade tunnel)

- lift force

l - length (referring to cascade blade)

N - number of blades in cascade

p - static pressure

p_o - stagnation pressure

Q - volume rate of flow

q - velocity head $(\rho V^2/2)$

- heat transfer per unit mass of gas

SYMBOLS

A - cross-sectional area

a - distance, measured along chord line, from leading edge of airfoil to point of maximum camber

a_0 - $dC_L/d\alpha$

C - velocity

C_D - drag coefficient

C_{D_0} - profile drag coefficient

C_L - lift coefficient

c - chord of airfoil

c_v - pressure loss coefficient through screen - $\dfrac{\phi^2}{(1-\phi)^2}$

D - drag force

F - screen area

F_0 - projected size area of screen

f - coefficient of friction

h - enthalpy per unit mass of gas

L - length (referring to cascade tunnel)

- lift force

l - length (referring to cascade blade)

N - number of blades in cascade

p - static pressure

p_0 - stagnation pressure

q - volume rate of flow

q - velocity head $(\rho V^2/2)$

- heat transfer per unit mass of gas

R - r/r_t

R_o - r_h/r_t

r - radius

s - gap between blades

- entropy per unit mass of gas

T - torque force

V - velocity

v - specific volume

w - mass rate of flow

X - axial force

z - exponent denoting variation with radius of circulation around a cascade blade

α - air angle measured from radial plane along axis of tunnel (Fig. 2)

α_{L_o} - angle of attack of airfoil at zero lift

Γ - circulation

δ - deflection angle (Fig. 2)

θ - angular distance measured from some fixed radial line

ρ - density

σ - stagger angle

ϕ - blockage ratio, F_r/F

Subscripts:

o - denotes stagnation condition

1, 2, etc. - stations along tunnel as per Fig. 1

1, 2 - stations forward and aft cascade respectively

h - at hub

r - r/r_0

r_n - r_n/r_0

r - radius

s - gap between blades

- Entropy per unit mass of gas

T - tangent force

t - velocity

v - specific volume

w - mass rate of flow

X - axial force

x - exponent denoting variation with radius of circulation around a cascade blade

α - air angle measured from radial plane along axis of tunnel (Fig. 2)

α_n - angle of attack of airfoil at zero lift

Γ - circulation

δ - deflection angle (Fig. 2)

θ - angular distance measured from some fixed radial line

ρ - density

σ - stagger angle

ϕ - blockage ratio, F_c/F

Subscripts:

o - denoted stagnation condition

1, 2, etc. - stations along tunnel as per Fig. 1

1, 2 - stations forward and aft cascade respectively

b - at hub

m - mean value (Sketches, pages 25 and 26)

t - at tip

u - tangential component

x - axial component

m - mean value (30-1000), pages 42 and 46)

f - at 1Hz

o - incremental acceleration

x - total acceleration

I THE LOW SPEED ANNULAR CASCADE TUNNEL

Description

Overall Length (with 9 screens).....	157 inches
Center Line Height (above deck).....	38 inches
Maximum Inside Diameter.....	$27\frac{1}{4}$ inches
Test Section Inside Diameter.....	$15\frac{3}{4}$ inches
Capacity.....	8500 cfm
Velocity at Test Section:	
(with $9\frac{1}{4}$" diameter core).....	159 ft/sec
(with $7\frac{7}{8}$" diameter core).....	138 ft/sec

The general outline and basic dimensions of the tunnel are shown in Figure 1. A view of the completed tunnel is shown in Figure 8.

The tunnel is powered by a Buffalo Forge Company A8A4W5 CCW Axial Flow Fan, rated to deliver 8000 cu. ft/min at three inches of water static pressure at 1750 rpm. The fan is followed by a straight diffuser section 46 inches in length, enclosing a tapered conical fairing mounted on the rear of the fan motor. An angle of $8\frac{1}{2}$ degrees is included between the cone and the straight side of the diffuser.

Seven sixteen-mesh screens spaced at two inch intervals are placed behind the diffuser section. An accelerating section follows and reduces the tunnel diameter from $27\frac{1}{4}$ inches to $15\frac{3}{4}$ inches

I. THE LOW SPEED GENERAL CAPACITY TUNNEL

SPECIFICATIONS

Overall Length (with 4 screens)..... 137 inches

Center Line Height (above deck)..... 58 inches

Minimum Inside Diameter..... 77½ inches

Test Section Inside Diameter..... 15¾ inches

Capacity..... 8000 cfs

Velocity at Test Section:

(with $\frac{7}{8}$" diameter core)..... 157 ft/sec

(with $\frac{7}{8}$" diameter core)..... 158 ft/sec

The general outline and basic dimensions of the tunnel are shown in Figure 1. A view of the completed tunnel is shown in Figure 2.

The tunnel is powered by a Buffalo Force Ventilator Model [illegible] Axial Flow Fan, rated to deliver 8000 cfs/min at three inches of water static pressure at 1750 rpm. The fan is followed by a straight diffuser section in tunnel in length, enclosing a tapered nozzle fairing downstream of the rear of the fan motor. An angle of 45 degrees is included between the cone and the straight side of the diffuser.

Tunnel distance-speed horizon spaced at the tank intervals are placed along the diffuser nozzle. A constantly motion follows and reduces the tunnel diameter from 77½ inches to 15¾ inches

in a length of 24 inches.

Two additional sixteen-mesh screens are placed immediately behind the accelerating section. All screens are individual units and are located between flanges of the duct so that the number of screens may be increased or decreased as desired.

An approach section eighteen inches in length completes the installation upstream of the test section.

Each duct section is supported in its own wooden cradle. The individual duct sections are bolted together to form the complete tunnel assembly.

The test section is a straight section 19¼ inches in length mounting the traversing mechanism and probes, and containing the cascade, a center core and nose section, and the mechanism for rotating the cascade. Front and rear views of the test section assembly are shown in Figures 9 and 10. The cascade presently mounted in the tunnel is the inlet guide vane assembly (54 airfoils) taken from an aircraft engine.

The traversing mechanism is designed to permit a radial traverse of the cascade, measuring total pressure and flow angles. Traversing in the tangential direction is accomplished by rotating the cascade. The traversing mechanism is illustrated in detail in Figure 11.

The remaining instrumentation presently contemplated for

in a length of 14 inches.

Two additional sixteen-mesh screens are placed immediately behind the accelerating section. All screens are individual units and are located between flanges of the duct so that the number of screens may be increased or decreased as desired.

An approach section eighteen inches in length completes the installation upstream of the test section.

Each duct section is supported in its own wooden cradle. The individual duct sections are bolted together to form the complete tunnel assembly.

The test section is a straight section 19½ inches in length mounting the traversing mechanism and probes, and containing the cascade, a center core and nose section, and the mechanism for rotating the cascade. Front and rear views of the test section assembly are shown in Figures 9 and 10. The cascade presently mounted in the tunnel is the inlet guide vane assembly (54 airfoils) taken from an aircraft engine.

The traversing mechanism is designed to permit a radial traverse of the cascade, mounting total pressure and flow angles. Traversing in the tangential direction is accomplished by rotating the cascade. The traversing mechanism is illustrated in detail in Figure 11.

The remaining instrumentation presently contemplated for

measuring total and static pressure upstream of the cascade is outlined in Figure 1.

Discussion of Design Details

The decision to make use of a low speed tunnel was dictated by three considerations: (1) It was desirable to avoid compressibility effects during tests for correlation with theoretical predictions. (2) Several other projects were scheduled to be operated in the M.I.T. Gas Turbine Laboratory high speed duct at approximately the expected time of completion of the annular cascade tunnel. (3) A Navy surplus fan of suitable capacity for the low speed tunnel was available in the Gas Turbine Laboratory.

A preliminary test run of this fan proved satisfactory and it was made the cornerstone of the project.

After several fruitless efforts had been made to obtain a suitable cascade of airfoils for test, and in order to determine the necessary duct dimensions for design purposes, it was tentatively decided to design a set of blades. The General Electric Company, Lynn, Massachusetts, was approached, and offered to manufacture the proposed set of blades and permit their use by the Gas Turbine Laboratory on a loan basis.

Simultaneously, a separate effort resulted in the salvaging of an inlet guide vane assembly from an aircraft engine. The tunnel was designed, therefore, to accomodate the basic dimensions of this

measuring total and static pressure systems of the nozzle is outlined in Figure 1.

Dimensions of Design Details

The decision to make use of a low speed tunnel was dictated by three considerations: (1) It was necessary to avoid compressibility effects during tests for correlation with theoretical predictions. (2) Several other projects were scheduled to be operated in the M.I.T. Gas Turbine Laboratory high speed duct at approximately the expected time of completion of the tunnel's vacuum tunnel. (3) A Navy surplus fan of suitable capacity for the low speed tunnel was available in the Gas Turbine Laboratory.

A preliminary test run of this fan proved satisfactory and it was made the cornerstone of the project.

After several fruitless efforts had been made to obtain a suitable compass of airfoils for test, and in order to determine the necessary test dimensions for design purposes, it was tentatively decided to design a set of blades. The General Electric Company, Lynn, Massachusetts, was approached, and offered to manufacture the proposed set of blades and permit their use by the Gas Turbine Laboratory on a loan basis.

Simultaneously, a concrete effort resulted in the salvaging of an inlet guide vane assembly from an aircraft engine. The tunnel was designed, therefore, to accommodate the basic dimensions of this

assembly (Cascade A), and the design of the blades to be manufactured (Cascade B) was continued in conformance with the tunnel dimensions.

Since Cascade A was constructed with a 1/8 inch outer shroud, it was considered desirable to keep this shroud out of the airflow in order to avoid excessive local turbulence at the outer diameter. A recess was provided at the forward end of the test section outer casing to accept the shroud. This fixed the inside diameter of the outer casing at $15\frac{3}{4}$ inches. Cascade B was designed without a shroud and its greater chord length precluded any fit into the recessed section. Consequently, Cascade B was designed to a nominal overall diameter of $15\frac{3}{4}$ inches. When this cascade is to be used in the tunnel, the recessed section must be filled by using a 1/8 inch annular ring, 16 inches overall diameter and 1-4/10 inches long, or by filling the cavity with modelling clay.

In addition, Cascade A has a hub-tip ratio of .586 while the hub-tip ratio of Cascade B is .500. The $9\frac{1}{4}$ inch diameter tunnel core was built for use with Cascade A. Therefore, a 7-7/8 inch diameter core must be provided to replace the $9\frac{1}{4}$ inch diameter core when Cascade B is to be installed in the tunnel.

It was planned to avoid the use of a clumsy settling chamber in the tunnel design. The straight sided diffuser section and cone fairing greatly simplified the design and permitted a neat installation. The use of a straightening tube honeycomb at the rear of the diffuser section was planned, if tunnel calibration tests indicated

assembly (Section A), and the design of the blades to be manufactured (Cascade A) was continued in conformance with the tunnel dimensions.

Since Cascade A was constructed with a 1/8 inch outer shroud, it was considered desirable to keep this shroud out of the airflow in order to avoid excessive local turbulence at the outer diameter. A recess was provided at the forward end of the test section outer casing to accept the shroud. This fixed the inside diameter of the outer casing at 15 1/2 inches. Cascade B was designed without a shroud and its greater chord length permitted any fit into the reduced section. Consequently, Cascade A was designed to a nominal overall diameter of 15 1/2 inches. Since this cascade is to be used in the tunnel, the reduced section must be filled by using a 1/8 inch annular ring, 14 inches overall diameter and 1-3/16 inches long, or by filling the cavity with modelling clay.

In addition, Cascade B has a hub-tip ratio of .500 while the hub-tip ratio of Cascade B is .500. The 9 inch diameter tunnel core was built for use with Cascade A. Therefore, a 7-7/8 inch diameter core must be provided to replace the 9 inch diameter core when Cascade B is to be installed in the tunnel.

It was planned to avoid the use of a dummy cutting number in the tunnel design. The straight sided diffuser section and cone fairing greatly simplified the design and permitted a neat installation. The use of a straightening tube honeycomb at the rear of the diffuser section was planned, if tunnel calibration tests indicated

undesirable rotational flow at the test section. A preliminary tuft survey, however, has indicated an axial flow pattern with negligible rotation, hence the use of a straightening honeycomb appears unnecessary.

In order to make traverses behind the cascade of airfoils in both radial and tangential directions, the traversing mechanism must either travel tangentially around the casing or the cascade must be capable of rotation. The latter solution gave promise of ease of operation and simplicity of construction. The idea of employing a central shaft supported on two bearings manually centered by the use of six bolts tapped through the casing to form two spider supports was first suggested by Mr. Lustwerk, and was adopted after further study. The rotation of the cascade is obtained by the use of a pair of bevel gears operated by a turning bar projecting through one side of the outer casing and fitted with a friction brake. This has the advantage of offering a relatively small additional resistance to the airflow in the test section and keeping the exit clear in the event that it might later be decided to add a diffusing section. A two to one gear tooth ratio permits positioning the cascade tangentially within 1/2 degree or less.

The traversing mechanism is mounted on a pad on the top of the test section outer casing and is secured in place by six set screws. The yawmeter is of the claw type and is rotated by a worm and gear and moved radially by a calibrated threaded bolt. The

undesirable rotational flow at the test section. A preliminary tuft survey, however, has indicated an axial flow pattern with negligible rotation, hence the use of a straightening honeycomb appears unnecessary.

In order to make traverses behind the cascade of airfoils in both radial and tangential directions, the traversing mechanism must either travel tangentially around the casing or the cascade must be capable of rotation. The latter solution gave promise of ease of operation and simplicity of construction. The idea of employing a central shaft supported on two bearings annually centered by the use of air bulbs turned through the casing to form two rotor supports was first suggested by Mr. Lustwerk, and was adopted after further study. The rotation of the cascade is obtained by the use of a pair of bevel gears operated by a turning bar projecting through one side of the outer casing and fitted with a friction brake. This has the advantage of offering a relatively small additional resistance to the airflow in the test section and keeping the unit clear in the event that it might later be decided to add a diffusing section. A two to one gear tooth ratio permits positioning the cascade tangentially within 1/8 degree or less.

The traversing mechanism is mounted on a pad on the top of the test section outer casing and is secured in place by six set screws. The pedestal is of the clad type and is rotated by a cam and gear and moved radially by a calibrated threaded bolt. The

traversing mechanism may be located axially in any number of positions, limited only by the number of holes drilled through the mounting pad to allow the probes into the tunnel behind the cascade.

No provisions are presently provided for removing boundary layers. This poses a fairly difficult problem, since annular manifolds must be provided for both inner and outer surfaces of the annulus. The location of the test cascade just aft of a flange, however, should permit the installation of such manifolds if they appear desirable.

No provision is available for obtaining photographic data.

A calculation of the forces expected to be exerted on the cascade by the airflow was made in Phase II for Cascade B. The results, an axial force of 4.9 pounds and a torque of 126 inch-pounds, were used to determine component dimensions required for structural rigidity of the test section assembly. Generally comparable forces may be expected from Cascade A.

Pressure Losses in Tunnel

The design operating point of the fan was determined from the fan performance curves and the following calculation of pressure losses through the tunnel:

traversing mechanism may be located axially in any number of positions, limited only by the number of holes drilled through the mounting pad to allow the probes into the tunnel behind the cascade.

No provisions are presently provided for removing boundary layers. This poses a fairly difficult problem, since annular manifolds must be provided for both inner and outer surfaces of the annulus. The location of the test cascade just aft of a flange, however, should permit the installation of such manifolds if they appear desirable.

No provision is available for obtaining photographic data.

A calculation of the forces expected to be exerted on the cascade by the airflow was made in Phase II for Cascade A. The results, an axial force of 4.0 pounds and a torque of 126 inch-pounds, were used to determine component dimensions required for structural rigidity of the test section assembly. Generally comparable forces may be expected from Cascade A.

Pressure Losses in Tunnel

The design operating point of the fan was determined from the fan performance curves and the following calculation of pressure losses through the tunnel:

<u>Wall friction loss:</u> $\frac{\Delta p_o}{q} = f \frac{L}{D}$ Darcy-Weisbach Equation Ref. (5)

<u>Loss through screens:</u> $\frac{\Delta p_o}{q} = c_w = \frac{\phi^2}{(1 - \phi)^2}$

where ϕ is the blockage ratio Ref. (6)

<u>Core, spider drag losses:</u>

$$\frac{\Delta p_o}{q} = C_D \frac{A_{body}}{A_{duct}}$$ Ref. (8)

where A_{body} is cross section or projected frontal area

<u>Loss through cascade:</u> $\frac{\Delta p_o}{q} = \frac{C_D}{s/c} \quad \frac{1}{\cos^3 \alpha_m}$ Ref. (12)

Assuming incompressible flow, $Q = \frac{AV}{144}$, where $V = C_{x_1}$ ft/sec

Station (See Fig.1)	0	1	2	3	4	5	6	7	8	0
A, sq. in.	∞	430	583	583	195	195	130	130	130	∞
C_x	0	C_{x_1}	.738 C_{x_1}	.738 C_{x_1}	2.20 C_{x_1}	2.20 C_{x_1}	3.31 C_{x_1}	3.31 C_{x_1}	3.31 C_{x_1}	0
q	0	q_1	.544 q_1	.544 q_1	4.84 q_1	4.84 q_1	10.95 q_1	10.95 q_1	10.95 q_1	0

Wall friction loss: $\frac{\Delta p_o}{q} = f \frac{L}{D}$ Darcy-Weisbach equation Ref. (5)

Loss through screens: $\frac{\Delta p_o}{q} = c_s = \frac{\phi^2}{(1-\phi)^2}$

where ϕ is the blockage ratio Ref. (6)

Cone, swirling wake losses:

$$\frac{\Delta p_o}{q} = C_D \frac{A_{body}}{A_{net}} \qquad \text{Ref. (8)}$$

where A_{body} is cross section of projected frontal area

Loss through cascade: $\frac{\Delta p_o}{q} = \frac{C_p}{\sigma/c} \frac{1}{\cos^2 \alpha_s}$ Ref. (10)

Assuming incompressible flow, $u = \frac{AV}{144}$, where $V = C_{x_1}$ ft/sec

Station (See Fig. 1)	0	1	2	3	4	5	6	7	8	9
A, sq. in.	∞	130	563	589	195	195	130	130	130	∞
C_s	0	C_{x_1}	.736 C_{x_1}	.735 C_{x_1}	2.40 C_{x_1}	2.20 C_{x_1}	3.31 C_{x_1}	3.71 C_{x_1}	3.31 C_{x_1}	0
u	0	u_1	.344 u_1	.344 u_1	4.44 u_1	4.44 u_1	10.95 u_1	10.95 u_1	10.95 u_1	0

Assuming standard sea level conditions,

$$\rho_o = .002378 \text{ slugs per cubic foot}$$

Average Reynolds Number = 500,000, $\therefore$ f = .015 , Ref. (5)

<u>Station 1 - 2</u>

$$\frac{\Delta p_o}{\frac{q_1 + q_2}{2}} = .015 \left[\frac{46}{27.25} + \frac{40}{7}\right] = .111$$

$$\frac{\Delta p_o}{q_1} = .086$$

<u>Station 2 - 3</u>

$$\phi = \frac{F_r}{F} = \frac{2 \times 16 \times .010}{1.000} = .32$$

$$C_w = \frac{(.32)^2}{(1 - .32)^2} = .221$$

$$\frac{\Delta p_o}{q_2} = .015\ (14/27.25) + (7)\ .221 = 1.552$$

$$\frac{\Delta p_o}{q_1} = 1.200$$

<u>Station 3 - 4</u>

$$\frac{\Delta p_o}{\frac{q_3 + q_4}{2}} = .015 \left[\frac{24}{(27.25 + 15.75)/2}\right] = .0154$$

$$\frac{\Delta p_o}{q_1} = .041$$

Assuming standard and I-mod conditions,

ρ_0 = .00237 slugs per cubic foot

Assuming Prandtle Theory = (20)(.00) , $\therefore$ Γ = .0[illegible] , and (1)

Iteration 1 - 1

$$\frac{\frac{\rho_0 \Delta_0}{\rho_1 + \rho_2}}{\frac{1}{2}} = .0[illegible] \left[\frac{\rho_1}{\rho} + \frac{\rho_2}{\rho}\right] = .[illegible]$$

$$\frac{\Delta_1}{\rho_1} = .00[illegible]$$

Iteration 1 - 2

$$\rho = \frac{\rho}{\rho_0} = \frac{2.[illegible] \times .00[illegible]}{1.000} = .0[illegible]$$

$$\Delta_1 = \frac{[illegible]}{(1 - .0[illegible])^2} = .00[illegible]$$

$$\frac{\Delta_1 \rho_0}{\rho_1} = .0[illegible] (1-(0/.29)) + (1) .00[illegible] = 1.[illegible]$$

$$\frac{\Delta_1 \rho_0}{\rho_1} = 1.[illegible]$$

Iteration 2 - 1

$$\frac{\frac{\rho_0 \Delta_1}{\rho_1 + \rho_2}}{\frac{1}{2}} = .00[illegible] \left[\frac{\rho_1}{[illegible] + [illegible]}\right] = .[illegible]$$

$$\frac{\Delta_2 \rho_0}{\rho_1} = .00[illegible]$$

Station 4 - 5

$$\frac{\Delta p_o}{q_4} = (2)\ C_W = 2 \times .221 = .442$$

$$\frac{\Delta p_o}{q_1} = 2.140$$

Station 5 - 6

$A_{core} = 67.1$ sq.in.

$C_D = (.30)$ Ref. (8)

Drag: $\frac{\Delta p_o}{q_5} = .30 \times 67.1/195 = .103$

Friction: $\frac{\Delta p_o}{q_6} = .015 \left[\frac{18}{15.75} + \frac{15}{9.125}\right] = .037$

Total: $\frac{\Delta p_o}{q_1} = .500 + .406 = .906$

Station 6 - 7

$$C_D = C_{D_p} + .02\ s/l + \frac{.06\ C_L^2}{(l/c)}$$

Estimated Average Drag Coefficient (Cascade B)

$$C_D = .02 + .02\ (1.00/3.94) + .06\ (.7)^2\ (1.70/3.94)$$

$$C_D = .038$$

Average $\alpha_m = 15$ degrees (Cascade B)

$s/c = .61$ at mean radius

$$\frac{\Delta p_o}{q_6} = \frac{.038}{.61} \times \frac{1}{(.965)^3} = .069$$

$$\frac{\Delta p_o}{q_1} = .760$$

Station 7 - 8

A_{rods}, = 6 (3.25 x .50) = 9.75

A_{shaft} = 3.25 x .75 = 2.44

12.19 sq.in.

C_D = .30 Ref. (8)

$$\frac{\Delta p_o}{q_7} = .015 \left[\frac{19}{15.75} + \frac{19}{9.125}\right] + .30\ (12.19/130)$$

$$\frac{\Delta p_o}{q_7} = .039 + .028 = .067$$

$$\frac{\Delta p_o}{q_1} = .740$$

Station	$\Delta p_o/q_1$
1 - 2	0.086
2 - 3	1.200
3 - 4	0.041
4 - 5	2.140
5 - 6	0.906
6 - 7	0.760
7 - 8	0.740
	5.873 $= \sum \Delta p_o/q_1$

$$\Delta p_o = 5.873\ \frac{\rho_o\ C_{x_1}^2}{2} \times \frac{1}{144} \times 2.307 \times 12, \text{ inches of water}$$

$$Q = \frac{430}{144}\ C_{x_1} \times 60 \text{ cubic feet per minute}$$

$$\Delta p_o = .00134\ C_{x_1}^2$$

$$Q = 179\ C_{x_1}$$

Eliminating C_{x_1}, with Q in cubic feet per minute,

$$\Delta p_o = .00134 \left(\frac{Q}{179}\right)^2 \text{ inches of } H_2O$$

Section I - A

$$\Delta_{max} = 2\,(0.25 + .75) = 2.00$$

$$\Delta_{min} = 1.25 + .75 = \frac{1.00}{2.00} = 0.50$$

$$\sigma_{\rho} = .50 \qquad \text{Eqn. (1)}$$

$$\frac{\Delta}{\sigma^2} = .500 \left[\frac{1}{0.50} + \frac{1}{1.00}\right] + .50\,(1.25 + 0.25)$$

$$\frac{\Delta}{\sigma^2} = .500 + .500 + .500 + .500$$

$$\frac{\Delta}{\sigma^2} = 2.00$$

Section	$\frac{\Delta}{\sigma^2}$
1 - 2	.500
2 - 3	1.000
3 - 4	0.500
4 - 5	1.250
5 - 6	.500
6 - 7	1.250
7 - 8	0.750
	$\sum \frac{\Delta}{\sigma^2} = 5.750$

$$\Delta_{\sigma} = 5.750 \quad \frac{\rho_{\sigma}^2}{2} = \frac{1}{2\mu} = 2.500 = 1.0, \text{ Ratio of value}$$

$$0 = \frac{\Delta\rho}{2\mu} \quad \sigma_{\rho} = 50 \text{ mils low per blade}$$

$$\Delta_{\rho} = .0025 \quad \sigma_{\rho}^2$$

$$0 = 2\mu \quad \sigma_{\rho}$$

Eliminating σ_{ρ}^2, when σ is .0025 low per blade,

$$\Delta_{\rho} = .0025 \left(\frac{\sigma}{2\mu}\right)^2 \qquad \text{Ratio of } \frac{\Delta_{\rho}}{\Delta_{\sigma}}$$

The design point of the fan is found to be the intersection of the curve of pressure drop and the fan characteristic curve, Figure (5). An airflow capacity of 8500 cubic feet per minute is indicated, resulting in an axial velocity at the test section of 159 feet per second (Cascade A) or 138 feet per second (Cascade B).

Design Drawings

A complete folder of blueprints for the tunnel and cascades is included in copies No. (1) and No. (2) of the thesis. A complete list of the drawing numbers is included here. Copies of all drawings are on file in the MIT Gas Turbine Laboratory.

Drawing Number	Item
N-1210	Bearing Sleeve
N-1211	Collar
N-1212	Quadrant
N-1213	Friction Clamp
N-1214	Mounting Pad
N-1215	Thrust Washer
N-1216	Bevel Pinion
N-1217	Shaft Bearings and Collars
N-2218	Aft Section-Inner Casing
N-3219	Shaft
N-3220	Shaft and Flanges
N-4221	Aft Section-Outer Casing Sub-Assembly
N-1222	Boss
N-1223	Bolt
N-4224	Aft Section Assembly
N-1225	Bevel Gear
N-2226	Traversing Mechanism Assembly
N-1227	Micrometer Head-Traversing Mechanism
N-1228	End Plate - " "
N-1229	Quadrant - " "
N-3230	Base Plate - " "
N-2231	Carriage - " "
N-1232	Worm Gear and Collar- " "
N-1233	Micrometer Head- " "

The design point of the fan is found to be the intersection of the curve of maximum duty and the fan characteristic curve, Figure (9). An airflow capacity of 4500 cubic feet per minute is influenced, resulting in an axial velocity at the test section of 139 feet per second (Section A) or 150 feet per second (Section B).

Design Drawings

A complete folder of blueprints for the tunnel and extensions is included in copies No. (1) and No. (2) of the tunnels. A complete list of the drawing numbers is included here. Copies of all drawings are on file in the MIT Gas Turbine Laboratory.

Drawing Number	Item
[illegible]	Bearing Flange
[illegible]	Collar
[illegible]	Lubricant
[illegible]	Friction Flange
[illegible]	Bearing Rod
[illegible]	Thrust Washer
[illegible]	Dowel Pinion
[illegible]	Shaft Bearing and Collars
[illegible]	Aft Section-Inner Casing
[illegible]	Shaft
[illegible]	Shaft and Flanges
[illegible]	Aft Section-Outer Casing Sub-Assembly
[illegible]	Nose
[illegible]	Shaft
[illegible]	Aft Section Assembly
[illegible]	Dowel Gear
[illegible]	Traversing Mechanism Assembly
[illegible]	Microscopy Head-Traversing Mechanism
[illegible]	Box Flange - " "
[illegible]	Bearing - " "
[illegible]	Box Flange - " "
[illegible]	Bearing - " "
[illegible]	Bore Gear and Collars " "
[illegible]	Microscopy Head- " "

Drawing Number	Item
N-1234	Traversing Screw and Worm Shaft-Traversing Mechanism
N-2237	Yawmeter
N-5238	Inlet Guide Vane-Blade Sections (Cascade B)
N-1239	Spacer
N-1240	"
N-1241	"
N-1242	"
N-1243	Nose Piece-Inner Casing
N-4244	Test Assembly-Inlet Guide Vanes (Cascade B)
N-3245	Diffuser Cone
N-5254	Inlet Guide Vane Assembly (Cascade A)
N-5255	Inlet Guide Vane (Cascade A)
N-5256	Annular Cascade Wind Tunnel-Assembly Layout and Casing Details

Drawing Number	Item
A-1101	Interior Door and Door Hardware Schedule
A-1201	Elevation
A-1211	Exterior Door Hardware Schedule (Door No 1)
A-1212	Frame
A-1213	"
A-1214	"
A-1215	"
A-1216	"
A-1301	Base Floor-Lower Ceiling
A-1311	Fire Alarm-Lower Ceiling Plan (Drawing 1)
A-1312	Offices Plan
A-1313	Base Floor Plan Revised (Drawing 1)
A-1314	Base Floor Plan (Drawing 2)
A-1401	Section Detail Plan Tunnel-Kenedy Square and Section Details.

II THE ANNULAR CASCADE OF AIRFOILS

Two Dimensional Theory of Flow

Consider an annular element in the flow field, of unit axial length. Flow is assumed symmetrical about the axis.

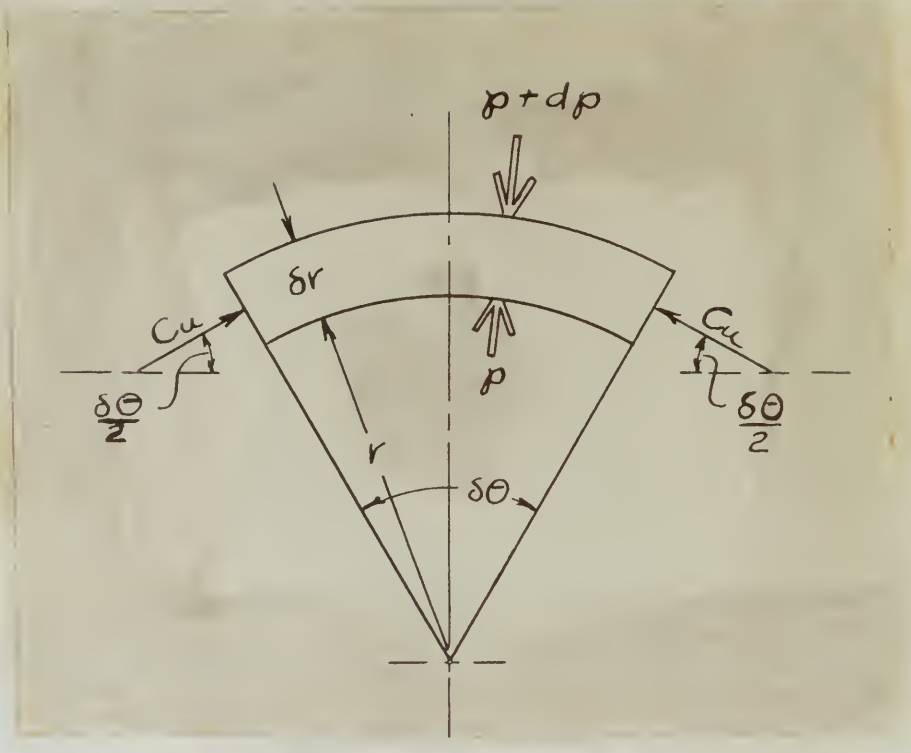

Mass Flow $= \rho C_u \, \delta r$

Summation of Forces in Radial Direction

$$(p + \delta p)\,(r + \delta r)\,\delta\theta = pr\,\delta\theta + \left(p + \frac{\delta p}{2}\right)\delta r\,\delta\theta + \rho\, C_u^2\,\delta\theta\,\delta r$$

$$pr\,\delta\theta + p\,\delta r\,\delta\theta + r\,\delta p\,\delta\theta + \delta p\,\delta r\,\delta\theta - pr\,\delta\theta - p\,\delta r\,\delta\theta - \frac{\delta p}{2}\,\delta r\,\delta\theta$$

$$-\rho C_u^2\,\delta\theta\,\delta r = 0$$

Simplifying and eliminating second order differentials

$$r\,\delta p = \rho C_u^2 \delta r$$

$$\frac{dp}{dr} = \rho \frac{C_u^2}{r}$$

or $$v \frac{dp}{dr} = \frac{C_u^2}{r}$$

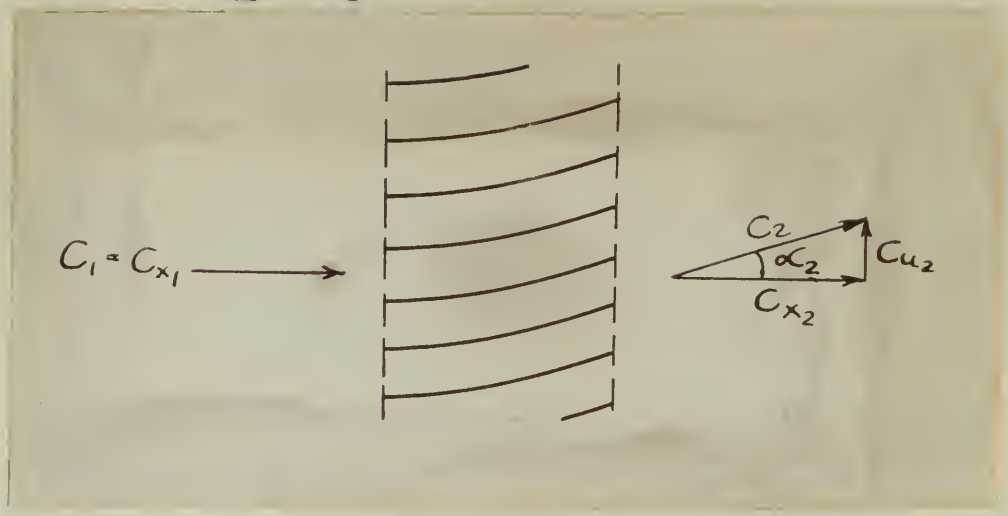

If a cascade of airfoils is placed in the annulus, and adiabatic steady airflow traverses the cascade, the total energy remains constant

$$dq = dh + d\frac{C^2}{2} = 0$$

$$dh = -\,d\frac{(C_x^2 + C_u^2)}{2}$$

For assumed isentropic flow

$$T\,ds = dh - v\,dp = 0$$

$$\therefore\ d\frac{(C_x^2 + C_u^2)}{2} + \frac{C_u^2}{r}\,dr = 0$$

$$2\,\frac{C_u^2}{r} + \frac{d}{dr}\,C_x^2 + \frac{d}{dr}\,C_u^2 = 0$$

$$\frac{d}{dr}\,C_x^2 + \frac{1}{r^2}\,\frac{d}{dr}\,(rC_u)^2 = 0$$

It is further assumed that for the flow through the annular cascade, a point (1) is taken far upstream and a point (2) is taken far downstream, such that

1. $C_1 = C_{x_1}$ = constant at all radii

2. The product of the radius and the tangential velocity at (2) varies as a function of the radius raised to some power, z

$$\frac{r\ C_{u_2}}{r_t C_{u_{2_t}}} = \left(\frac{r}{r_t}\right)^z$$

Then $$\frac{d}{dr} C_x^2 = -\frac{1}{r^2} \frac{C_{u_{2_t}}^2}{r_t^{2z-2}} \frac{d}{dr} r^{2z}$$

$$\frac{d}{dr} C_x^2 = -\frac{2z}{r_t}\left(\frac{r}{r_t}\right)^{2z-3} C_{u_{2_t}}^2$$

Letting $\frac{r}{r_t} = R$

$$\frac{d}{dR} C_{x_2}^2 = -2z\, R^{2z-3}\, C_{u_{2_t}}^2$$

$$\int_r^{r_t} d\ C_{x_2}^2 = -2z\, C_{u_{2_t}}^2 \int_R^1 R^{2z-3}\ dR$$

Integrating between r and r_t

$$C_{x_{2_t}}^2 - C_{x_2}^2 = -\frac{2z}{2z-2} \; C_{u_{2_t}}^2 \left(1 - R^{2z-2}\right)$$

$$C_{x_2} = \left\{C_{x_{2_t}}^2 + \frac{2z}{2z-2} \; C_{u_{2_t}}^2 \left(1 - R^{2z-2}\right)\right\}^{\frac{1}{2}}$$

The continuity equation for mass flow through the cascade, assuming incompressible flow, is

$$\int_r^{r_t} C_{x_1} \; 2\pi r \; dr = \int_r^{r_t} C_{x_2} \; 2\pi r \; dr$$

or, since C_{x_1} is assumed constant at all radii

$$C_{x_1} \int_R^1 R \; dR = \int_R^1 C_{x_2} \; R \; dR$$

$$C_{x_1} \frac{(1 - R^2)}{2} = \int_R^1 \left[C_{x_{2_t}}^2 + \frac{2z}{2z-2} \; C_{u_{2_t}}^2 \; (1 - R^{2z-2})\right]^{\frac{1}{2}} \frac{dR^2}{2}$$

But $\quad C_{u_{2_t}} = C_{x_{2_t}} \tan\alpha_t$

Hence
$$\frac{C_{x_1}}{C_{x_{2_t}}} = \frac{\int_R^1 \left[1 + \frac{2z}{2z-2} \tan^2\alpha_t (1 - R^{2z-2})\right]^{\frac{1}{2}} dR^2}{(1 - R^2)}$$

$$\frac{C_{x_1}}{C_{x_{2_t}}} = \frac{\left(\frac{2z \tan^2\alpha t}{2z-2}\right)^{\frac{1}{2}} \int_R^1 \left[\frac{z(1 - \tan^2\alpha t) - 1}{z \tan^2\alpha t} - R^{2z-2}\right]^{\frac{1}{2}} dR^2}{(1 - R^2)}$$

Therefore, because ξ and ζ_1

$$\frac{\partial \zeta_1}{\partial \xi} = \zeta_1^2 \, \alpha - \frac{\gamma\alpha}{2\gamma-1} \, \frac{\zeta_1^2}{\xi^{2\gamma}} \left(1 - \zeta_1^{2\gamma-1}\right)$$

$$\frac{\partial \zeta_1}{\partial \xi} = \left\{ \zeta_1^2 + \frac{\gamma\alpha}{2\gamma-1} \, \zeta_1^2 \, \xi \left(1 - \zeta_1^{2\gamma-1}\right) \right\}^{\frac{1}{2}}$$

The constants involving the boundary flow conditions, can be determined. Integrating Eqn. 12

$$\int_0^{\zeta_1} \frac{d\zeta}{\zeta^2} = \int_0^{\xi} \frac{d\xi}{\xi^{\gamma}}$$

or, since ζ_1 is assumed constant at all radii

$$\int_0^{\zeta_1} \frac{d\zeta}{\zeta^2} = \int_0^{\xi} \frac{d\xi}{\xi^{\gamma}}$$

$$\int_0^{\zeta_1} \frac{d\zeta}{\left\{ \zeta^2 + \frac{\gamma\alpha}{2\gamma-1} \, \zeta^2 \, \xi \left(1 - \zeta^{2\gamma-1}\right) \right\}^{\frac{1}{2}}} = \int_0^{\xi} \frac{d\xi}{\xi^{\gamma}}$$

Since $\zeta = \zeta_1^{\gamma} \cos\alpha$,

$$\int_0^{\zeta_1} \frac{d\zeta}{\left\{ \zeta^2 \left[1 + \frac{\gamma\alpha}{2\gamma-1} \zeta^{2\gamma-1} \xi \left(1 - \zeta^{2\gamma-1}\right) \right] \right\}^{\frac{1}{2}}} = \int_0^{\xi} \frac{d\xi}{\xi^{\gamma}}$$

$$\int_0^{\zeta_1} \frac{d\zeta}{\left\{ \left(\frac{\gamma\alpha \cos^{2\gamma-1}\alpha}{2\gamma-1} \right) \left[\frac{\left(1 - \cos^{2\gamma-1}\alpha\right)}{\alpha \cos^{2\gamma-1}\alpha} - 1 - \zeta^{2\gamma-1} \right] \right\}^{\frac{1}{2}}} = \int_0^{\xi} \frac{d\xi}{\xi^{\gamma}}$$

Integrating

$$\frac{C_{x_1}}{C_{x_{2_t}}} = \left(\frac{\frac{z \tan^2\alpha_t}{z-1}}{1-R^2}\right)^{\frac{1}{2}} \left\{ \frac{R^2}{2}\left(\frac{z(1-\tan^2\alpha t)-1}{z \tan^2\alpha t} - R^{2z-2}\right)^{\frac{1}{2}} \right.$$

$$\left. + \frac{z(1-\tan^2\alpha t)-1}{2z \tan^2\alpha t} \sin^{-1} \frac{R^{z-1}}{\left(\frac{z(1-\tan^2\alpha t)-1}{z \tan^2\alpha t}\right)^{\frac{1}{2}}} \right\}_R^1$$

Also,

$$C_{x_2} = \left[C_{x_{2_t}}^2 + \frac{2z}{2z-2} C_{u_{2_t}}^2 \left(1 - R^{2z-2}\right)\right]^{\frac{1}{2}}$$

$$C_{u_{2_t}} = C_{x_{2_t}} \tan \alpha t$$

$$\frac{r\, C_{u_2}}{r\, C_{u_{2_t}}} = \left(\frac{r}{r_t}\right)^z$$

Thus, by assigning desired values to z and α_t, the velocity pattern may be determined for all blade radii.

INTEGRATING

$$\frac{\sin\alpha_1}{\sin\alpha_2} = \left(\frac{\frac{2 - \sin^2\alpha_2}{2 - \sin^2\alpha_1}}{\frac{2 - \sin^2\alpha_2}{2 - \sin^2\alpha_1}}\right)^{\frac{1}{2}} \left\{\frac{1}{2}\left(\frac{2 + \sin^2\alpha_1}{2 + \sin^2\alpha_2}\right)^{\frac{1}{2}} \int_0^{\alpha_2} \left(\frac{2 + \sin^2\alpha_2}{2 + \sin^2\alpha_1}\right)^{\frac{1}{2}} d\alpha_2\right\}$$

$$+ \frac{(1 + \sin^2\alpha_1) - 1}{2\sin\alpha_1\cos\alpha_1} \int_0^{\alpha_2} \frac{\cos\alpha_2}{\left(\frac{(1 + \sin^2\alpha_1) - 1}{2\sin\alpha_1\cos\alpha_1}\right)^{\frac{1}{2}}}$$

Also,

$$\log\frac{\sin\alpha_1}{\sin\alpha_2} = \left[\log\frac{\sin\alpha_1}{\sin\alpha_2} + \frac{\sin\alpha_1}{2\sin\alpha_2}\int_0^{\alpha_2} \frac{\cos\alpha_2}{(1 - \sin^2\alpha_2)^{\frac{1}{2}}}\right]^{\frac{1}{2}}$$

$$\sin\alpha_1 = \sin\alpha_2 \tan\alpha_1$$

$$\frac{\sin\alpha_1}{\sin\alpha_2} = \left(\frac{\alpha_1}{\alpha_2}\right)^{\alpha_1}$$

Thus, by evaluating definite values in α_1 and α_2, the variation of latitude may be determined for all values (real).

Forces on an Airfoil in Cascade

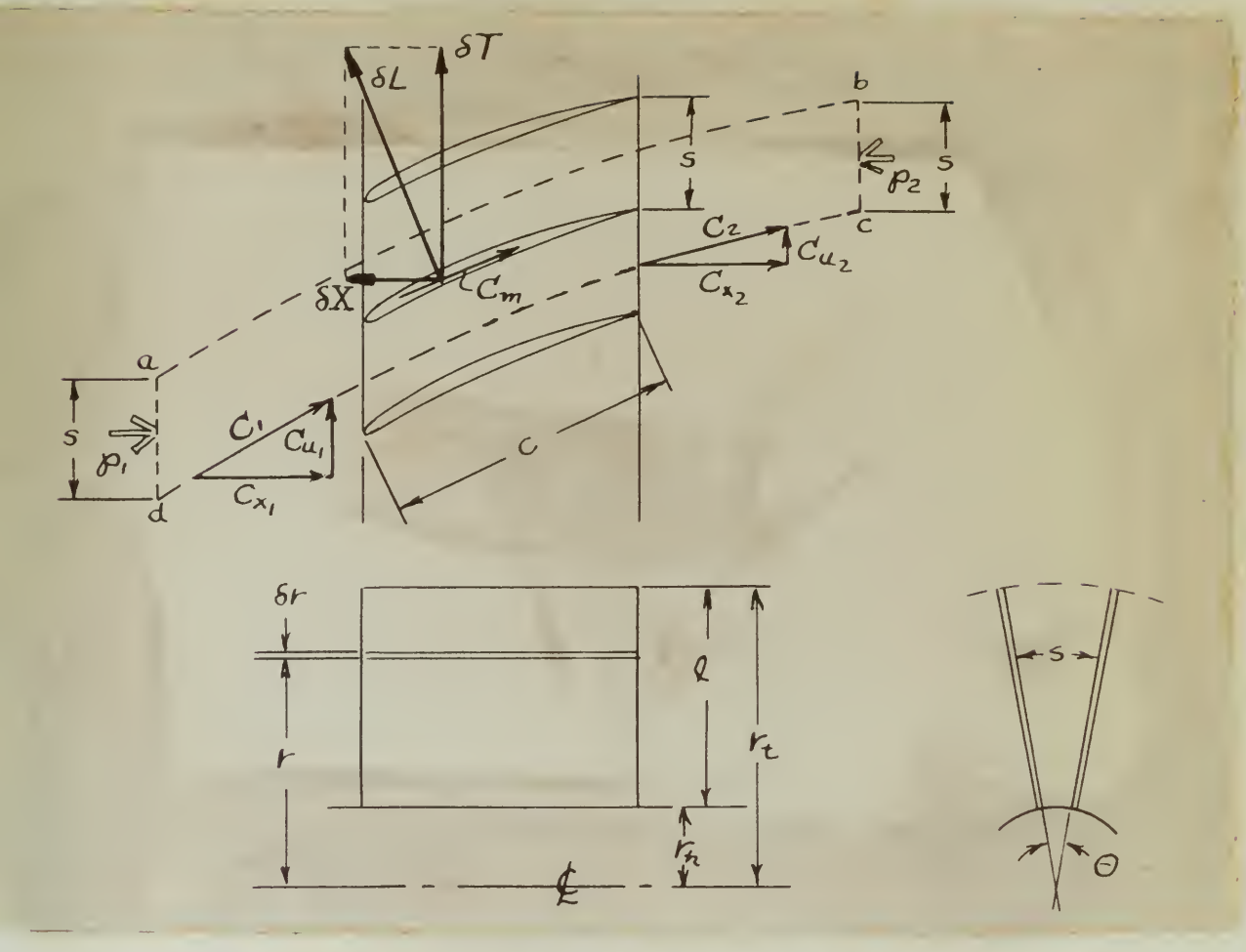

At any given radius, r, a control surface abcd is drawn around an airfoil of the cascade. Flow is assumed isentropic and incompressible. If radial flow is also assumed negligible

Mass flow, $\delta w = \rho C_{x_1} \, s \, \delta r = \rho C_{x_2} \, s \, \delta r$

$$\therefore \quad C_{x_1} = C_{x_2}$$

$$- \delta T = \delta w (C_{u_1} - C_{u_2})$$

$$\delta X = \delta w (C_{x_2} - C_{x_1}) + (p_2 - p_1) \; s \, \delta r$$

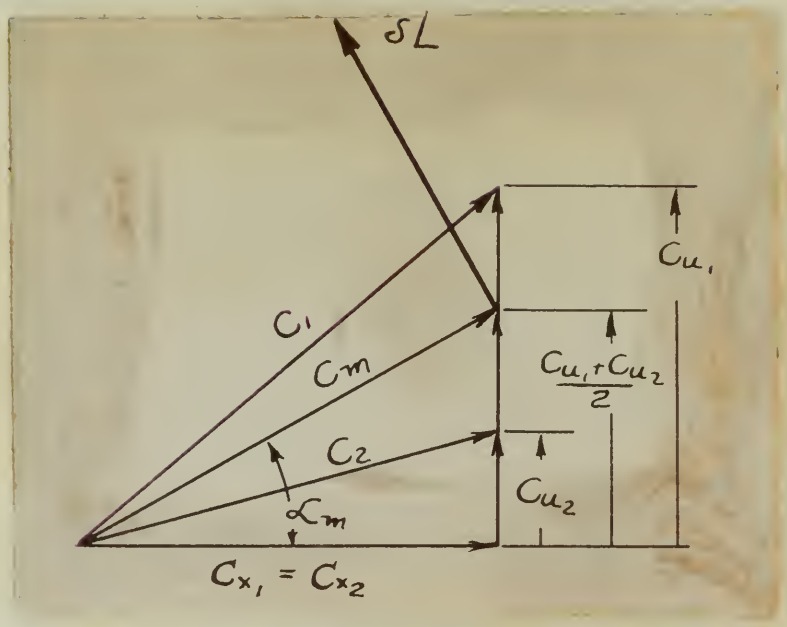

$$\tan \alpha_m = \frac{\delta X}{\delta T} = \frac{\frac{C_{u1} + C_{u2}}{2}}{C_x}$$

$$\delta L = \sqrt{\delta X^2 + \delta T^2}$$

$$\delta L = \delta T \sqrt{\left(\frac{\delta X}{\delta T}\right)^2 + 1}$$

$$\delta L = \frac{\delta T}{C_x} \sqrt{\left(\frac{C_{u1} + C_{u2}}{2}\right)^2 + C_x^2}$$

$$\delta L = \frac{\rho C_x \, s \, \delta r (C_{u1} - C_{u2})}{C_x} \sqrt{C_m^2}$$

$$\delta L = \rho C_m \, s (C_{u1} - C_{u2}) \, \delta r$$

By airfoil theory

$$\delta L = C_L \frac{\rho}{2} C_m^2 \, c \, \delta r$$

$$\therefore C_L = \frac{2 \, s/c \, (C_{u1} - C_{u2})}{C_m}$$

If radial flow is appreciable, then $C_{x_1} \neq C_{x_2}$

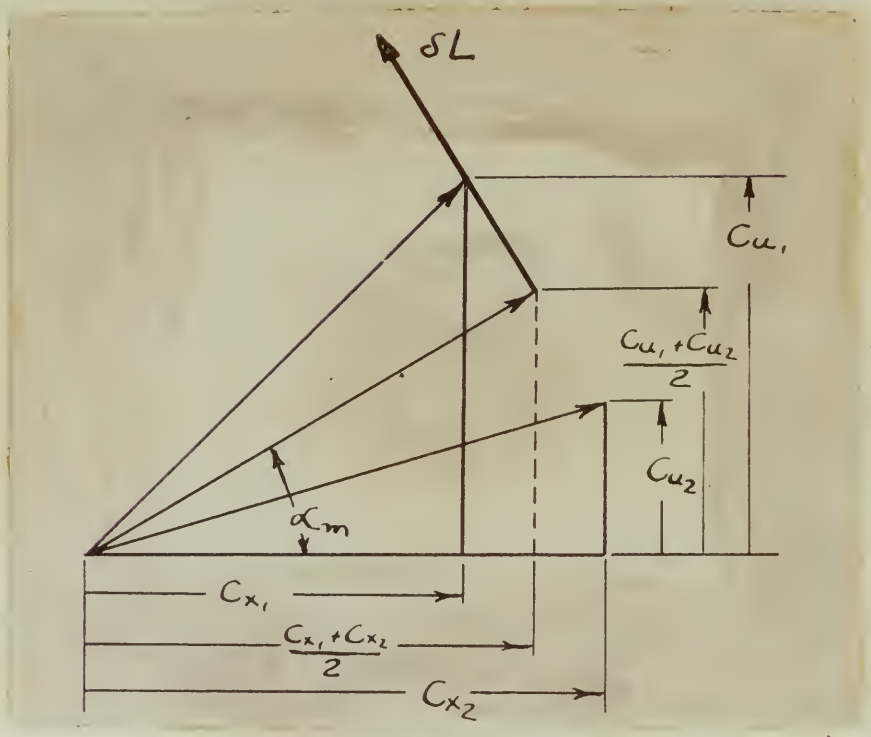

$$\tan \alpha_m = \frac{\delta X}{\delta T} = \frac{\dfrac{C_{u_1} + C_{u_2}}{2}}{\dfrac{C_{x_1} + C_{x_2}}{2}}$$

$$C_m = \sqrt{\left(\frac{C_{u_1} + C_{u_2}}{2}\right)^2 + \left(\frac{C_{x_1} + C_{x_2}}{2}\right)^2}$$

For inlet guide vanes, entering flow is axial and $C_{u_1} = 0$

$$\therefore \quad C_L = \frac{2\ s/c\ \ C_{u_2}}{\sqrt{\left(\dfrac{C_{u_2}}{2}\right)^2 + \left(\dfrac{C_{x_1} + C_{x_2}}{2}\right)^2}}$$

Now $s = r\theta$, where $\theta = \frac{2\pi}{N}$ (Number of vanes)

$$C_L = \frac{4\pi r}{Nc} \frac{C_{u_2}}{\sqrt{\left(\frac{C_{u_2}}{2}\right)^2 + \left(\frac{C_{x_1} + C_{x_2}}{2}\right)^2}}$$

Cascade A

Cascade A is the inlet guide vane assembly from an aircraft engine. It consists of 54 airfoils welded between an inner and an outer shroud, and was originally split on a diameter into two assemblies. In order to mount the cascade in the tunnel the two halves were brazed together to form a single assembly. This assembly was fitted on a wooden disk and held in axial position on the central shaft in the tunnel by means of bolts through the wooden disk. The assembly is best shown on Drawing Nos. N-5254 and N-4224.

The blade profile and planform are shown in Figure (3). Design velocity triangles at hub and tip and variation of turning angle with radius are also shown on Figure (3).

The radius at the blade root is 4.625 inches and the tip radius is 7.875 inches, giving a hub-tip ratio, $R_o = .5875$.

$$\frac{r_h C_{u_{2h}}}{C_{x_1}} = r_h \tan \alpha_{2h} = 2.65$$

$$\frac{r_t C_{u_{2t}}}{C_{x_1}} = r_t \tan \alpha_{2t} = 6.90$$

$$\frac{r_h C_{u_{2h}}}{r_t C_{u_{2t}}} = \frac{2.65}{6.90} = .384$$

(Below or above)

$$\frac{\pi r}{\lambda_0} = \frac{U w^2}{\sqrt{\left(\frac{\rho_0 w^2}{\lambda_0}\right)^2 + \left(\frac{\rho_0 w^2}{2}\right)^2}}$$

Example 1

Suppose ρ_0 is the total axial force acceleration field in circular motion. It consists of an arbitrary uniform pressure on inner and an outer shell, and two orthogonally equal on a diameter line the antinodal. In order to avoid the singular in the tension the two forces over lapped together in form a single assembly. This assembly was fixed on a support line and only in which particles on the inertial shell in the tension in order of total through the vector line. The assembly is just along on having zero. $\lambda_0 = 1.0$ and $\rho_0 = 1.0$.

The flank profile and pressure are shown in Figure (3). During velocity variation it was and the variation of pressure and is with radius are clear shown on Figure (3).

The ratio of the flank root is 1.0 inches and the tip radius is 0.75 inches giving a hub-tip radio, $\delta_0 = .5075$.

$$\frac{\lambda_0 \, \rho_0 w^2}{\rho_0 \, \lambda_0} = \tan \alpha_0 = 1.0$$

$$\frac{\lambda_0 \, \rho_0 w^2}{\rho_0} = \tan \alpha_{\frac{1}{2}} = 0.50$$

$$\frac{\lambda_0 \, \rho_0 w^2}{\rho_0 \, \rho_0 w^2} = \frac{1.00}{0.50} = .384$$

$$\frac{r_h \, C_{u2h}}{r_t \, C_{u2t}} = (R_o)^z$$

$$.384 = (.5875)^z$$

$$\therefore \quad z = 1.8$$

It is interesting to note here that for free vortex flow, $z = 0$; for "solid body" rotational flow, $z = 2$; and Cascade B is designed with $z = 3$.

Cascade B

Cascade B was designed using the three dimensional theory of Appendix A. It consists of 36 airfoils retained in a central disk. The tip radius is 7.875 inches and the hub radius is 3.938 inches, giving a hub-tip ration, $R_o = .5$.

A cubic variation of circulation with blade radius is obtained by setting $z = 3$, in order to provide a severe test of theory. The turning angle at the tip was arbitrarily set at 45 degrees as representing the maximum that could be obtained with the available value of solidity and with a moderate lift coefficient.

The number of blades was selected as a compromise to give a good approximation to the infinite requirement of the three dimensional theory without excessive manufacturing cost. The blades were tapered linearly from tip to hub to obtain suitable values of lift coefficient.

After selection of these design parameters, the design

$$\frac{T_h\, C_{mp}}{T_h\, C_{mp}} = (\delta_a)^n$$

$$.344 = (1.5075)^n$$

$$\therefore \quad n = 1.4$$

It is interesting to note that for free vortex flow, $n = 0$; for "solid body" rotational flow, $n = 2$; and Example B is designed with $n = 3$.

Example B

Example B was designed using the three dimensional theory of Appendix A. It consists of 17 airfoils mounted in a general disc. The tip radius is 7.[illegible] inches and the hub radius is [illegible] inches, giving a hub-tip radius, $\delta_a = .5$.

A double variation of circulation with blade radius is obtained by setting $n = 3$, in order to provide a severe test of theory. The spacing angle at the tip was arbitrarily set to 45 degrees as representing the maximum that could be obtained with the available value of solidity and with a moderate lift coefficient.

The number of blades was selected as a compromise to give a good approximation to the infinite requirement of the three dimensional theory without excessive manufacturing cost. The blades were tapered linearly from tip to hub to obtain variation value, of lift coefficient.

After selection of these design parameters, the design

proceeded as follows:

Design constants:

$z = 3$

$\alpha_{2t} = 45^\circ$ at $r_t = 7.875$ inches

$R_o = .5$

$N = 36$

R	c	s	s/c
1.0	2.000	1.373	.685
.9	1.875	1.236	.660
.8	1.750	1.100	.630
.7	1.625	.962	.591
.6	1.500	.825	.550
.5	1.375	.687	.500

From the previous development of cascade theory, substituting these design constants

$$\frac{C_{x_1}}{C_{x_{2t}}} = \frac{\left(\frac{3\tan^2 45^\circ}{2}\right)^{\frac{1}{2}}}{(1 - R_o^2)} \left[\frac{R^2}{2} \left(\frac{3(1-\tan^2 45^\circ) - 1}{3\tan^2 45^\circ} - R^4 \right) + \frac{3(1-\tan^2 45^\circ) - 1}{3\tan^2 45^\circ} \sin^{-1} \frac{R^2}{\frac{3(1-\tan^2 45^\circ) - 1}{3\tan^2 45^\circ}} \right]_{R_o}^{1}$$

$\frac{C_{x_1}}{C_{x_{2t}}} = 1.35$, or $C_{x_{2t}} = .741\ C_{x_1}$

Also, $C_{x_{2t}} = C_{u_{2t}} = .741\ C_{x_1}$

Proceeded as follows:

Design constants:

$z = 3$

$\alpha E_t = 45^\circ$ at $r_1 = 7.875$ inches

$R_0 = .5$

$N = 36$

α	α	α	α/α
1.0	2.000	1.973	.625
.9	1.875	1.236	.660
.8	1.750	1.100	.630
.7	1.625	.960	.591
.6	1.500	.825	.550
.5	1.375	.687	.500

From the previous development of cascade theory, substituting these design constants

$$\frac{C_{\alpha_1}}{C_{\alpha_2}} = \left(\frac{\frac{3\tan^2 45^\circ}{2}}{(1 - R_0^2)}\right)^{\frac{1}{2}} \left[\frac{R_0^2}{2}\left(\frac{3(1-\tan^2 45^\circ) - 1}{3\tan^2 45^\circ} - R_0^4\right)\right.$$

$$\left. + \frac{3(1-\tan^2 45^\circ) - 1}{3\tan^2 45^\circ} \sin^{-1} \frac{R_0^2}{\frac{3(1-\tan^2 45^\circ) - 1}{3\tan^2 45^\circ}}\right]_{R_0}^{1}$$

$\frac{C_{\alpha_1}}{C_{\alpha_2}} = 1.35$, or $C_{\alpha_2} = .741\ C_{\alpha_1}$

Also, $C_{\alpha_2} = C_{\alpha_2} = .741\ C_{\alpha_1}$

$$C_{x_2} = .741\, C_{x_1} \left[1 + \frac{3}{2}(1 - R^4)\right]^{\frac{1}{2}}$$

$$C_{u_2} = .741\, C_{x_1} R^2$$

$$\tan\alpha_2 = \frac{C_{u_2}}{C_{x_2}}$$

But, from Appendix A, it is recalled that the blade performs as if it were in a flow field, C_m.

Therefore

$$\tan\alpha_{2_{design}} = \frac{C_{u_2}}{\dfrac{C_{x_1} + C_{x_2}}{2}}$$

$$C_L = 4\pi r_t \frac{R}{Nc} \frac{.741\, C_{x_1} R^2}{\dfrac{.741\, C_{x_1}}{2} \sqrt{R^4 + \left[\left(\frac{5}{2} - \frac{3}{2} R^4\right)^{\frac{1}{2}} + \frac{1}{.741}\right]^2}}$$

$$C_L = \frac{8\pi r_t}{Nc} \frac{R^3}{\sqrt{4.32 - \frac{R^4}{2} + 2.70\left(\frac{5}{2} - \frac{3}{2} R^4\right)^{\frac{1}{2}}}}$$

R	C_{u_2}	C_{x_2}	C_m	α_m	α_2	$\alpha_{2\,design}$	C_L
1.0	$.741C_{x_1}$	$.741C_{x_1}$	$.947C_{x_1}$	23.0°	45.0°	40.4°	1.07
.9	.600	.911	1.001	17.4	33.4	32.2	.79
.8	.474	1.018			25.0	25.2	.57
.7	.363	1.082	1.055	9.9	18.6	19.2	.41
.6	.267	1.124			13.4	14.1	.27
.5	.185	1.150	1.080	4.9	9.15	9.75	.17

Four sections are determined, at R = 1.0, .9, .7, and .5. The basic section for the blade is taken from reference (3), increased

$$C_{x_2} = .741\, C_{x_1} \left[1 + \frac{3}{2}(1 - R^4) \right]^{\frac{1}{2}}$$

$$C_{z_2} = .741\, C_{x_1} R^2$$

$$\tan \alpha_2 = \frac{C_{z_2}}{C_{x_2}}$$

Obj. from Appendix A, it is recalled that the blade performs as if it were in a flow field, C_a.

Therefore

$$\tan \alpha_2 \text{ design} = \frac{C_{z_2}}{\frac{C_{x_1} + C_{x_2}}{2}}$$

$$C_L = 4\pi r_s \frac{R}{Rd} \frac{.741\, C_{x_1} R^2}{\sqrt{\frac{.741\, C_{x_1}}{2} \left[R^4 + \left(\frac{3}{2} - \frac{1}{2} R^4 \right)^{\frac{1}{2}} - \frac{1}{.741} \right]^2}}$$

$$C_L = \frac{4\pi r_s}{Rd} \frac{R^3}{\sqrt{4.50 - \frac{R^4}{2} - 2.70 \left(\frac{3}{2} - \frac{1}{2} R^4 \right)^{\frac{1}{2}}}}$$

R	C_{x_2}	C_{x_1}	C_a	α_a	α_2	α_2 design	C_L
1.0	.741 C_{x_1}	.741 C_{x_1}	.847 C_{x_1}	23.0°	45.0°	48.4°	1.07
.9	.660	.911	1.001	17.4	33.4	32.3	.79
.8	.654	1.018			25.0	25.2	.57
.7	.763	1.080	1.056	9.9	18.0	19.2	.41
.6	.867	1.124			13.4	14.1	.27
.5	.889	1.150	1.080	4.9	9.15	9.75	.17

Four sections are determined, at R = 1.0, .9, .7, and .5.

The basic section for the blade is taken from reference (5), increased

in thickness from 6% to 10% for manufacturing purposes. This section is designated 64(B)-10. It is an experimentally derived section and gives the required turning angle at R = 1.0 with peak-free pressure distribution. In order to achieve a smoothly faired blade, the remaining sections are obtained from the basic section by an empirical construction based on the tangent to the mean camber line at the trailing edge. The distribution of camber and thickness along the chord are held constant while the camber is reduced to give the desired turning angle. The thickness ration of ten percent remains constant.

Comparison is made to other referencesto validate the choice of section, as follows:

$$C_L\left(\begin{matrix}\text{isolated}\\ \text{airfoil}\end{matrix}\right) = \begin{matrix}\text{Slope of } C_L\\ \text{vs. Angle of}\\ \text{Attack Curve}\end{matrix} \times \left(\begin{matrix}\text{Angle}\\ \text{of}\\ \text{Attack}\end{matrix} - \begin{matrix}\text{Angle of}\\ \text{Attack,}\\ \text{Zero Lift}\end{matrix}\right)$$

(1) $$C_{L_{\left(\begin{matrix}\text{isolated}\\ \text{airfoil}\end{matrix}\right)}} = a_o \left[(\alpha_m - \sigma) - \alpha_{L_o}\right]$$ Ref. (7)

where α_{L_o} is determined by construction Ref. (8)

(2) $$C_{L_{\text{cascade}}} = C_{L_{\begin{matrix}\text{isolated}\\ \text{airfoil}\end{matrix}}} \times \frac{2a/c}{\pi \cos \alpha_2},$$ Ref. (12)

(3) $$\delta = \theta \sqrt{\frac{S}{C}} \left[.23 \left(\frac{2a}{C}\right)^2 + \frac{.10\,\alpha_2}{500}\right],$$ Ref. (9)

Another value of δ for comparison is taken from reference (14).

in thickness from 6% to 10% for manufacturing purposes. This section is designated 64(B)-10. It is an experimentally derived section and gives the required turning angle at R = 1.0 with peak-free pressure distribution. In order to achieve a smoothly faired blade, the remaining sections are obtained from the basic section by an additional construction based on the tangent to the chord camber line at the trailing edge. The distribution of camber and thickness along the chord are held constant while the camber is reduced to give the desired turning angle. The thickness ratios of ten percent remains constant.

Comparison is made to other references to validate the choice of section, as follows:

$$C_{L\,(\text{isolated airfoil})} = \text{Slope of } C_L \text{ vs. Angle of Attack Curve} \times \left(\text{Angle of Attack} - \text{Angle of Attack, Zero Lift} \right)$$

(1) $$C_{L\,(\text{isolated airfoil})} = s_0 \left[(\alpha_s - \sigma) - \alpha_{L_0} \right]$$ Ref. (7)

where α_{L_0} is determined by construction Ref. (8)

(2) $$C_{L\,\text{cascade}} = C_{L\,\text{isolated airfoil}} \times \frac{2\sigma/c}{\pi \cos \alpha_0} ,$$ Ref. (10)

(3) $$\delta = \theta \sqrt{\frac{2}{c}} \left[.23 \left(\frac{2\sigma}{c} \right)^2 + \frac{.10\,\alpha_0}{500} \right] ,$$ Ref. (9)

Another value of δ for comparison is taken from reference (14).

All constructions were made to a scale of ten to one to insure reasonable accuracy. Some slight compromises were necessary during the layout to obtain smooth contours between blade sections. In addition, the thickness of the trailing edge was increased to .015 inches for manufacturing purposes.

A comparison of the lift coefficients and outflow angles of the derived sections, as determined from the above sources are compared with the design values in the following table:

All constructions were made to a scale of 1in to one be inserve reasonable accuracy. Some slight compromises were necessary during the layout to obtain smooth contours between blade sections. In addition, the thickness of the trailing edge was increased to .01½ inches for manufacturing purposes.

A comparison of the lift coefficients and outflow angles of the derived sections, as determined from the above sources are compared with the design values in the following table:

R	1.0	.9	.7	.5	Remarks
Camber (%)	12.1(1)	8.9 (2)	7.2 (2)	4.8 (2)	(1) Ref. (3) (2) Empirical Constr.
σ	-27.0°(1)	-22.4°(2)	-13.2°(2)	-4.° (2)	
$\alpha_m - \sigma$	4.°	5.°	3.3°	-0.9°	
θ	68.0°	55.5°	44.3°	33.8°	Constr.
α'_1	21.0°	18.0°	18.8°	20.8°	Constr.
α'_2	-47.0°	-37.5°	-24.5°	-13.°	Constr.
α_{L_o}	-13.4°	-9.9°	-6.5°	-	Constr. Ref.(8)
a_o	.105	.105	.105	-	
C_L isolated airfoil	1.83(3)	1.56 (3)	.81(3)	.41(4)	(3) Eqn. (1) (4) Ref. (7)
C_L cascade	1.04	.78	.42	.127	Eqn. (2)
C_L design	1.07	.79	.41	.17	Page 30
δ	6.8°(1)	5.3°	4.3°	3.25°	Empirical Constr.
δ	8.3°	6.6°	5.0°	3.5°	Eqn. (3)
δ	8.7°	7.0°	5.4°	3.3°	Ref. (14)
α_2	-40.2°(1)	-32.2°	-20.2°	-9.75°	Empirical Constr.
α_2	-38.7°	-30.9°	-20.5°	-9.50°	Ref. (9)
α_2	-38.3°	-30.5°	-20.1°	-9.70°	Ref. (14)
α_2 design	-40.4°	-32.2°	-19.2°	-9.75°	Page 30

Ordinates of the mean camber line of the four sections, measured from the chord line, are tabulated in Table I. Ordinates of the four section profiles, also measured from the chord line, were determined from layouts and are tabulated in Table II.

A calculation of the forces acting on this cascade was made, for use in designing components of the annular cascade tunnel such as

Remarks	.5	.7	.9	1.0	R
Ref. (1) Empirical Constr.	[illegible]	[illegible]	[illegible]	[illegible]	Camber (R)
	[illegible]	[illegible]	[illegible]	[illegible]	σ
	[illegible]	[illegible]	[illegible]	[illegible]	$\alpha_0 - \sigma$
Constr.	[illegible]	[illegible]	[illegible]	[illegible]	β
Constr.	[illegible]	[illegible]	[illegible]	[illegible]	α_1
Constr.	[illegible]	[illegible]	[illegible]	[illegible]	α_2
Constr. Ref. (2)	-	[illegible]	[illegible]	[illegible]	α_3
	-	[illegible]	[illegible]	[illegible]	α_0
Ref. (1) Ref. (2)	[illegible]	[illegible]	[illegible]	[illegible]	C_L isolated airfoil
Ref. (3)	[illegible]	[illegible]	[illegible]	[illegible]	C_L measure
Page 30	[illegible]	[illegible]	[illegible]	[illegible]	C_L design
Empirical Constr.	[illegible]	[illegible]	[illegible]	[illegible]	δ
Ref. (1)	[illegible]	[illegible]	[illegible]	[illegible]	δ
Ref. (1)	[illegible]	[illegible]	[illegible]	[illegible]	δ
Empirical Constr.	[illegible]	[illegible]	[illegible]	[illegible]	α_2
Ref. (2)	[illegible]	[illegible]	[illegible]	[illegible]	α_3
Ref. (1)	[illegible]	[illegible]	[illegible]	[illegible]	α_2
Page 30	[illegible]	[illegible]	[illegible]	[illegible]	α_2 design

Ordinates of the same camber line of the four sections, measured from the chord line, are tabulated in Table I. Ordinates of the four section profiles, also measured from the chord line, were determined from formula and are tabulated in Table II.

A calculation of the forces acting on this cascade was made, for use in designing components of the annular cascade tunnel room as

shafts, bevel gears, and friction brake. Since an exact figure was not required, the assumption was made that $C_{x_1} = C_{x_2}$ in order to simplify the calculation, particularly in the case of determining the axial force, X.

<u>Axial Force X</u>

From Page

$$\delta X = \delta w \, (C_{x_2} - C_{x_1}) + (p_2 - p_1) \, s \, \delta r$$

Applying the above assumption,

$$\delta X = (p_{o_2} - p_{o_1}) - \frac{\rho}{2} (C_2^2 - C_1^2) \quad s \, \delta r$$

$$dX = -\frac{\rho}{2} C_{u_2}^2 \; s \, dr$$

and $C_{u_2} = .741 \, C_{x_1} \, R^2$

$$X = -\frac{\rho}{2} s \, r_t \int_{.5}^{1.0} (.741 \, C_{x_1} \, R^2)^2 \, dR$$

$$X = -\frac{\rho}{2} s \, r_t \, (.741 \, C_{x_1})^2 \left[\frac{R^5}{5} \right]_{.5}^{1.0}$$

For $\rho =$ .002378 slugs/cu.ft.

$s_{avg} = 1.031/12$ feet

$$X = -.715 \times 10^{-6} \, C_{x_1}^2$$

$C_{x_1} = 138$ feet per second (See page 17)

shafts, bevel gears, and friction drain. Since the exact figure was not required, the assumption was made that $C_{x_1} = C_{x_2}$ in order to simplify the calculation, particularly in the case of determining the axial force, X.

Axial Force X

From Page

$$\delta u = \delta w\,(C_{x_2} - C_{x_1}) + (p_2 - p_1) \times \delta r$$

applying the above assumption,

$$\delta u = (p_2 - p_1) - \frac{\rho}{2}\left(C_2^2 - C_1^2\right) \times \delta r$$

$$\Delta E = -\frac{\rho}{2}\, C_{x_2}^2 \times \delta r$$

and $C_{x_2} = .741\, C_{x_1}\, R^2$

$$X = -\frac{\rho}{2} \times r_e \int_{.5}^{1.0} (.741\, C_{x_1}\, R^2)^2\, dR$$

$$X = -\frac{\rho}{2} \times r_e\, (.741\, C_{x_1})^2 \left[\frac{R^5}{5}\right]_{.5}^{1.0}$$

For ρ = .000375 slugs/cu.ft.

r_{avg} = 1.[illegible]/12 feet

$$X = -.715 \times 10^{-6}\, C_{x_1}^2$$

C_{x_1} = 130 feet per second (See page 17)

$X = -.136$ pounds/blade

X (Total) $= -4.9$ pounds

<u>Torque Force, T</u>

$$-\delta T = \delta w \, (C_{u_1} - C_{u_2})$$

$$-dT = -\rho \, C_{x_1} \, s \, r_t \, C_{u_2} \, dR$$

$$T = \rho \, C_{x_1} \, s \, r_t \int_{.5}^{1.0} .741 \, C_{x_1} \, R^2 \, dR$$

$$T = .741 \rho \, C_{x_1}^2 \, s \, r_t \left[\frac{R^3}{3} \right]_{.5}^{1.0}$$

$$T = 29 \times 10^{-6} \, C_{x_1}^2$$

$T = .552$ pounds/blade

*Torque/blade $= .552 \times .8 \times 7.875$

Torque/blade = 3.5 inch-pounds

Torque (Total) = 126 inch-pounds

---

*.8 r_t taken as center of forces since turning angle is increasing toward tip of blade.

$T = -.136$ pounds/blade

T (total) $= -1.7$ pounds

Torque force, $\underline{T}$

$$-\delta T = \delta \times (C_{n_1} - C_{n_2})$$

$$-\delta T = -\rho C_{n_1} \times r_b C_{n_2} \, dR$$

$$T = \rho C_{n_1} \times r_b \int_{.5}^{1.0} .741 \, C_{n_1} R^2 \, dR$$

$$T = .741 \rho C_{n_1}^2 \times r_b \left[\frac{R^3}{3} \right]_{.5}^{1.0}$$

$$T = 28 \times 10^{-4} \, r_{n_1}^2$$

$T = .552$ pounds/blade

ΣTorque/blade $= .552 \times .8 \times 7.375$

Torque/blade $= 3.5$ inch-pounds

Torque (Total) $= 126$ inch-pounds

---

*.8 r_b taken as center of forces since turning angle is increasing toward tip of blade.

III EXPERIMENTAL INVESTIGATION

Results

It has been previously noted that the design and construction aspects of the current project were not completed until mid-April 1949. After installation and adjustment the equipment was ready for calibration early in May and a temporary manometer setup was improvised in order to obtain some preliminary data. Test runs were made during the second week in May and approximately three hundred and fifty test points were taken and recorded. It should be emphasized, however, that these data should be regarded as tunnel calibration data rather than as accurate information applied to the performance of the cascade.

Results of the tunnel survey, with the cascade removed are presented in Figure 6. These tests indicate a good velocity profile at the test section of the tunnel. Boundary layer thicknesses are of the order of 1/2 inch at the outer wall, and 3/8 inch at the inner core. Since inlet guide vanes to an aircraft engine must be designed to operate in a duct where a similar build-up of boundary layer must be expected, this is not presently considered objectionable. The magnitude of the absolute velocity at the test section appears considerably lower than the calculated value, when using a manometer vented to ambient static pressure. The true tunnel velocity cannot be determined until provisions are available for obtaining the static pressure in the test section.

III EXPERIMENTAL INVESTIGATION

Results

It has been previously noted that the design and construction aspects of the current project were not completed until mid-April 1949. After installation and adjustment the equipment was ready for calibration early in May and a temporary manometer setup was improvised in order to obtain some preliminary data. Test runs were made during the second week in May and approximately three hundred and fifty test points were taken and recorded. It should be emphasized, however, that these data should be regarded as tunnel calibration data rather than as accurate information applied to the performance of the balance.

Results of the tunnel survey, with the cascade removed are presented in Figure 6. These tests indicate a good velocity profile at the test section of the tunnel. Boundary layer thicknesses are of the order of 1/2 inch at the outer wall, and 1/8 inch at the inner core. Since inlet guide vanes in an aircraft engine must be designed to operate in a wet where a similar build-up of boundary layer must be expected, this is not necessarily considered objectionable. The magnitude of the absolute velocity at the test section appears considerably lower than the calculated value, when using a manometer vented to ambient station pressure. The true tunnel velocity cannot be determined until provisions are available for obtaining the static pressure in the test section.

Maximum rotation of the flow was 2½ degrees, near the outer diameter. Since a satisfactory method for zeroing the yawmeter in the true axial direction has not yet been developed, the zero setting was established by line of sight. Since there is no reason for the airflow to rotate in opposite directions at inner and outer radius, as might appear from Figure 6, it is assumed that the flow at the inner radius is axial, and a one degree correction is added to all subsequent yawmeter readings. This appears to be of the correct order of magnitude for the accuracy to be expected from the sighting method used for zeroing the yawmeter.

With Cascade A placed in the tunnel, radial traverses were made at .100 inch intervals over an arc of 12 degrees. Tangential traverses were made at one degree intervals over an arc of 14 degrees, at .500 inch radial intervals. Representative flow characteristics are presented in Figure 7.

The results are generally excellent judged on the basis of reproducibility and cyclic repetition. A comparison of these preliminary data with the design values for Cascade A is made in Figure 3, but no conclusions are drawn from these early findings.

It is apparent that some separation is occurring from the upper surface of the airfoil, thus reducing the outflow angle in this region. Total pressure losses are relatively low in this region. As the wake region behind the trailing edge is traversed from upper surface to lower surface, the turning angle increases sharply, accompanied

Maximum rotation of the flow was 15 degrees, with the outer diameter. Since a satisfactory method for turning the pressure in the true axial direction was not yet been developed, the cars setting was established by line of sight. Since there is no reason for the airflow to rotate in opposite directions at inner and outer radius, it might appear from Figure 1. It is assumed that the flow at the inner radius is radial, but a cam degree correction is added to all subsequent pressure readings. This appears to be of the correct order of magnitude for the accuracy to be expected from the aligning method used for turning the pressure.

Data Cascade 4 showed in the tunnel, radial traverses were made at .100 inch intervals over an arc of 22 degrees. Tangential traverses were made at one degree intervals over an arc of 14 degrees, at .500 inch radial intervals. Representative flow characteristics are presented in Figure 7.

The results are generally considered judged on the basis of reproducibility and cyclic repetition. A comparison of these preliminary data with the design values for Cascade 4 is made in Figure 3, but no conclusions are drawn from these early findings.

It is apparent that some separation is occurring from the upper surface of the airfoil, thus reducing the orbiter angle in this region. Total pressure losses are relatively low in this region. In the wake region behind the trailing edge is traversed from upper surface to lower surface, the turning angle increases sharply, accompanied

by a loss in total pressure, indicating a considerable boundary layer on the lower surface of the airfoil. Between these regions, across an arc of 2-3 degrees (airfoils are spaced 6.67°), the outflow angle is relatively constant, and pressure losses are low. The outflow angle in this central region is taken as the average outflow angle for the comparison on Figure 3.

Within the boundary layer at both the inner and the outer tunnel walls, the outflow angle increases sharply. It seems probable that secondary flow circulation from the lower surface of one airfoil to the upper surface of the adjacent airfoil may cause the considerable increase in turning angle in these regions of low velocity.

Much additional data must be obtained on Cascade A and Cascade B, when it is built, before any valid conclusions may be drawn concerning the correlation of the experimental results with the theory outlined in Appendix A.

Suggestions for Further Work

As a result of the preliminary test runs, the following suggestions are offered to improve the performance of the tunnel and enhance the value of future experimental investigations:

1. Complete instrumentation.

2. Determine true axis of tunnel and scribe inside of test section outer casing in order to properly zero yawmeter in axial direction.

3. Provide a vernier on indicating quadrant of cascade rotating mechanism to permit accurate setting to tenths of a degree.

by a loss in total pressure, indicating a considerable boundary layer on the lower surface of the airfoil. Between these regions, across an arc of 0-3 degrees (Airfoils are spaced 0.67"), the outflow angle is relatively constant, and pressure losses are low. The outflow angle in this central region is taken at the average outflow angle for the comparison on Figure 4.

Within the boundary layer at both the inner and the outer tunnel walls, the outflow angle increases sharply. It seems probable that secondary flow circulation from the lower surface of one airfoil to the upper surface of the adjacent airfoil may cause the considerable increase in turning angle in these regions of low velocity.

Most analytical data must be obtained on Cascade g and Cascade h, when it is built, before any valid conclusions may be drawn concerning the correlation of the experimental results with the theory outlined in Appendix A.

<u>Suggestions for further work</u>

As a result of the preliminary test runs, the following suggestions are offered to improve the performance of the tunnel and increase the value of future experimental investigations:

1. Cascade instrumentation.

2. Cascading from axis of tunnel and active inside of test section outer axis in order to properly vary cascades in axial direction.

3. Provide a vernier on indicating pressure of expense rotating attention to permit accurate setting to tenths of a degree.

4. Reduce friction in cascade rotating mechanism and eliminate backlash in system when rotating cascade to left (viewed from rear). No significant backlash exists when cascade is rotated to right.

5. Reduce roughness and fitting irregularities in the vicinity of the cascade.

6. Remove or reduce boundary layer by use of annular manifolds, or possibly by shortening the approach section preceding the test section.

7. Seal plywood spacers separating screens to prevent air leakage from the tunnel.

8. Possibly add a low resistance straightening honeycomb in an attempt to eliminate the slight flow rotation.

4. Unknown difficulties in assembly operating mechanisms and stability limitations in system when controlling towards to Left (viewed from rear). No significant unwanted motions/disturbances results be induced by flight.

5. Unknown problems and little investigability in low stability of the towards.

6. Danger of motion becoming large by use of control sensitivity, or possibly in overcoming the governor torque preventing the last section.

7. Tail pivoted system controlling towards is involves air leakage from the tunnel.

8. Finally, with a low pressure monitoring unpowered is an attempt to eliminate the slight flow variation.

APPENDIX A

VORTEX THEORY OF ANNULAR CASCADES*

The vortex theory of airfoils and propellers may be applied to the flow through an annular cascade (Ref. 15). Assuming incompressible flow, in the case of a ring of blades designed to give free vortex flow downstream the blades may be replaced by vortices bound to the respective locations of the blades. Each blade may be represented by a single vortex line whose circulation, Γ, is independent of radius and whose axis is a straight line which intersects the axis of the annulus, Fig. 1A. A uniform axial velocity, C_x, is superimposed on the velocities produced by the bound vortices. A path ABCDA enclosing one blade and following similar streamlines in adjacent blade passages will have a circulation $2\pi rC_u/Z$ where Z is the number of blades. Since the circulation, Γ, is constant, rC_u is constant and the downstream flow, being additionally one with constant entropy and stagnation enthalpy, must be free vortex.

The representation above does not give a complete picture of the flow. The influence of such bound vortex lines downstream at infinity is negligible, but the circulation along a path, BCB, enclosing the hub or cylinder which forms the inner wall of the

*This development by Dr. W. R. Hawthorne, George Westinghouse Professor of Mechanical Engineering, Massachusetts Institute of Technology, Cambridge, Massachusetts.

APPENDIX A

VORTEX THEORY OF ANNULAR BLADES*

The vortex theory of airfoils and propellers may be applied to the flow through an annular cascade (Ref. 15). Assuming incompressible flow, in the case of a ring of blades designed to give free vortex flow downstream the blades may be replaced by vortices bound to the respective locations of the blades. Each blade may be represented by a single vortex line under circulation, Γ, is independent of radius and whose axis is a straight line which intersects the axis of the annulus, Fig. 11. A uniform axial velocity, C_u, is superimposed on the velocities produced by the bound vortices. A path which replaces one blade and following similar streamlines in adjacent blade passages will have a circulation $2\pi r C_u/N$ where N is the number of blades. Since the circulation, Γ, is constant, rC_u is constant and the downstream flow, being additionally one with constant entropy and stagnation enthalpy, must be free vortex.

The representation above does not give a complete picture of the flow. The influence of such bound vortex lines downstream at infinity is negligible, but the circulation along a path, PC_u, enclosing the hub or cylinder which forms the inner wall of the

---

*This development by Dr. [illegible], Chrysler Engineering, Professor of Mechanical Engineering, Massachusetts Institute of Technology, Cambridge, Massachusetts.

annulus equals $2\pi r C_u = Z\Gamma$. Therefore in representing the conditions at infinity it is necessary to turn the vortex lines replacing the blades through a right angle and let them trail off downstream enclosed within the inner wall of the annulus. If the trailing vortices pass downstream along the axis of the annulus and the bound vortices pass radially to infinity then the boundary condition of no radial velocity is satisfied at the inner and outer walls up and downstream at infinity and in the plane of the bound vortices representing the blades. For a finite number of blades the condition of zero radial velocity at the walls is not satisfied elsewhere and it does not appear possible to obtain a simple vortex representation of the flow for a finite number of blades. For an infinite or large number of blades the vortex representation of Fig. 2A along with a superimposed axial velocity gives stream surfaces which are concentric cylinders everywhere and satisfies the conditions of flow. This method of representing the flow for a cascade designed to give free vortex flow downstream may be extended to other types provided the number of blades is large.

Considering the case where the circulation varies along the blade span, a vortex sheet of strength $d\Gamma/dr$ per unit radial length trails downstream off the blade. To satisfy the boundary conditions at the walls each filament of these trailing vortex sheets requires multiple reflection in the walls. A number of equivalent diagrams may be drawn of which Fig. 3A is an example. In this figure

annulus equals $2\pi r C_u = 2\Gamma$. Therefore in representing the conditions at infinity it is necessary to turn the vortex lines emulating the blades through a right angle and let them trail off downstream enclosed within the inner wall of the annulus. If the trailing vortices pass downstream along the axis of the annulus and the bound vortices pass radially to infinity then the boundary condition of no radial velocity is satisfied at the inner and outer walls up and downstream at infinity and in the plane of the bound vortices representing the blades. For a finite number of blades the condition of zero radial velocity at the walls is not satisfied elsewhere and it does not appear possible to obtain a simple vortex representation of the flow for a finite number of blades. For an infinity or large number of blades the vortex representation of Fig. 2a along with a superimposed axial velocity gives stream surfaces which are concentric cylinders everywhere and satisfies the conditions of flow. This method of representing the flow for a cascade designed to give free vortex flow downstream may be extended to other types provided the number of blades is large.

Considering the case where the circulation varies along the blade span, a vortex sheet of strength $d\Gamma/dr$ per unit radial length trails downstream off the blade. To satisfy the boundary conditions at the walls each filament of these trailing vortex sheets requires multiple reflection in the walls. A number of equivalent diagrams may be drawn of which Fig. 2a is an example. In this figure

the circulation around each blade increases from a value Γ_h at the hub (inner wall). Each blade and its trailing vortices are represented by a bound vortex of circulation Γ_h extending from the axis radially to infinity, and a system of appropriate horseshoe vortices, each horseshoe vortex being of strength $d\Gamma/dr$ per unit radial length and combining with the bound vortex in the sense required to give the desired circulation. At the axis the bound vortex trails off downstream as above in order to reproduce the boundary conditions at the inner wall. In this example each of the existing trailing vortices is part of the horseshoe formed by reflecting it in the outer wall. This system is reflected in the inner wall, giving a system which in turn is reflected in the outer wall and so for an infinite number of reflections. The reflection in each wall is performed so that the product of the radius of the vortex and the radius of its reflection is the square of the radius of the wall in which it is reflected.

The trailing vortices lie along stream lines and therefore wind downstream along the annulus in approximately helical paths. With a superimposed axial velocity equal to the axial velocity upstream at infinity this system will represent the flow through an annular cascade consisting of a large number of blades. The circulation on any stream surface downstream at infinity is equal to the circulation $Z\Gamma$ at the radius at which this stream surface passes through the blades. In Fig. 4A is illustrated the procedure

the circulation around each blade increases from a value Γ_b at the hub (inner wall). Each blade and its trailing vortices are represented by a bound vortex of circulation Γ_b extending from the axis radially to infinity, and a system of appropriate horseshoe vortices, each horseshoe vortex being of strength $d\Gamma/dr$ per unit radial length and combining with the bound vortex in the same manner to give the desired circulation. At the axis the bound vortex trails off downstream as above in order to represent the boundary conditions at the inner wall. In this example each of the existing trailing vortices is part of the horseshoe formed by reflecting it in the outer wall. This system is reflected in the inner wall, giving a system which in turn is reflected in the outer wall and so for an infinite number of reflections. The reflection in each wall is performed so that the product of the radius of the vortex and the radius of the reflection is the square of the radius of the wall to which it is reflected.

The trailing vortices lie along stream lines and therefore wind downstream along the annulus in approximately helical paths. With a superimposed axial velocity equal to the axial velocity upstream at infinite this system will represent the flow through an annular cascade consisting of a large number of blades. The circulation on any stream surface downstream at infinity is equal to the circulation $d\Gamma$ at the radius at which this stream surface passes through the blades. In fig. 4 is illustrated the procedure

for proving this. Along the path ABCDA in which AB and CD are adjacent stream surfaces and the flow through the circle ADA equals that through BCB the circulation enclosed is $Z\Gamma$. This may be demonstrated by developing the surface ABCD and noting that it encloses all the blades. Now if AB and CD are made practically identical stream lines the contribution to the circulation from AB cancels that from CD. There is no contribution from AD if this is located far upstream, hence the circulation enclosed by BC is equal to $Z\Gamma$. The picture of the flow in Fig. 3A clearly satisfies this since contributions from complete horseshoe vortices enclosed by BC cancel out and the circulation equals that of the axial trailing vortices and those horseshoe trailing vortices of which only one trailing portion is within the circuit BC.

Only one blade and its associated trailing vortices is shown in Fig. 3A. The boundary conditions at the annulus walls, however, are satisfied everywhere only by an infinite number of blades with this representation. For this case the flow is axially symmetric and the trailing vorticity is distributed throughout the flow field. The vortex lines following the stream lines may be regarded as distributed uniformly over stream surfaces coaxial with the annulus. Due to the effect of velocities induced by one vortex surface on the other such stream surfaces are not generally cylindrical except at large distances from the blades. The approximately helical vortices in each stream surface may be resolved into components

for proving this. Along the path ABCDE in which AB and CD are adjacent stream surfaces and the flow through the circle EFA equals that through ECD the circulation enclosed is 2Γ. This may be demonstrated by developing the surface ABCD and noting that it encloses all the blades. Now if AB and CD are made practically identical stream lines the contribution to the circulation from AB cancels that from CD. There is no contribution from AB if this is located far upstream, hence the circulation enclosed by BC is equal to 2Γ. The picture of the flow in Fig. 34 clearly satisfies this since contributions from complete horseshoe vortices enclosed by BC cancel out and the circulation equals that of the axial trailing vortices and these horseshoe trailing vortices of which only one trailing portion is within the circuit BC.

Only one blade and its associated trailing vortices is shown in Fig. 34. The boundary conditions at the annulus walls, however, are satisfied everywhere only by an infinite number of blades with this representation. For this case the flow is axially symmetric and the trailing vorticity is distributed throughout the flow field. The vortex lines following the stream lines may be regarded as distributed uniformly over stream surfaces coaxial with the annulus. Due to the effect of velocities induced by one vortex surface on the other each stream surface are not generally cylindrical except at large distances from the blades. The approximately helical vortices in each stream surface may be resolved into components

in the tangential direction and components following the stream surface in an almost axial direction. Hence, the trailing vortices may be considered as a system of ring (or smoke ring) vortices and a system of vortices following the generating lines of the stream surface.

The radial velocities are largely induced by the ring vortices, the contributions from the vortices following the generating lines being small due to their small components in the radial direction. At a large distance downstream from the blades the stream surfaces become concentric cylinders, the generating line vortices induce no radial velocities, and the radial velocities induced by an infinite set of ring vortices similar to those of Fig. 5A is zero.

If it is assumed that the radial velocities are so small that the trailing vortices lie on concentric cylindrical surfaces, the velocities induced in the plane of the blades may be compared with those induced downstream at infinity in the following manner (Reference 11). The axial components of the trailing vortices, Fig. 6A, being uniformly distributed over the surface of a cylinder induce only tangential velocity components and no radial or axial components. Since the bound vortices induce no velocities either in their plane or at infinity, the induced velocity at the plane of the blades due to the semi-infinite axial vortices is half that induced by this

in the tangential direction and components following the stream surface in an almost axial direction. Hence, the trailing vortices may be considered as a system of ring (or quasi ring) vortices and a system of vortices following the generating lines of the stream surface.

The radial velocities are largely induced by the ring vortices, the contributions from the vortices following the generating lines being small due to their small components in the radial direction. At a large distance downstream from the blades the stream surfaces become concentric cylinders, the generating line vortices induce no radial velocities, and the radial velocities induced by an infinite set of ring vortices similar to those of Fig. 54 is zero.

If it is assumed that the radial velocities are so small that the trailing vortices lie on concentric cylindrical surfaces, the velocities induced in the plane of the blades are to compared with those induced downstream at infinity in the following manner (Reference 11). The axial components of the trailing vortices, Fig. 54, being uniformly distributed over the surface of a cylinder induce only tangential velocity components and no radial or axial components. Since the bound vortices induce no velocities either in their plane or at infinity, the induced velocity at the plane of the blades due to the semi-infinite axial vortices is half that induced by this

vortex system at an infinite distance downstream. If C_{u_1} and C_{u_2} are the tangential velocities at infinite distance upstream and downstream of the blades respectively, the induced tangential velocity due to the axial components of the vortices trailing from the blades is $(C_{u_2} - C_{u_1})$. The induced velocity due to these components at the blades is $(C_{u_2} - C_{u_1})/2$ and the tangential velocity in the plane of the blades will be $C_{u_1} + (C_{u_2} - C_{u_1})/2 = (C_{u_2} + C_{u_1})/2$.

The radial velocities induced by the trailing ring vortices cancel out downstream at infinity. The velocities induced by two ring vortices equidistant from a plane perpendicular to the axis of the annulus is shown in Fig. 5A. These have equal circulations and hence by symmetry induce no radial component of velocity. At an infinite distance downstream the ring vortex system is composed of an infinite number of such pairs of vortex rings, and thus no radial velocities are induced. Each pair of vortices, however, induces an axial velocity which is just twice that induced by a single ring. At the plane of the blades the ring vortex system is made up of an infinite number of rings formed by only the downstream member of each pair, Fig. 5A. The axial velocity induced at the plane of the blades by the system of ring vortices in that case will be just half that induced at an infinite distance downstream. If C_{x_1} and C_{x_2} are the axial velocities at infinite distances upstream and downstream of the blades respectively, the axial velocity induced by the ring vortices downstream at infinity will be $C_{x_2} - C_{x_1}$ and that induced

vortex system at an infinite distance downstream. If C_{u_1} and C_{u_2} are the tangential velocities at infinite distance upstream and downstream of the blades respectively, the induced tangential velocity due to the axial components of the vortices trailing from the blades is $(C_{u_2} - C_{u_1})$. The induced velocity due to these components at the blades is $(C_{u_2} - C_{u_1})/2$ and the tangential velocity in the plane of the blades will be $C_{u_1} + (C_{u_2} - C_{u_1})/2 = (C_{u_2} + C_{u_1})/2$.

The radial velocities induced by the trailing ring vortices cancel out downstream at infinity. The velocities induced by two ring vortices equidistant from a plane perpendicular to the axis of the annulus is shown in Fig. 5b. These have equal circulations and hence by symmetry induce no radial component of velocity. At an infinite distance downstream the ring vortex system is composed of an infinite number of such pairs of vortex rings, and thus no radial velocities are induced. Each pair of vortices, however, induces an axial velocity which is just twice that induced by a single ring. At the plane of the blades the ring vortex system is made up of an infinite number of rings formed by only the downstream member of each pair, Fig. 5a. The axial velocity induced at the plane of the blades by the system of ring vortices in that case will be just half that induced at an infinite distance downstream. If C_{z_1} and C_{z_2} are the axial velocities at infinite distance upstream and downstream of the blades respectively, the axial velocity induced by the ring vortices downstream at infinity will be $C_{z_2} - C_{z_1}$ and that induced

in the plane of the blades is $(C_{x_2} - C_{x_1})/2$. The axial velocity at the blades is, therefore, $C_{x_1} + (C_{x_2} - C_{x_1})/2 = (C_{x_2} + C_{x_1})/2$.

in the plane of the blades is $(\Omega r_2 - \Omega r_1)/2$. The axial velocity at the blades is, therefore, $\Omega r + (\Omega r_2 - \Omega r_1)/2 = (\Omega r_2 + \Omega r_1)/2$.

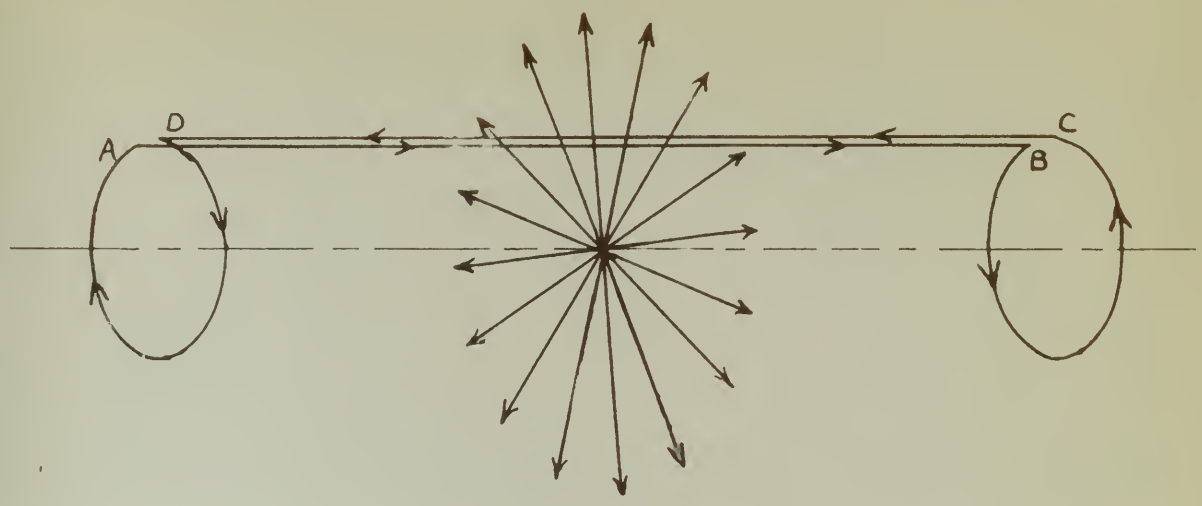

FIG 1A. VORTEX REPRESENTATION OF CASCADE DESIGNED TO GIVE FREE VORTEX FLOW.

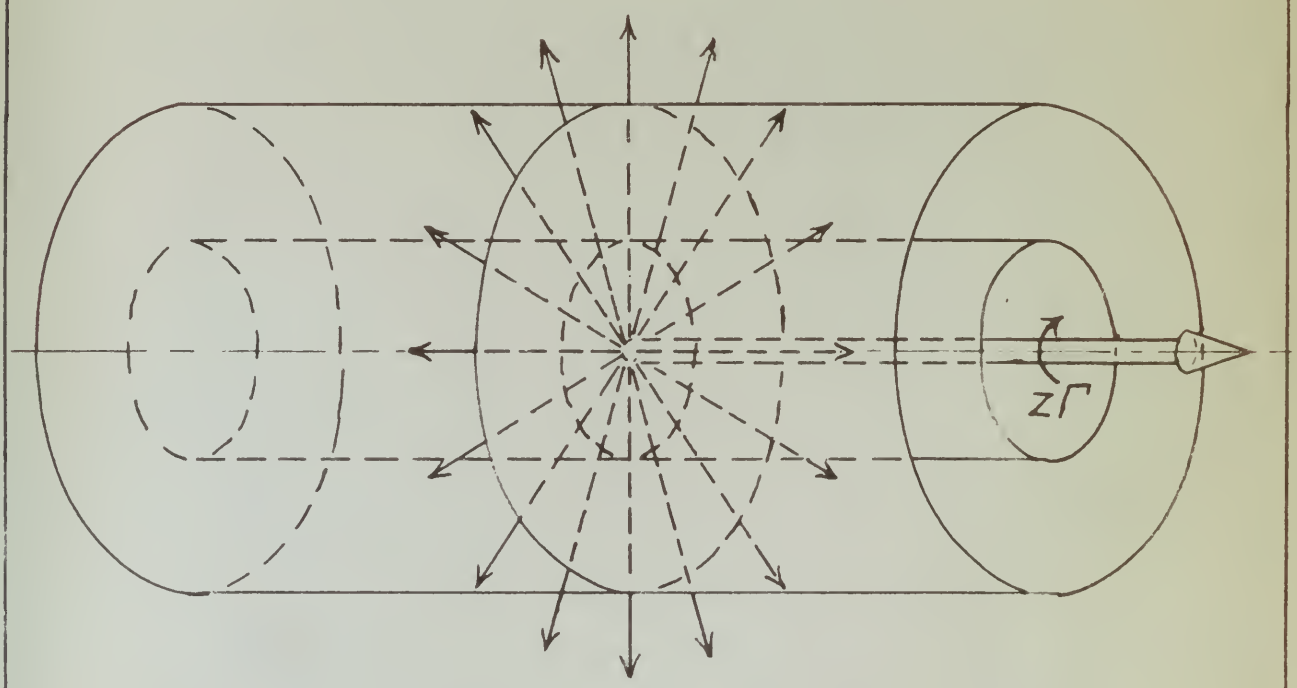

FIG 2A. VORTEX REPRESENTATION OF FREE VORTEX CASCADE IN AN ANNULUS.

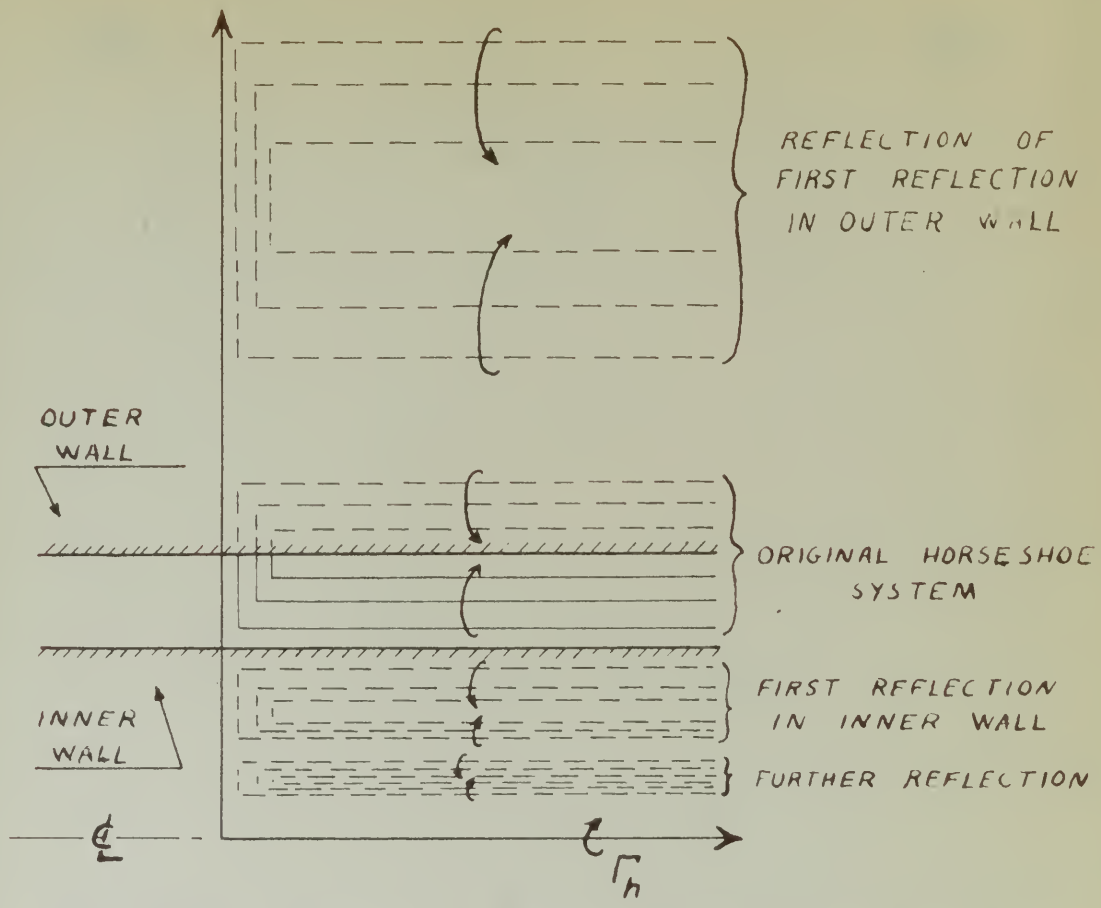

FIG. 3A. CASCADE BLADE WITH CIRCULATION INCREASING TOWARD TIP

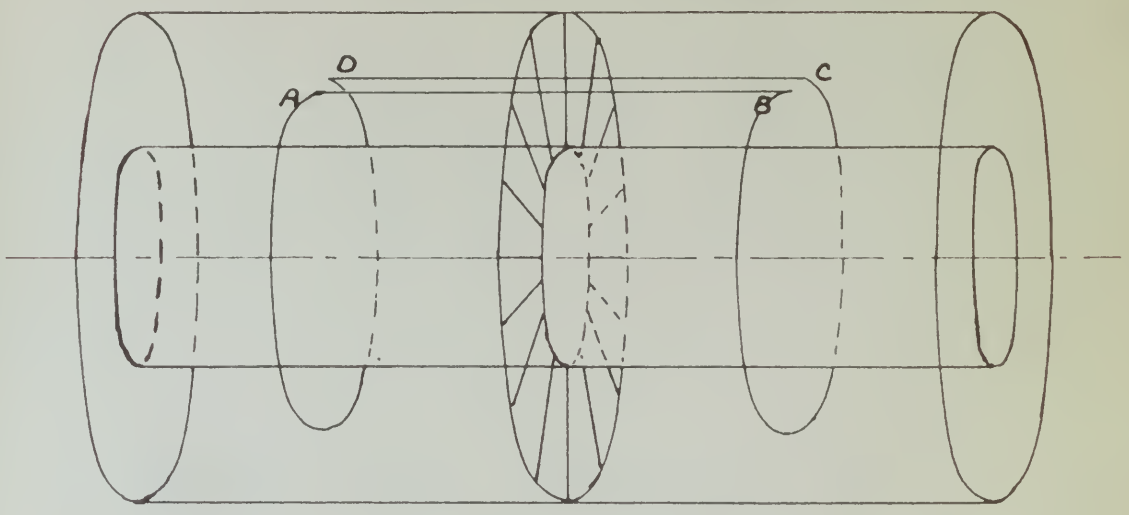

FIG. 4A. STREAM SURFACE IN AN ANNULUS WITH AN ANNULAR CASCADE

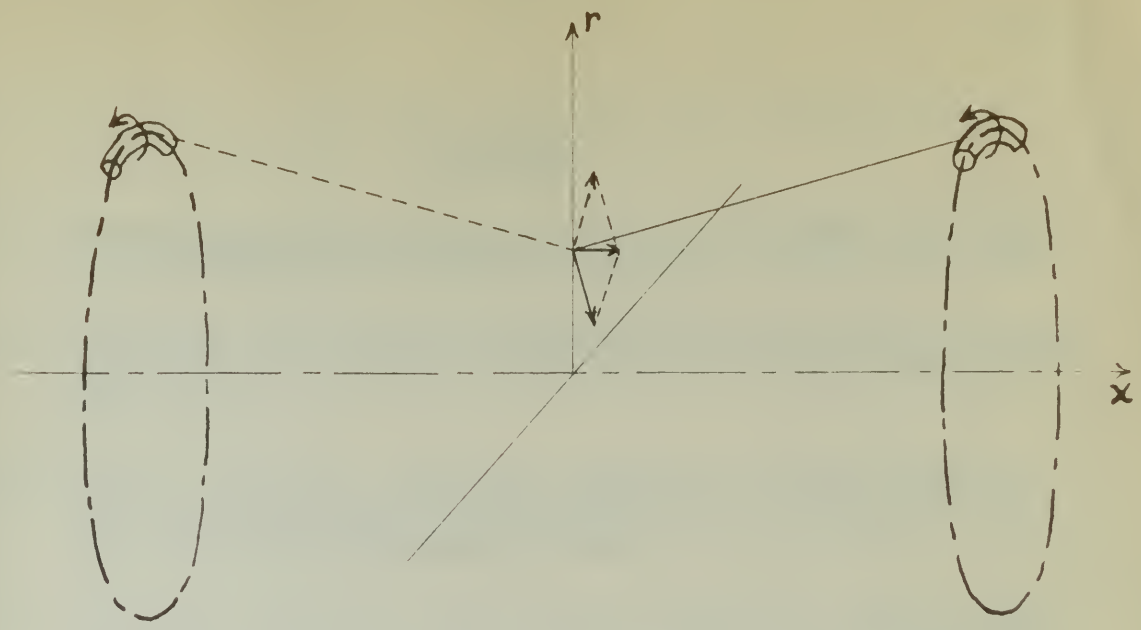

FIG. 5A. RING COMPONENTS OF TRAILING VORTICES

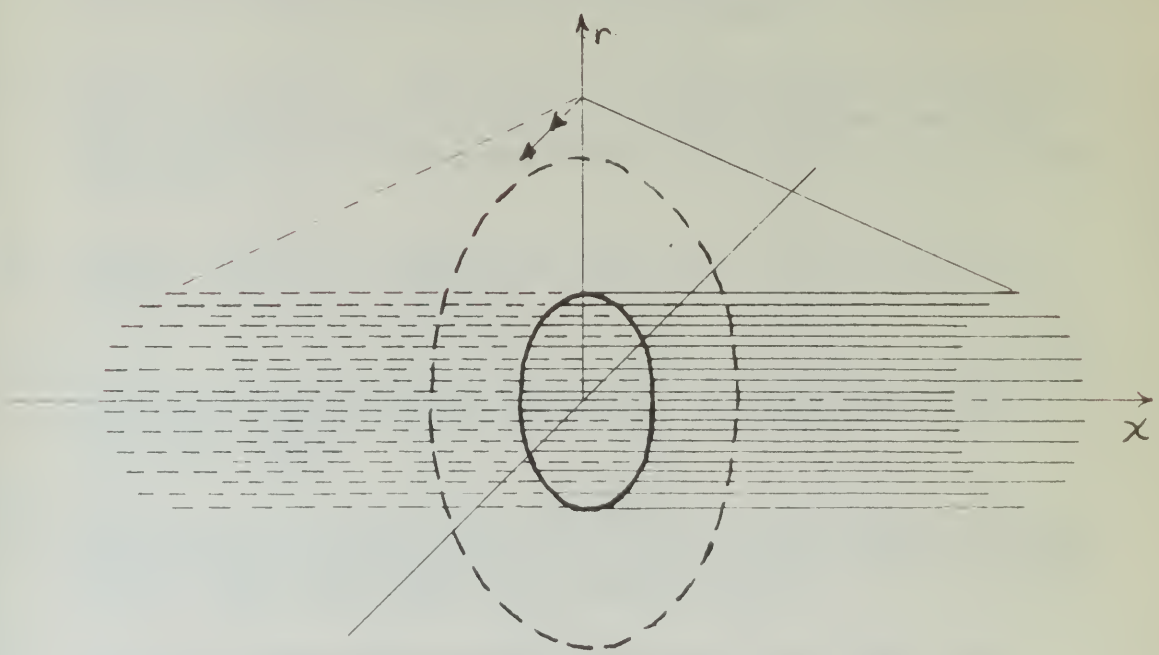

FIG 6A. AXIAL COMPONENTS OF TRAILING VORTICES

REFERENCES

1. Kantrowitz, Arthur, and Daum, Fred L.: Preliminary Experimental Investigation of Airfoils in Cascade. NACA CB, July 1942.

2. Bogdonoff, Seymour M., and Bogdonoff, Harriet E.: Blade Design Data for Axial Flow Fans and Compressors. NACA WR L-635, July 1945.

3. Zimney, Charles M., and Lappi, Viola M.: Data for Design of Entrance Vanes from Two-Dimensional Tests of Airfoils in Cascade. NACA WR-L5G18, October 1945.

4. Bogdonoff, Seymour M.: NACA Cascade Design Data for the Blade Design of High Performance Axial Flow Compressors. Journal of Aeronautical Sciences, February 1948.

5. Rouse, Hunter: Elementary Mechanics of Fluids. John Wiley and Sons, New York, 1946.

6. Eckert, B., and Pfluger, F.: The Resistance Coefficient of Round Wire Grids. NACA TM-1003 (Translation).

7. Jacobs, Eastman N., Ward, Kenneth E., and Pinkerton, Robert M.: The Characteristics of 78 Related Airfoil Sections from Tests in the Variable-Density Wind Tunnel. NACA Rept. No. 460, November 1933.

8. Diehl, Walter S.: Engineering Aerodynamics (Revised Edition), Ronald Press, New York, 1941.

9. Howell, A.R.: Cascade Theory and Performance (Part I); Compressor Theory and Performance (Part II). RAE Rept. Nos. E3946, and E3961, 1942.

10. Carter, A. D. S., and Cohen, Elizabeth M.: Preliminary Investigation into the Three Dimensional Flow through a Cascade of Airfoils. Power Jets Rept. R1180, February 1946.

11. Ruden, P.: Investigation of Single Stage Axial Fans. NACA TM-1062, 1944.

REFERENCES

1. Kantrowitz, Arthur, and Laus, Fred L.: Preliminary Experimental Investigation of Airfoils in Cascade. NACA CB, July 1942.

2. Hogdonoff, Seymour M., and Hogdonoff, Harriet P.: Blade Design Data for Axial Flow Fans and Compressors. NACA TN L-635, July 1945.

3. Blaney, Charles M., and Lapp, Viola M.: Data for Design of Entrance Vanes from Two-Dimensional Tests of Airfoils in Cascade. NACA WR-L9G10, October 1945.

4. Hogdonoff, Seymour M.: NACA Cascade Design Data for the Blade Design of High Performance Axial Flow Compressors. Journal of Aeronautical Sciences, February 1948.

5. Rouse, Hunter: Elementary Mechanics of Fluids. John Wiley and Sons, New York, 1946.

6. Eckert, M., and Pfluger, F.: The Resistance Coefficient of Round Wire Grids. NACA TM-1003 (Translation).

7. Jacobs, Eastman N., Ward, Kenneth E., and Pinkerton, Robert M.: The Characteristics of 78 Related Airfoil Sections from Tests in the Variable-Density Wind Tunnel. NACA Rept. No. 460, November 1933.

8. Diehl, Walter S.: Engineering Aerodynamics (Revised Edition), Ronald Press, New York, 1941.

9. Covell, A.D.: Cascade Theory and Performance (Part I); Compressor Theory and Performance (Part II). NAS Rept. Nos. E7946, and E7961, 1943.

10. Carter, A. D. S., and Cohen, Elizabeth W.: Preliminary Investigation into the Three Dimensional Flow through a Cascade of Airfoils. Power Jets Rept. R1100, February 1944.

11. Ruden, P.: Investigation of Single Stage Axial Fans. NACA TM-1062, 1944.

12. Hawthorne, W. R.: MIT Lecture Notes, Gas Turbines, Subject 2.213 (1948-49).

13. Sproule, Robert S.: Design of a Cascade Test Rig. S.M. Thesis, M.I.T. Department of Mechanical Engineering, 1947.

14. Merchant, W., and Hansford, J. T.: Flow of an Ideal Fluid Past a Cascade of Blades. Metropolitan-Vickers Ltd. Summary Report, June 1945.

15. Carter, A. D. S.: Three-Dimensional Flow Theories for Axial Compressors and Turbines. The Institution of Mechanical Engineers, Proceedings 1948, Vol. 159.

12. Southerne, F. C.: [illegible], Sea Vertebrae, Subject [illegible] (1946-47).

13. Wrobel, Robert G.: Design of a Cascade Test Rig, [illegible], M.I.T. Department of Mechanical Engineering, 1957.

14. Hartman, J., and Hartman, J. T.: Flow of an Ideal Fluid Past a Cascade of Blades. Aeropolitan-Thesis 118. Summer Report, June 1948.

15. Barton, J. G. C.: Terms-Dimensional Flow Theories for Axial Compressors and Turbines. The Institution of Mechanical Engineers, Proceedings 1949, Vol. 158.

TABLE I

Ordinates of Mean Camber Line -

Blade Sections - Cascade B

	R			
	1.0	.9	.7	.5
	27.°	22.4°	13.2°	4.°
c in.	2.000	1.875	1.625	1.375
Sta. % c.	Ordinates of Mean Camber Line			
0	0	0	0	0
1.25	1.38	1.01	.81	.55
2.50	2.59	1.90	1.53	1.04
5.00	4.56	3.36	2.69	1.82
7.50	6.02	4.43	3.55	2.40
10.	7.16	5.27	4.24	2.86
15.	8.82	6.50	3.84	3.53
20.	9.98	7.34	5.90	3.98
25.	10.90	8.02	6.45	4.36
30.	11.55	8.50	6.77	4.62
35.	11.95	8.80	7.06	4.79
40.	12.10	8.90	7.15	4.84
45.	12.06	8.87	7.12	4.82
50.	11.88	8.72	7.01	4.75
55.	11.42	8.41	6.75	4.57
60.	10.75	7.90	6.35	4.30
65.	9.83	7.24	5.81	3.94
70.	8.71	6.45	5.14	3.48
75.	7.57	5.57	4.48	3.03
80.	6.37	4.68	3.76	2.54
85.	5.01	3.69	2.96	2.01
90.	3.49	2.57	2.06	1.40
95.	1.80	1.32	1.06	.72
100.	0	0	0	0

All ordinates measured from chord line in percent of chord.

Table I

Relative Age of Some Cooper Ships -

Birth Stations - Tables I, II

Sta. | [illegible] | [illegible] | [illegible] | [illegible]

Sta. | [illegible] | [illegible] | [illegible] | [illegible]

[illegible]	[illegible]	[illegible]	[illegible]	[illegible]

TABLE II

Ordinates of Blade Sections -

Cascade B

R

Sta.	1.0		.9		.7		.5	
% c.	Upper	Lower	Upper	Lower	Upper	Lower	Upper	Lower
0	.037	.000	.025	.000	.019	.000	.017	-.000
1.25	.079	-.004	.051	-.006	.044	-.008	.032	-.010
2.50	.111	+.010	.074	+.002	.064	-.007	.047	-.011
5.00	.156	.032	.112	.016	.094	-.003	.066	-.010
10.	.224	.069	.165	.036	.132	+.006	.091	-.009
20.	.295	.111	.222	.058	.173	.022	.119	-.006
30.	.333	.135	.251	.070	.193	.032	.132	-.004
40.	.343	.145	.260	.078	.198	.038	.134	-.001
50.	.328	.144	.249	.081	.188	.041	.128	+.001
60.	.292	.136	.221	.078	.166	.040	.112	.003
70.	.237	.117	.180	.068	.136	.037	.092	.004
80.	.168	.086	.129	.049	.098	.026	.066	.002
90.	.090	.043	.070	.024	.054	.011	.039	-.002
95.	.049	.019	.040	.008	.032	.002	.024	-.005
100.	.008	-.009	.008	-.009	.008	-.009	.008	-.008
LER.	.022		.021		.018		.016	
TER.	.015		.015		.015		.015	

All ordinates measured in inches from chord line.

TABLE II

Ordinates of Blade Sections -

Canada E

Pos. % c.	1.0 Upper	1.0 Lower	.9 Upper	.9 Lower	.7 Upper	.7 Lower	.5 Upper	.5 Lower
0	.037	.000	.025	.000	.028	.000	.017	-.000
1.25	.079	-.004	.032	-.000	.044	-.002	.028	-.010
2.50	.111	+.010	.074	+.000	.084	-.007	.047	-.017
5.00	.156	.032	.112	.016	.114	-.003	.064	-.024
10.	.224	.009	.165	.039	.162	+.004	.091	-.037
20.	.295	.111	.229	.050	.203	.002	.119	-.049
30.	.333	.135	.231	.070	.201	.002	.132	-.004
40.	.343	.145	.208	.078	.198	.034	.134	-.001
50.	.328	.144	.209	.084	.186	.001	.128	+.001
60.	.292	.134	.201	.076	.166	.010	.112	.003
70.	.237	.117	.180	.064	.134	.037	.082	.004
80.	.168	.088	.129	.043	.098	.028	.048	.012
90.	.090	.043	.070	.024	.054	.011	.039	-.002
95.	.043	.010	.040	.006	.070	.002	.004	-.005
100.	.008	-.009	.008	-.009	.008	-.009	.008	-.002
[illegible]	.023		.023		.018		.018	
[illegible]	.015		.015		.015		.015	

All ordinates measured in inches from chord line.

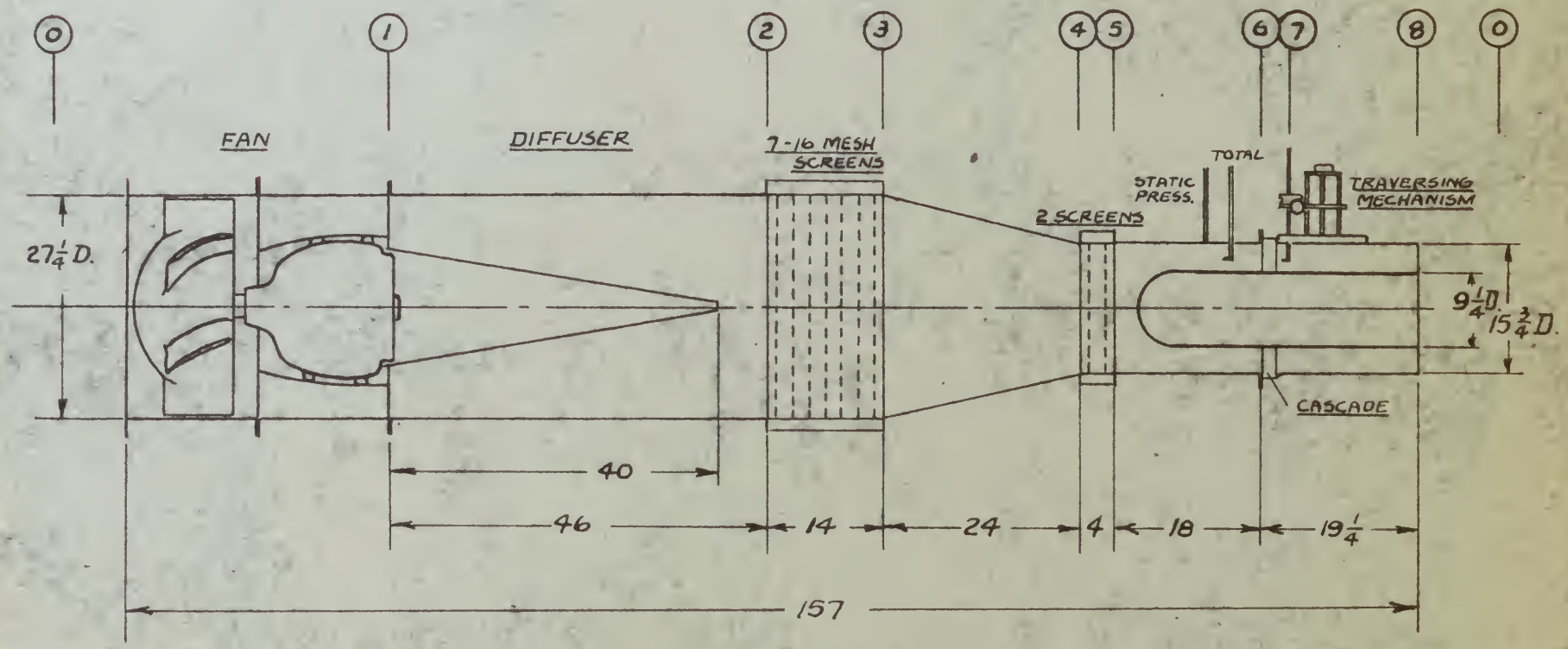

MIT LOW SPEED ANNULAR CASCADE TUNNEL

GENERAL ARRANGEMENT AND DIMENSIONS

4-25-49

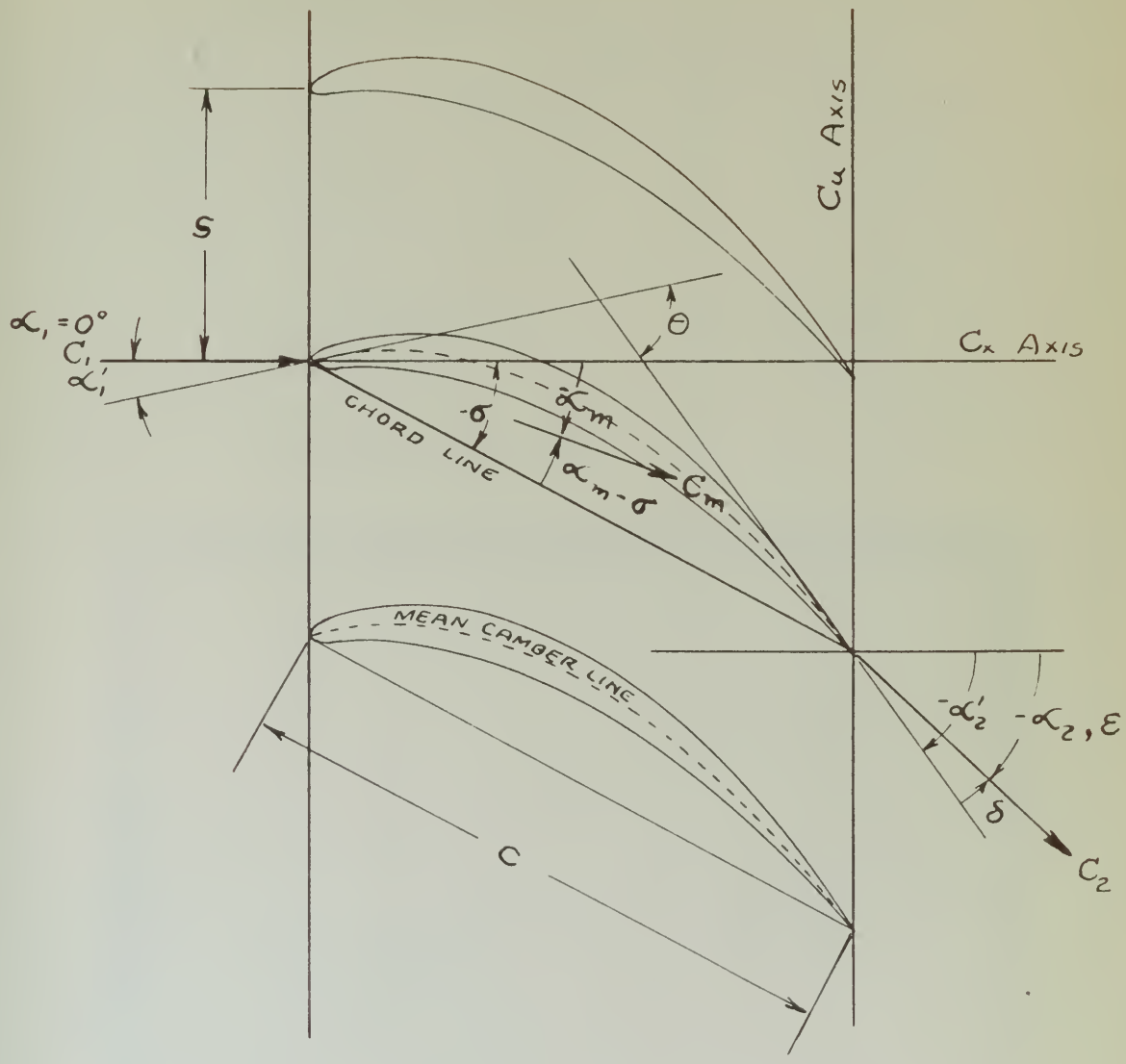

CASCADE NOMENCLATURE

INLET GUIDE VANE

5 5 49

CASCADE A

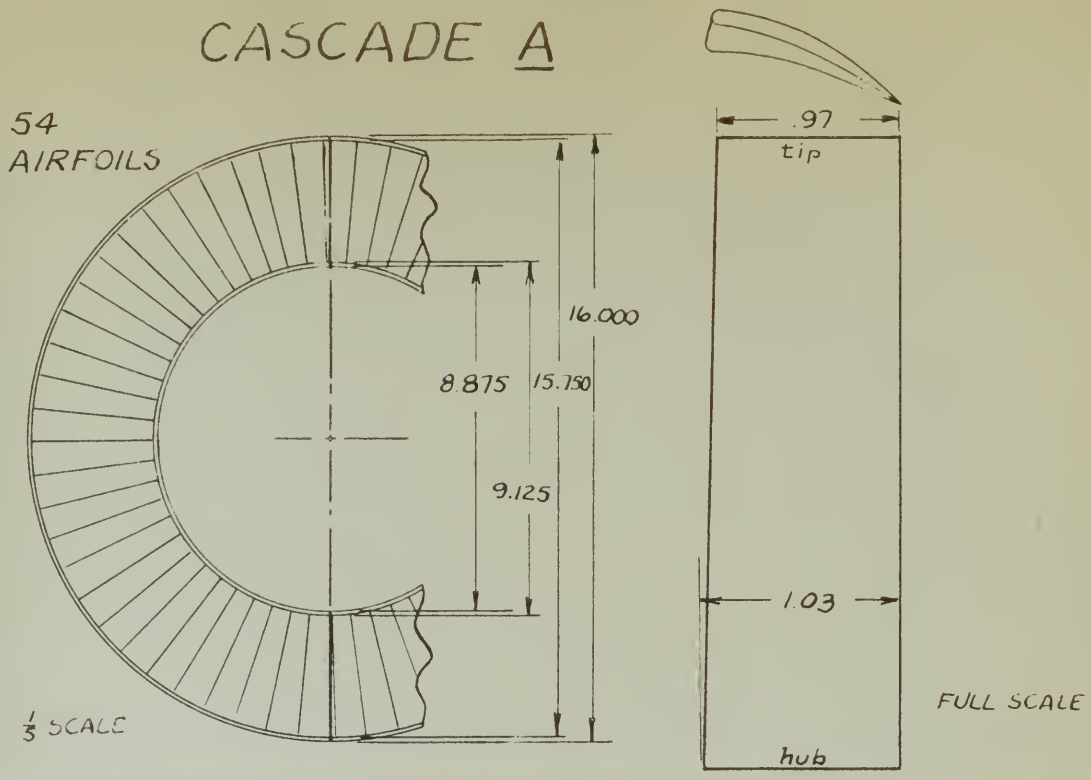
54
AIRFOILS
16.000
8.875
15.750
9.125
1/3 SCALE
.97
tip
1.03
hub
FULL SCALE

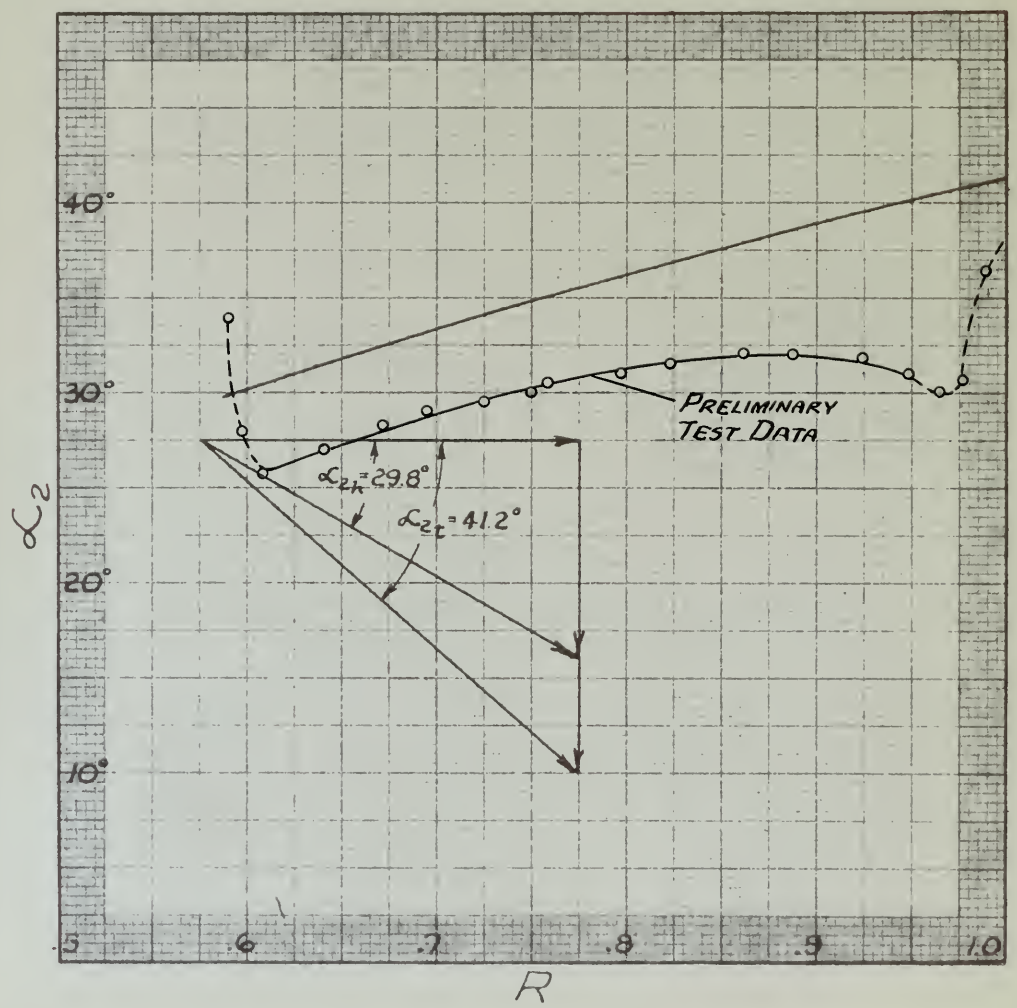
40°
30°
20°
10°
α_2
.5
.6
.7
.8
.9
1.0
R
PRELIMINARY
TEST DATA
α_{2h}=29.8°
α_{2t}=41.2°

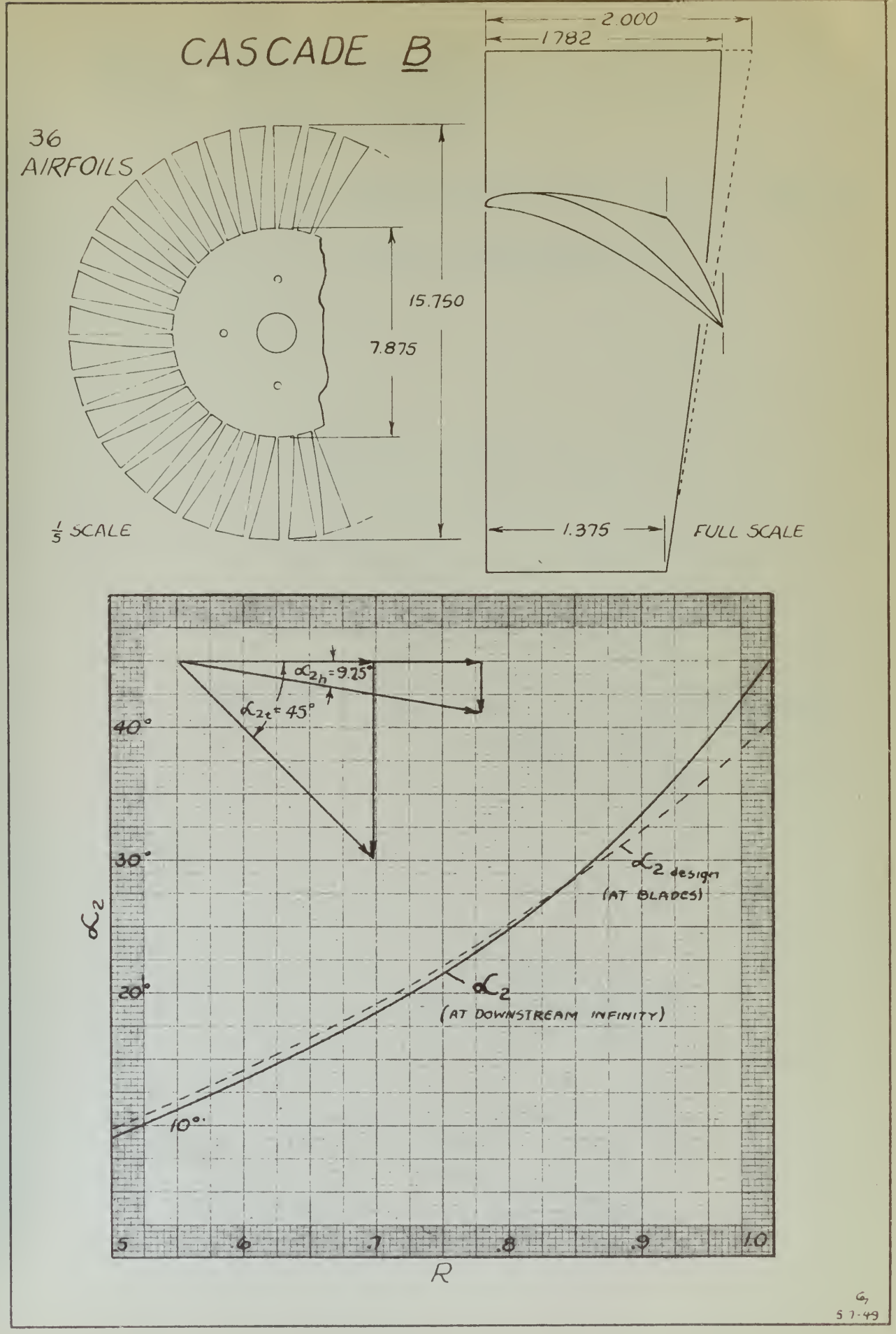
CASCADE B
36 AIRFOILS
15.750
7.875
1/5 SCALE
2.000
1.782
1.375
FULL SCALE
α_{2h} = 9.25°
α_{2t} = 45°
40°
30°
20°
10°
α_2
α_2 design (AT BLADES)
α_2 (AT DOWNSTREAM INFINITY)
.5
.6
.7
.8
.9
1.0
R
G
5-7-49

Figure 4

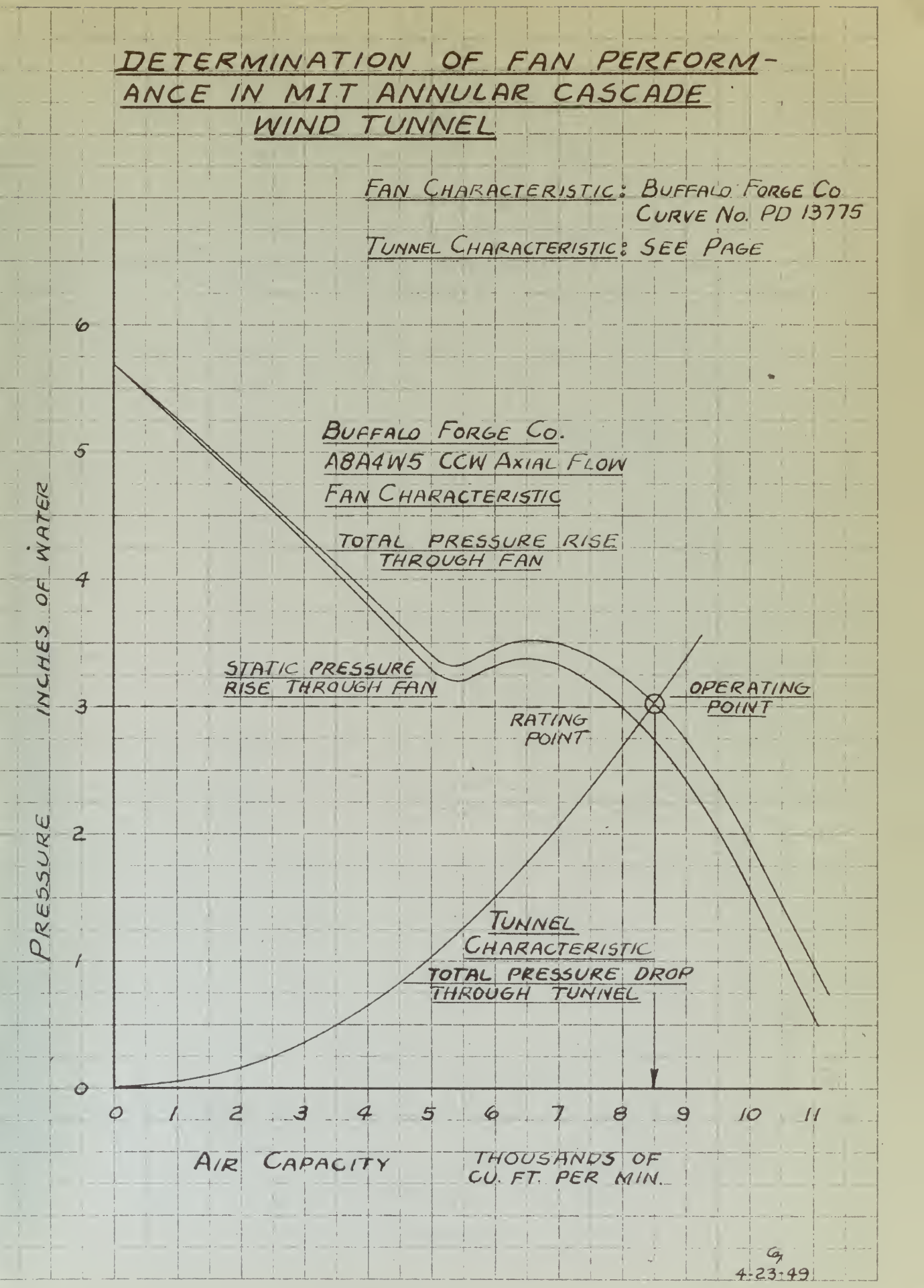
DETERMINATION OF FAN PERFORMANCE IN MIT ANNULAR CASCADE WIND TUNNEL
FAN CHARACTERISTIC: BUFFALO FORGE CO CURVE NO. PD 13775
TUNNEL CHARACTERISTIC: SEE PAGE
BUFFALO FORGE CO.
A8A4W5 CCW AXIAL FLOW
FAN CHARACTERISTIC
TOTAL PRESSURE RISE THROUGH FAN
STATIC PRESSURE RISE THROUGH FAN
OPERATING POINT
RATING POINT
TUNNEL CHARACTERISTIC
TOTAL PRESSURE DROP THROUGH TUNNEL
PRESSURE INCHES OF WATER
0
1
2
3
4
5
6
0
1
2
3
4
5
6
7
8
9
10
11
AIR CAPACITY THOUSANDS OF CU. FT. PER MIN.
4-23-49

Figure 5

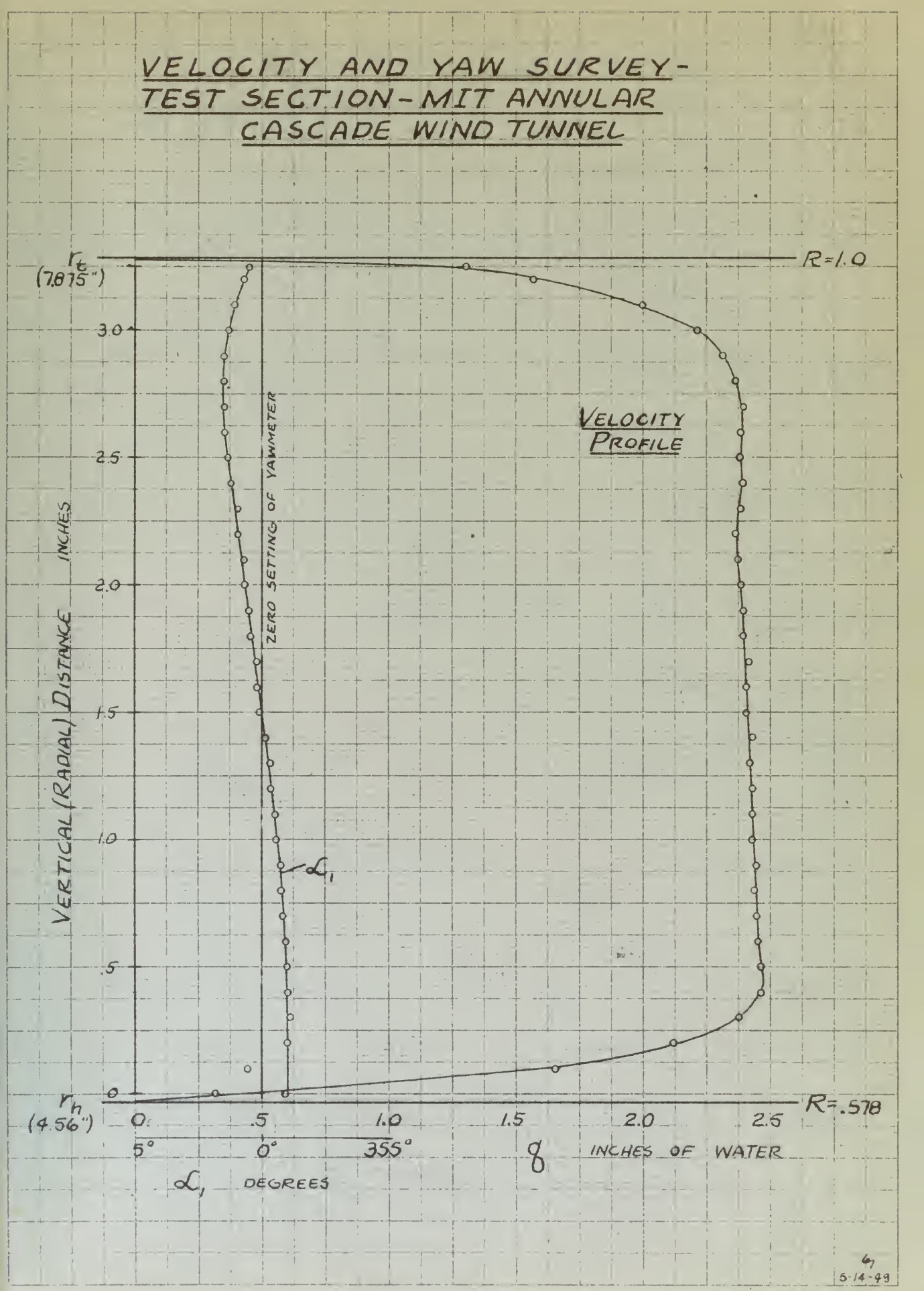
VELOCITY AND YAW SURVEY-
TEST SECTION-MIT ANNULAR
CASCADE WIND TUNNEL
r_t
(7.875")
R=1.0
3.0
2.5
2.0
1.5
1.0
.5
0
r_h
(4.56")
R=.578
VERTICAL (RADIAL) DISTANCE INCHES
ZERO SETTING OF YAWMETER
VELOCITY PROFILE
α_1
0
.5
1.0
1.5
2.0
2.5
5°
0°
355°
α_1 DEGREES
q INCHES OF WATER
4
5-14-49

Figure 6

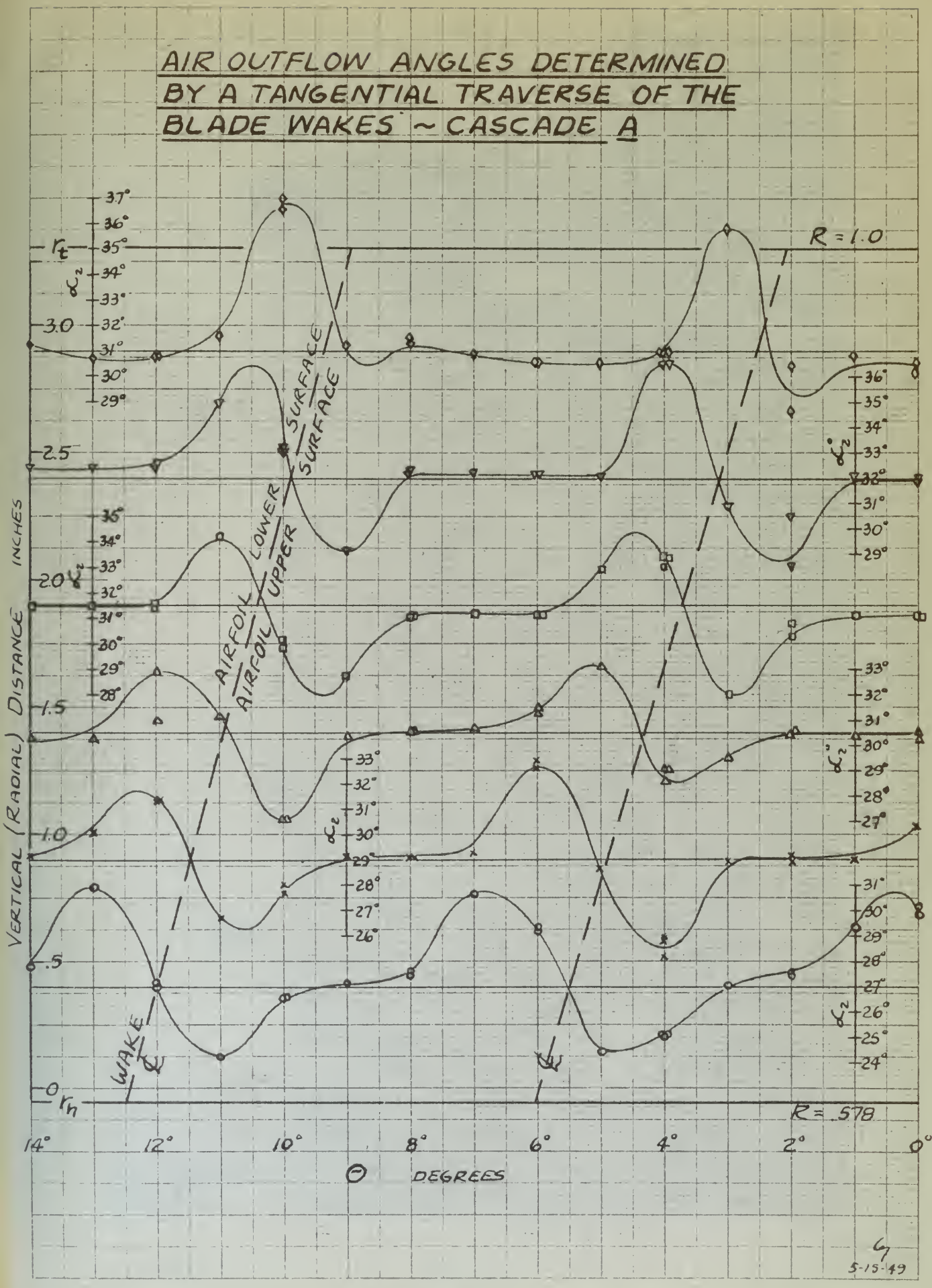
AIR OUTFLOW ANGLES DETERMINED BY A TANGENTIAL TRAVERSE OF THE BLADE WAKES ~ CASCADE A
R = 1.0
R = .578
SURFACE
SURFACE
LOWER
UPPER
AIRFOIL
AIRFOIL
WAKE
VERTICAL (RADIAL) DISTANCE INCHES
θ DEGREES
5-15-49

Figure 7

Annular Cascade Tunnel -- Overall View

Figure 8

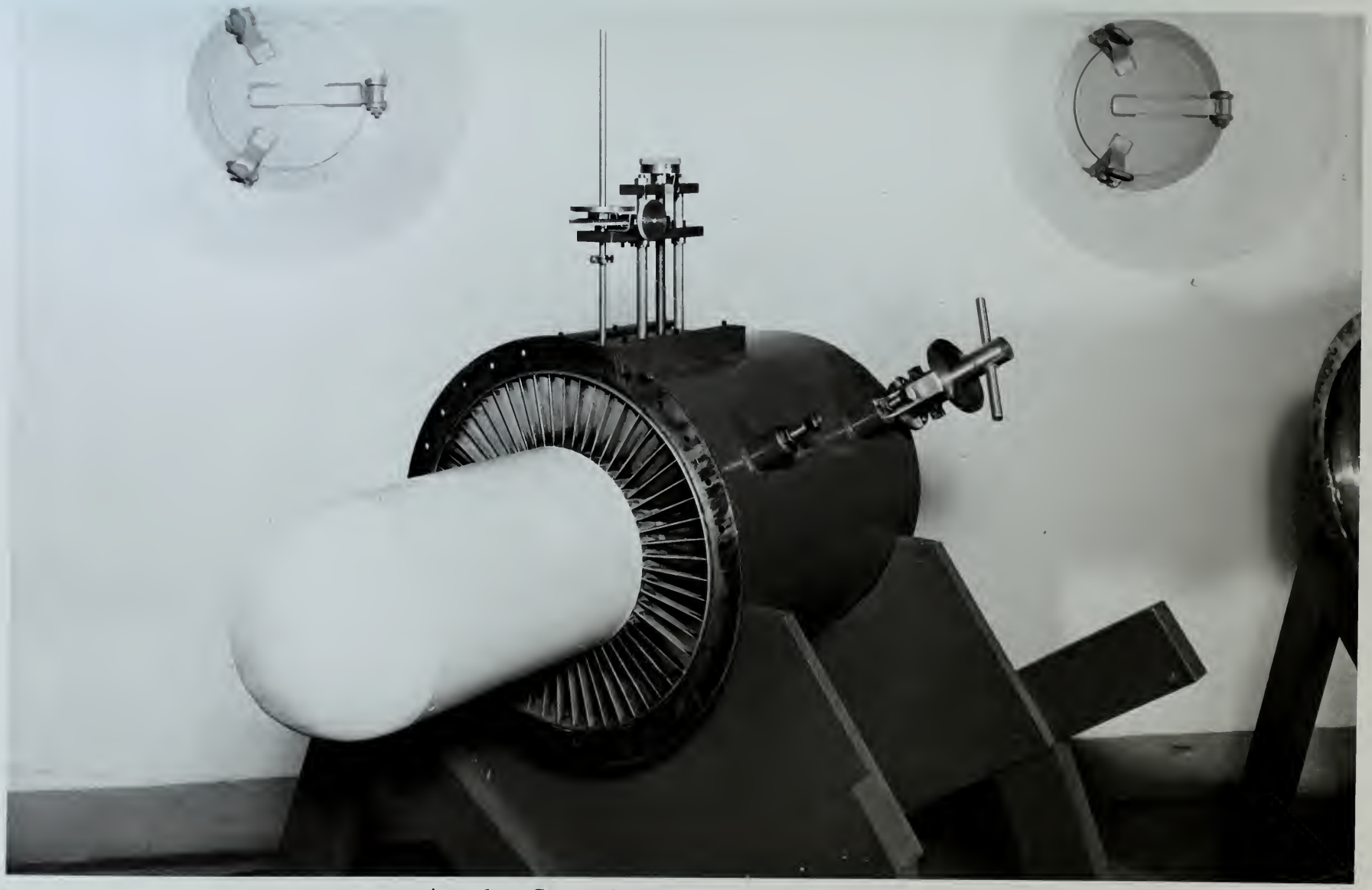

Annular Cascade Tunnel -- Test Section
Three Quarter Front View

Figure 9

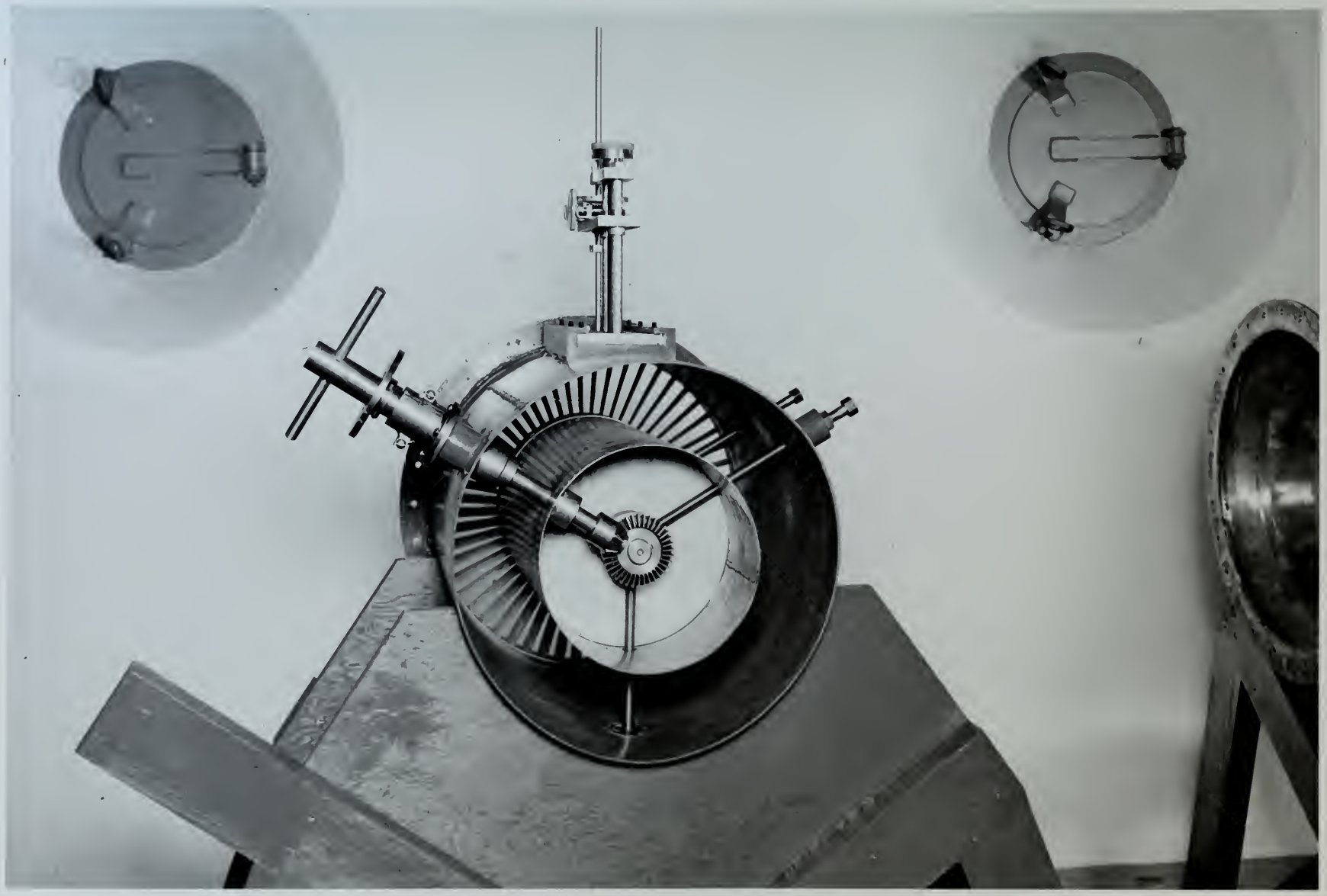

Annular Cascade Tunnel -- Test Section
Three Quarter Rear View

Figure 10

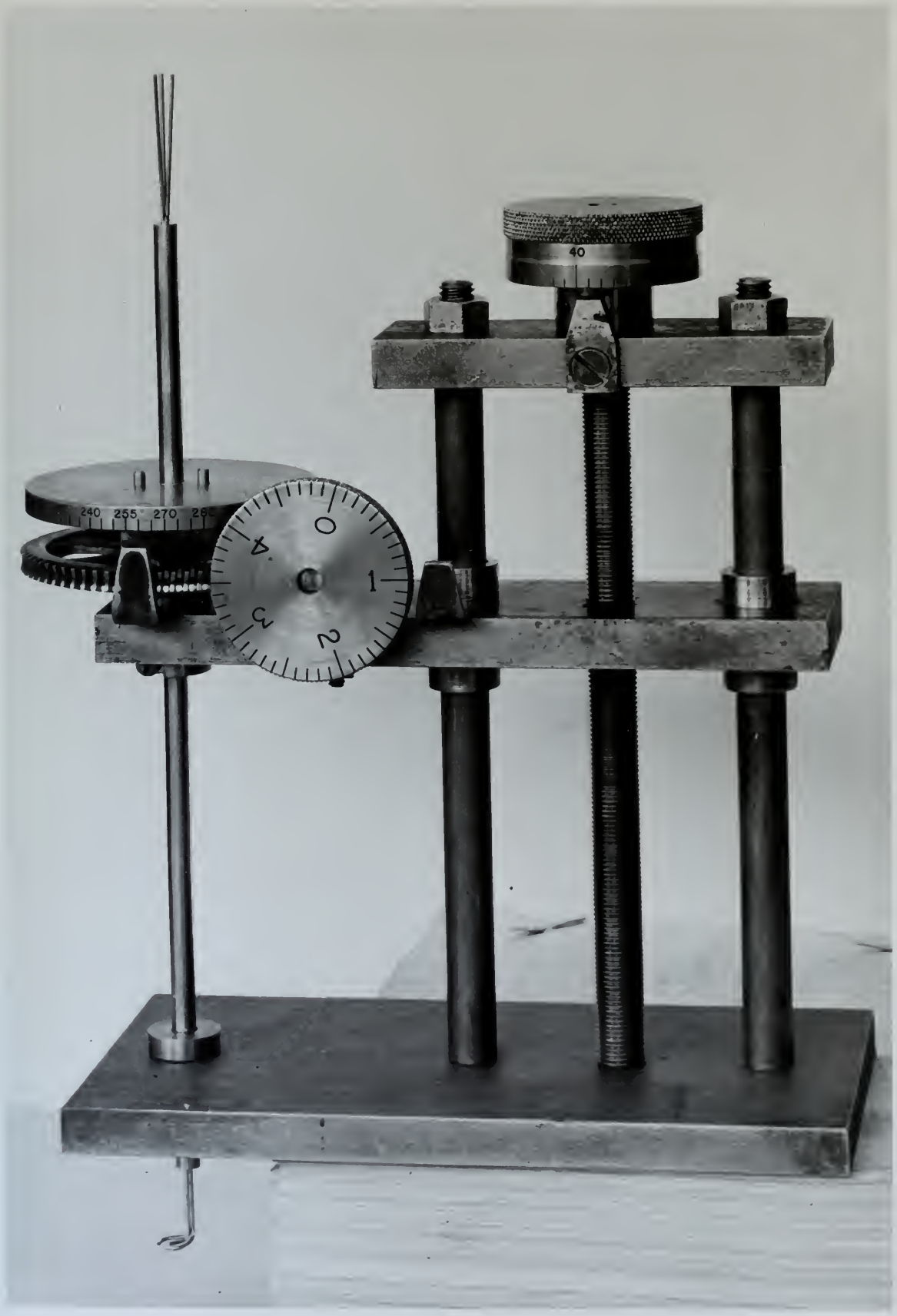

Traversing Mechanism -- Showing Claw-Type Yaw Head

Figure 11

NOTE
PRESS FIT IN
PIECE N-1214
AFTER ASSEMBLY

NO.	MATERIAL BRONZE	NO. REQ. 1

MASSACHUSETTS INSTITUTE OF TECHNOLOGY

GAS TURBINE LABORATORY

BEARING SLEEVE

DRAWN BY Gy	DATE 2-17-49
CHECKED BY	SCALE FULL
NEXT ASSEM.	N-1210

NO.	MATERIAL	NO. REQ.
1	STL	1

MASSACHUSETTS INSTITUTE OF TECHNOLOGY

GAS TURBINE LABORATORY

COLLAR

DRAWN BY Ca	DATE 2-19-49
CHECKED BY	SCALE FULL
HERE ASSEM.	N - 1211

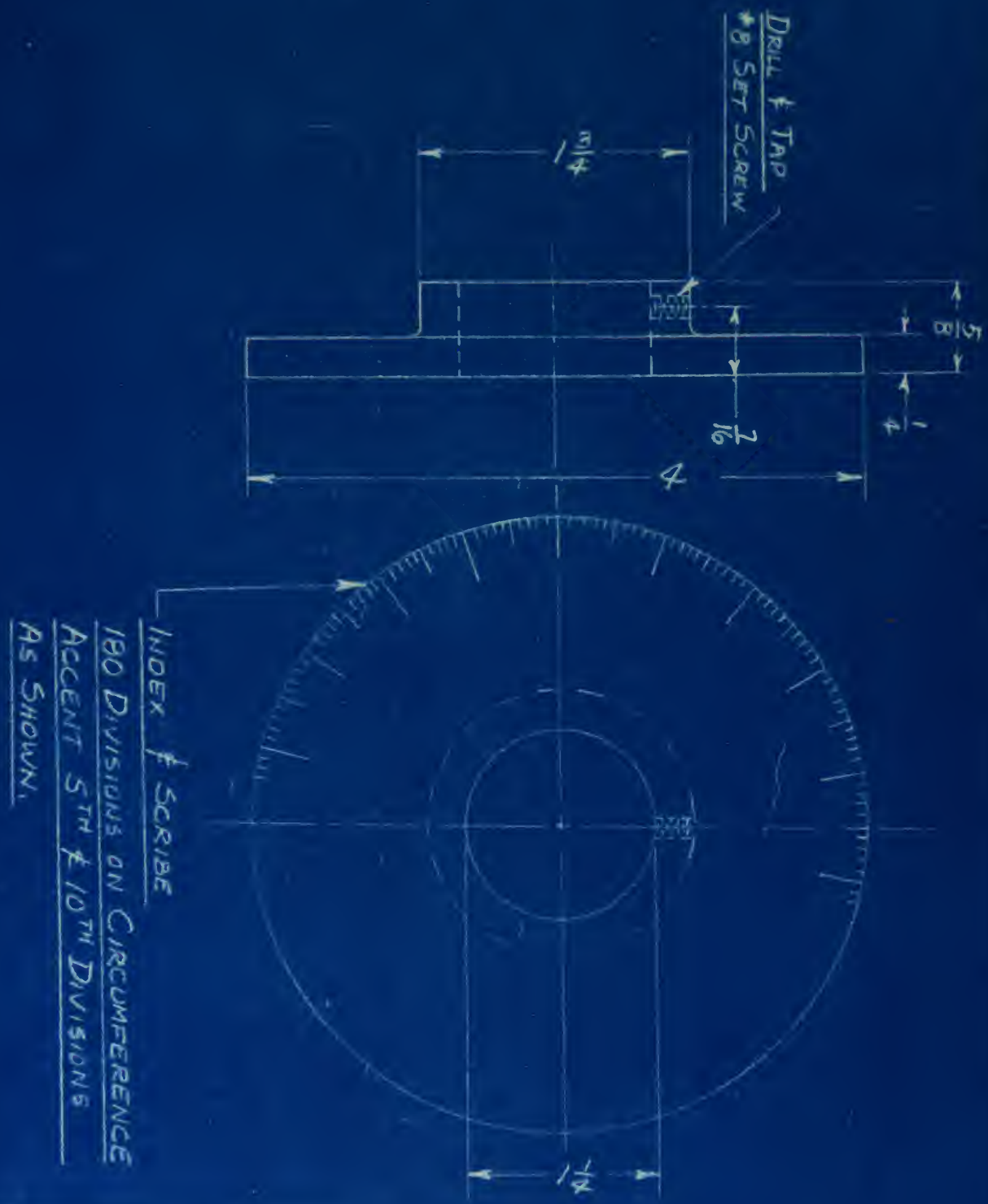

NO	MATERIAL	NO REQ
1	STL	1

MASSACHUSETTS INSTITUTE OF TECHNOLOGY

GAS TURBINE LABORATORY

QUADRANT

2-19-49 FULL SCALE

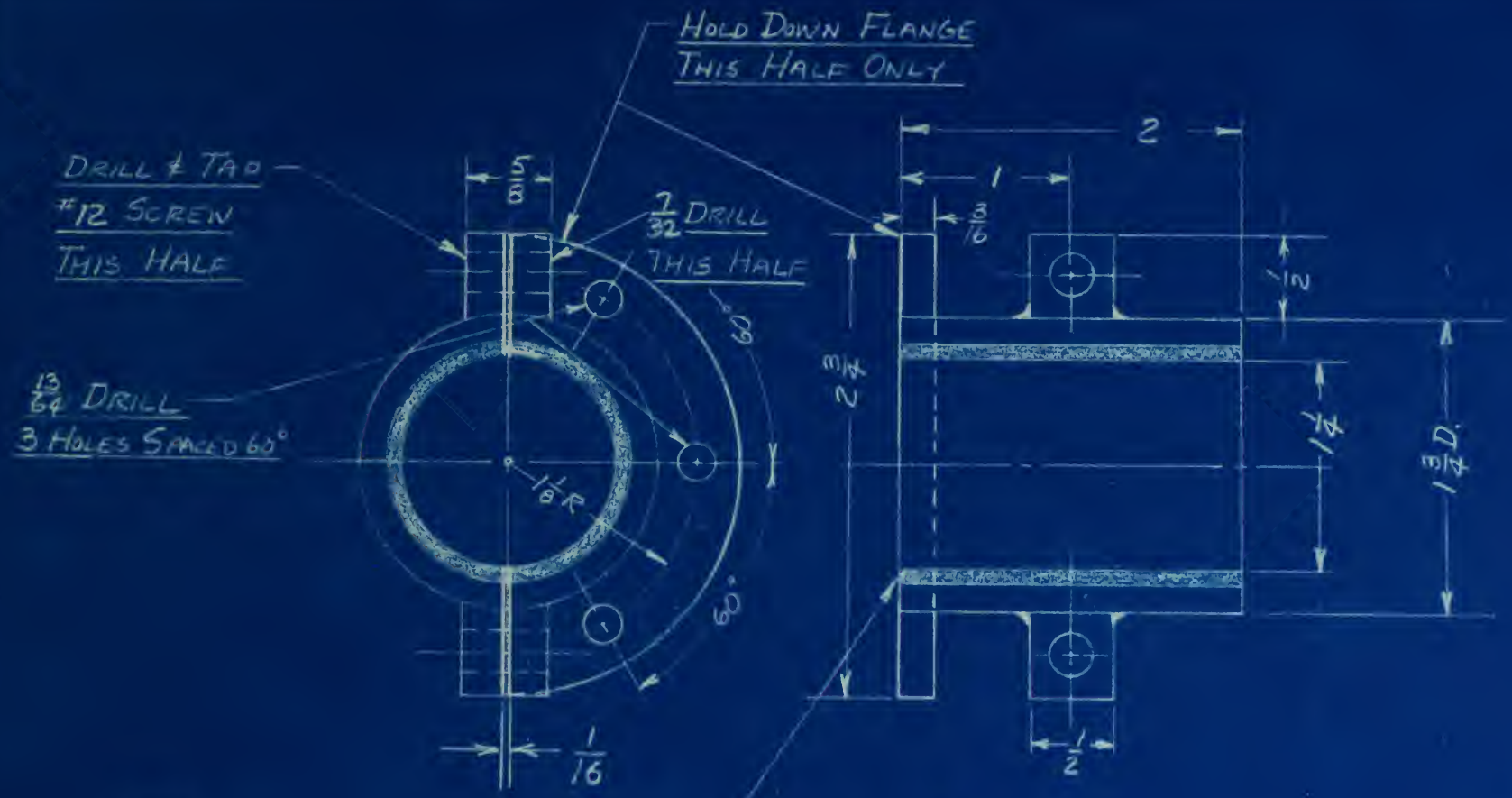

NOTE:
WELD LUGS TO SHELL
BEFORE SPLITTING SHELL

BRAKE LINING
OR SIMILAR MAT'L - 3/32 APPROX.
RIVET TO SHELL - FLUSH INSIDE

TWO HALVES
REQ'D

FULL SCALE

NOTE:
TEST AFTER ASSEMBLY
CLAMP MUST RESIST 150 INCH-POUNDS
OF TORQUE ON 1 1/4" SHAFT

NO.	MATERIAL STL.	NO. REQ
MASSACHUSETTS [illegible] TECHNOLOGY		
GAS TURBINE LABORATORY		
FRICTION CLAMP		

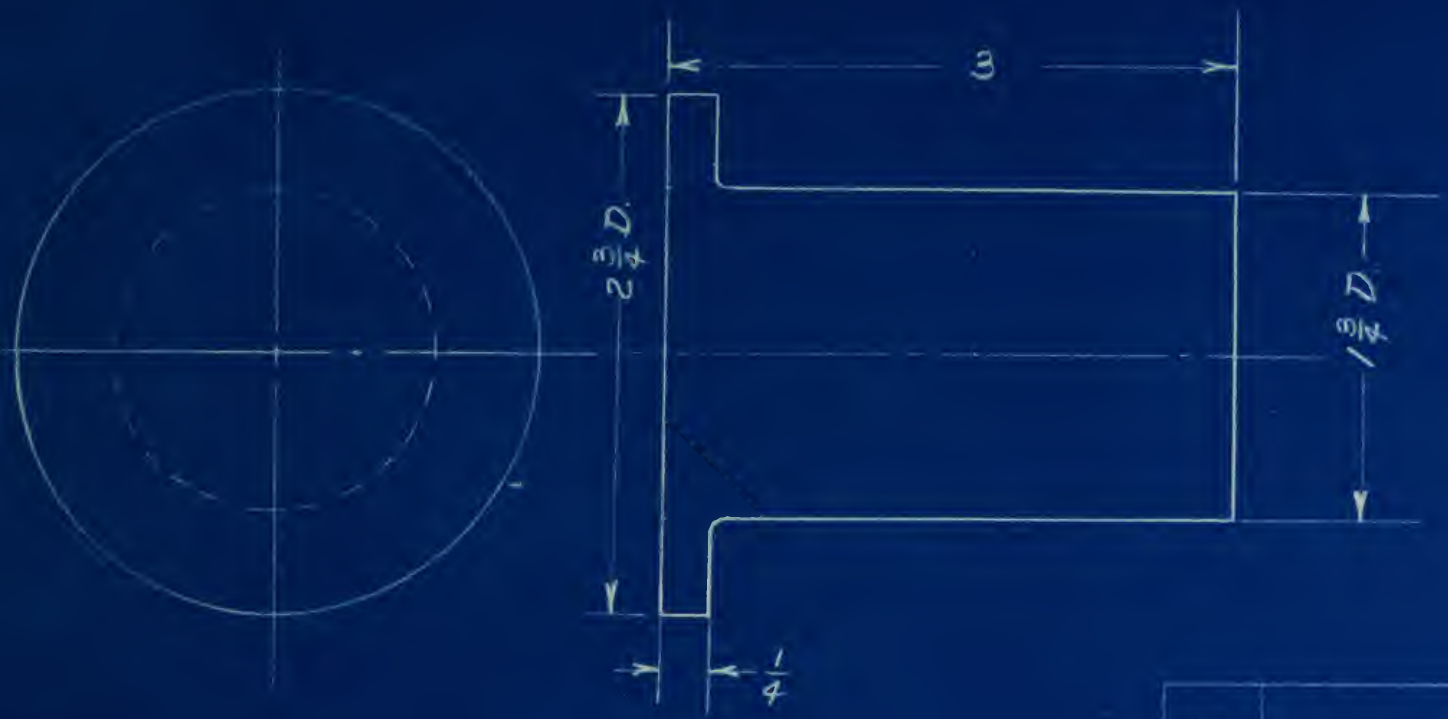

NO.	MATERIAL STL.	NO. REQ. 1

MASSACHUSETTS INSTITUTE OF TECHNOLOGY

GAS TURBINE LABORATORY

MOUNTING PAD

DRAWN BY G	DATE 2-17-49
CHECKED BY	SCALE FULL

NO.	MATERIAL BRONZE	NO. REQ. 1

MASSACHUSETTS INSTITUTE OF TECHNOLOGY

GAS TURBINE LABORATORY

THRUST WASHER

DRAWN BY G	DATE 2-17-49
CHECKED BY	SCALE FULL

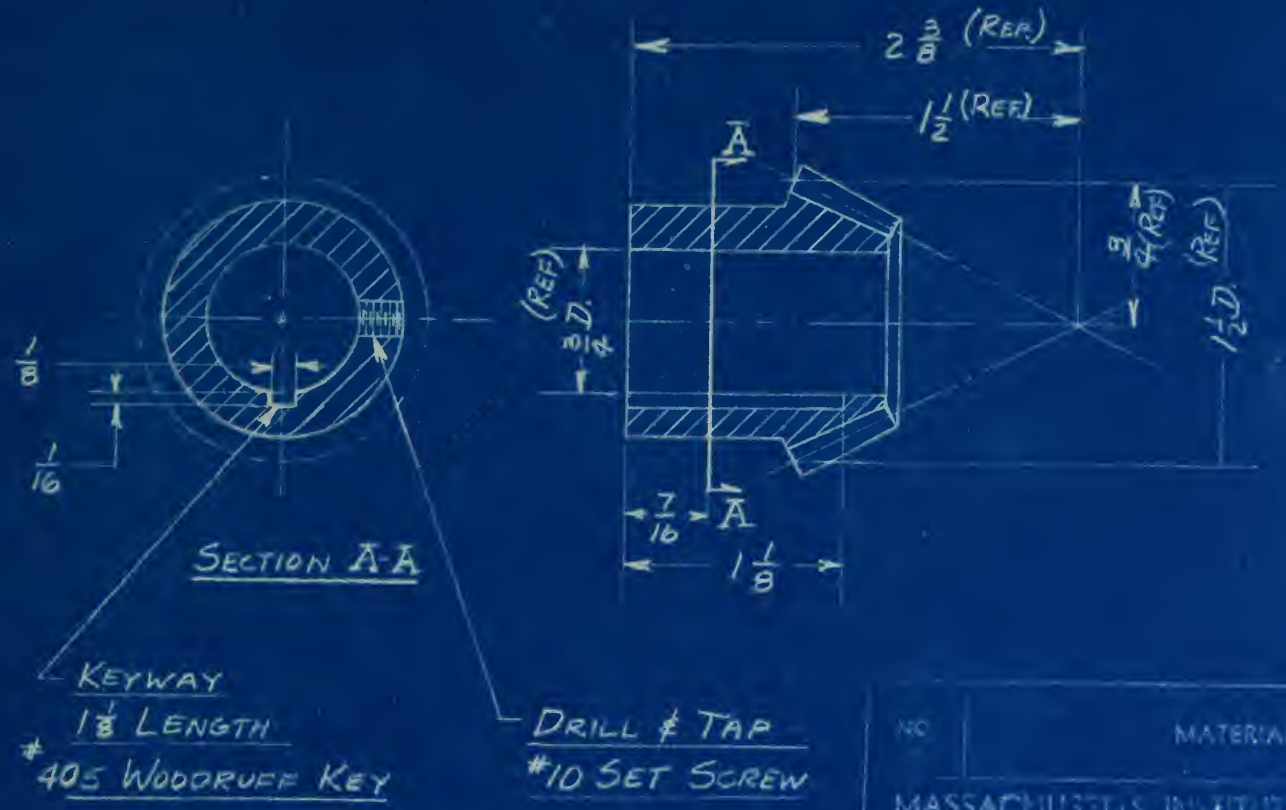

BOSTON GEAR COMPANY

L-152 BEVEL PINION

NO	MATERIAL STL.	NO REQ 1

MASSACHUSETTS INSTITUTE OF TECHNOLOGY

GAS TURBINE LABORATORY

BEVEL PINION

DRAWN BY G	DATE 2-17-49
CHECKED BY	SCALE FULL

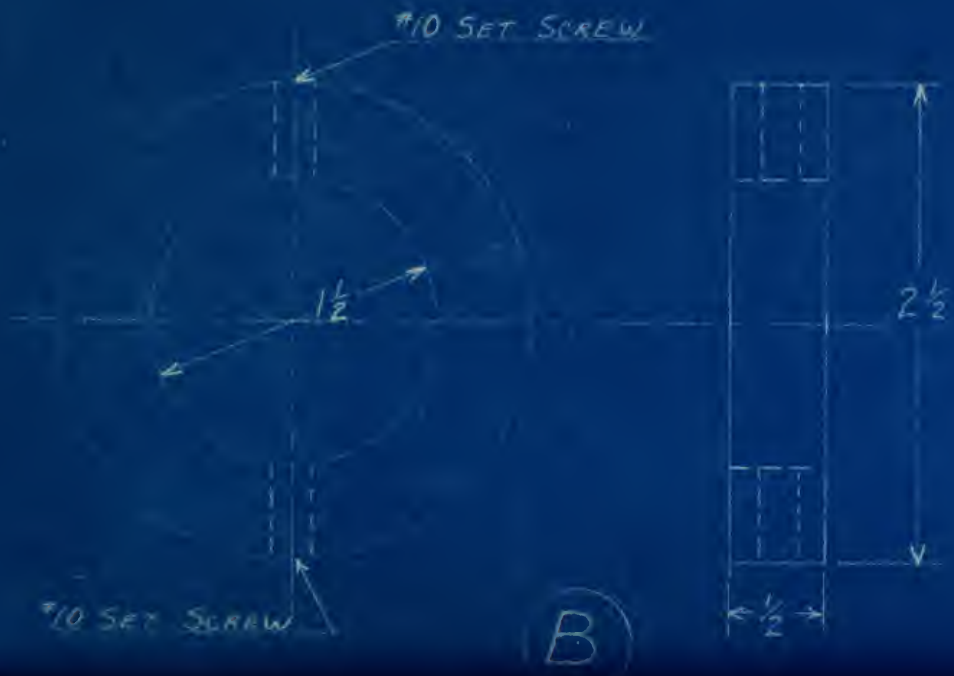

NO.	MATERIAL	NO. REQ'D
A	STEEL BACKED BRONZE BEARING	2
B	STEEL COLLAR	2

MASSACHUSETTS INSTITUTE OF TECHNOLOGY

GAS TURBINE LABORATORY

SHAFT BEARINGS AND COLLARS

DRAWN BY LASTER | DATE 2-17-49

CHECKED BY | SCALE FULL

NO.	MATERIAL STL	NO. REQ. 6
MASSACHUSETTS INSTITUTE OF TECHNOLOGY GAS TURBINE LABORATORY		
Boss		
DRAWN BY Cy	DATE 2-25-49	
CHECKED BY	SCALE FULL	
NEXT ASSEM. N-4221	N 1222	

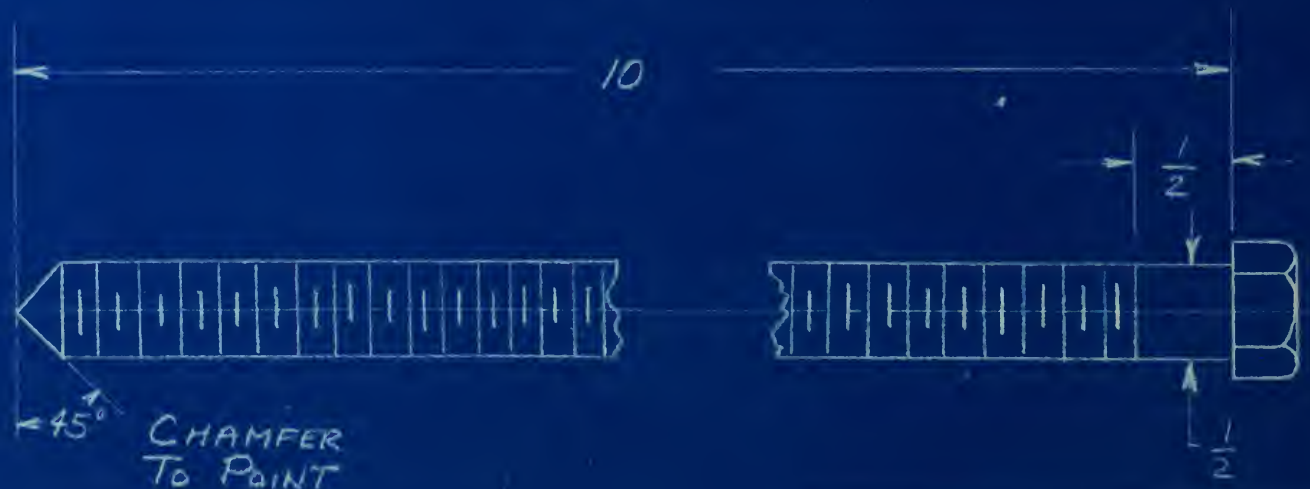

1/2" BOLT THREADED TO
WITHIN 1/2" OF HEAD.

NO.	MATERIAL	NO. REQ'D.
	STL	6

MASSACHUSETTS INSTITUTE OF TECHNOLOGY

GAS TURBINE LABORATORY

BOLT

DRAWN BY Cq	DATE 2-25-47
CHECKED BY	SCALE FULL
NEXT ASSEM.	N- 1223

SECTION AA

KEYWAY FOR
#606 WOODRUFF KEY

DRILL + TAP
#10 SETSCREW

BOSTON GEAR COMPANY
L-152 BEVEL GEAR

NO	MATERIAL	NO. REQ

MASSACHUSETTS INSTITUTE OF TECHNOLOGY
GAS TURBINE LABORATORY

BEVEL GEAR

DRAWN BY R	DATE 2-25-49
CHECKED BY	SCALE FULL
NEW ASSEM. N-4224	N - 1225

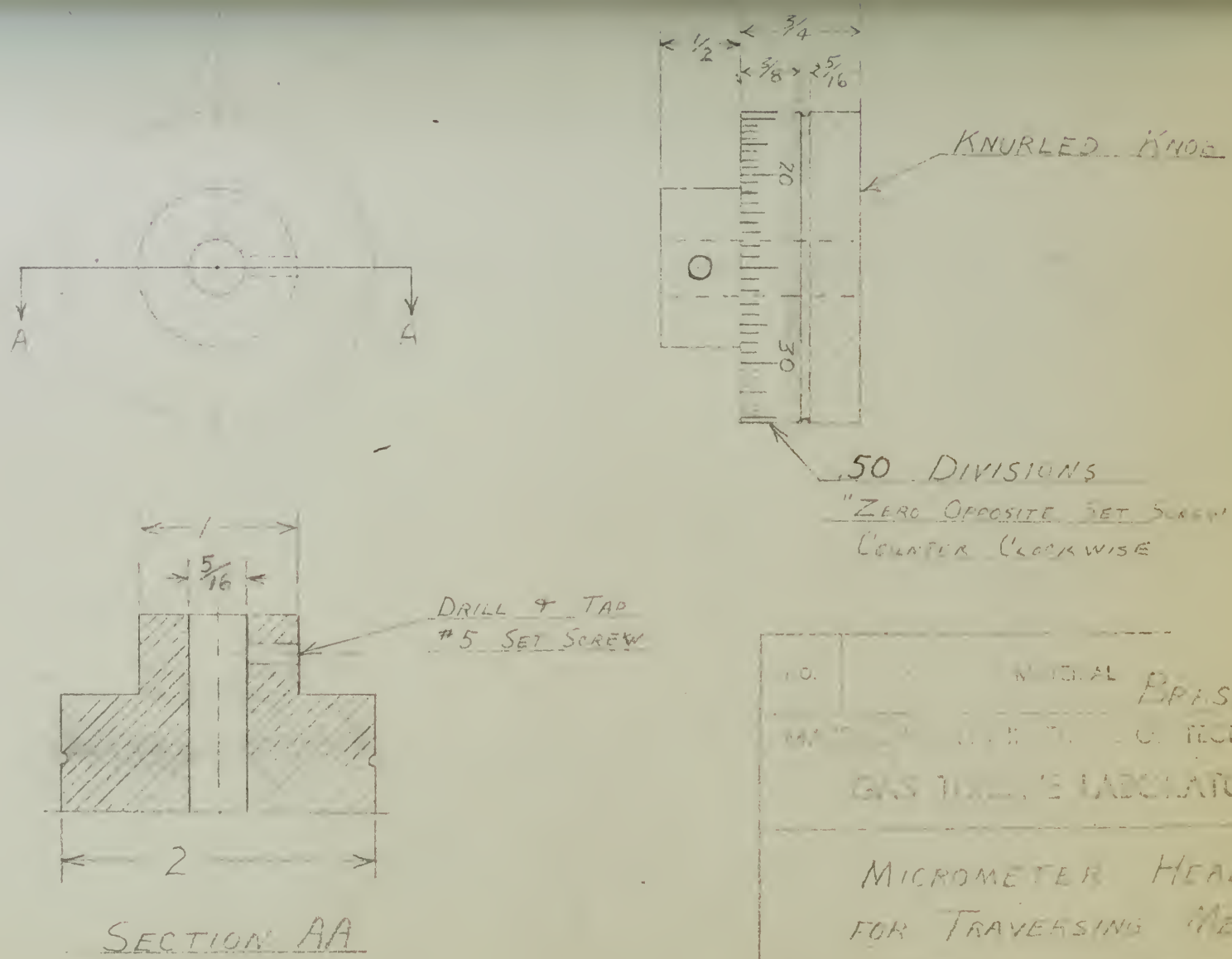

NO.	MATERIAL BRASS	
[illegible] TECHNOLOGY		
GAS TURBINE LABORATORY		
MICROMETER HEAD FOR TRAVERSING MECH.		
DRAWN BY LASTRA	DATE 2-25-49	
CHECKED BY	SCALE FULL	
NEXT ASSEM. N-2226	N = 1227	

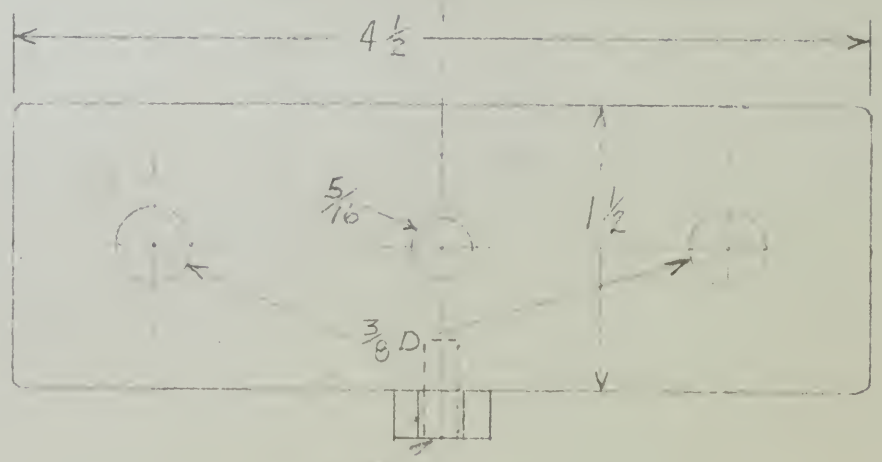

FASTENED
#10 MACHINE SCREW

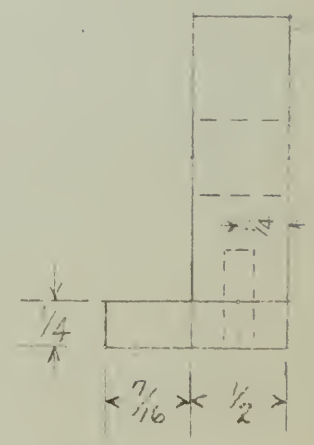

STEEL

END PLATE
TRAV. MESH

LASTER 3-1-4?
FUSE

N-2220 N - 1228

NOTE
SEE DWG N-1232
AND N-2226

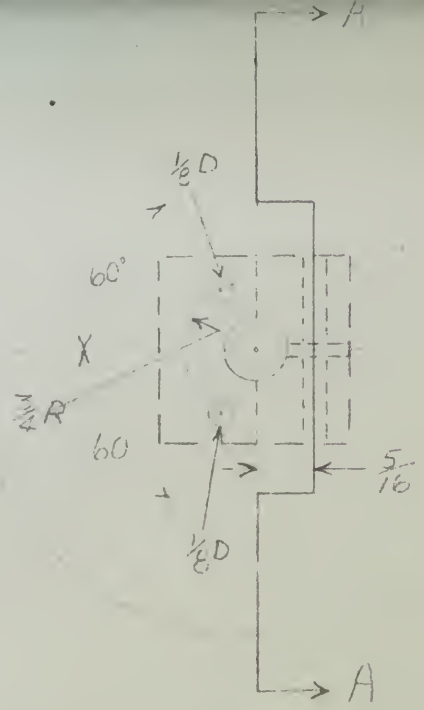

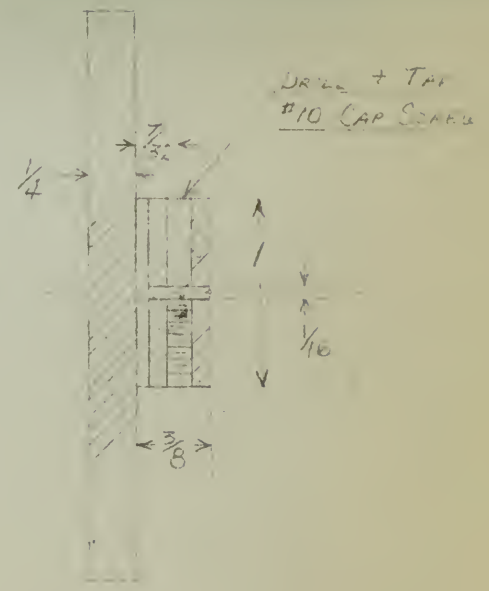

SECTION AA

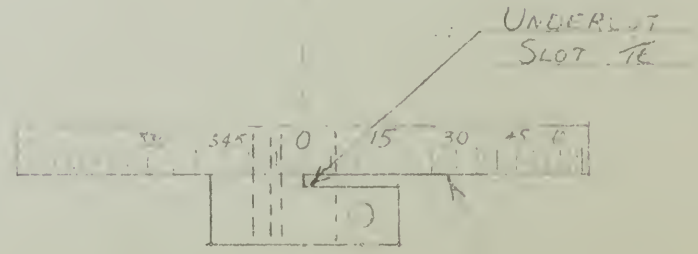

SCRIBE MARK EVERY 5°
NUMBERED EVERY 15°
COUNTER CLOCKWISE

NO.	MATERIAL BRASS	NO REQ
MASSACHUSETTS INSTITUTE OF TECHNOLOGY GAS TURBINE LABORATORY		
QUADRANT FOR TRAVERSING MECH.		
DRAWN BY LASTER	DATE 3-1-49	
CHECKED BY	SCALE FULL	
NEXT ASSEM. N-2226	N - 1229	

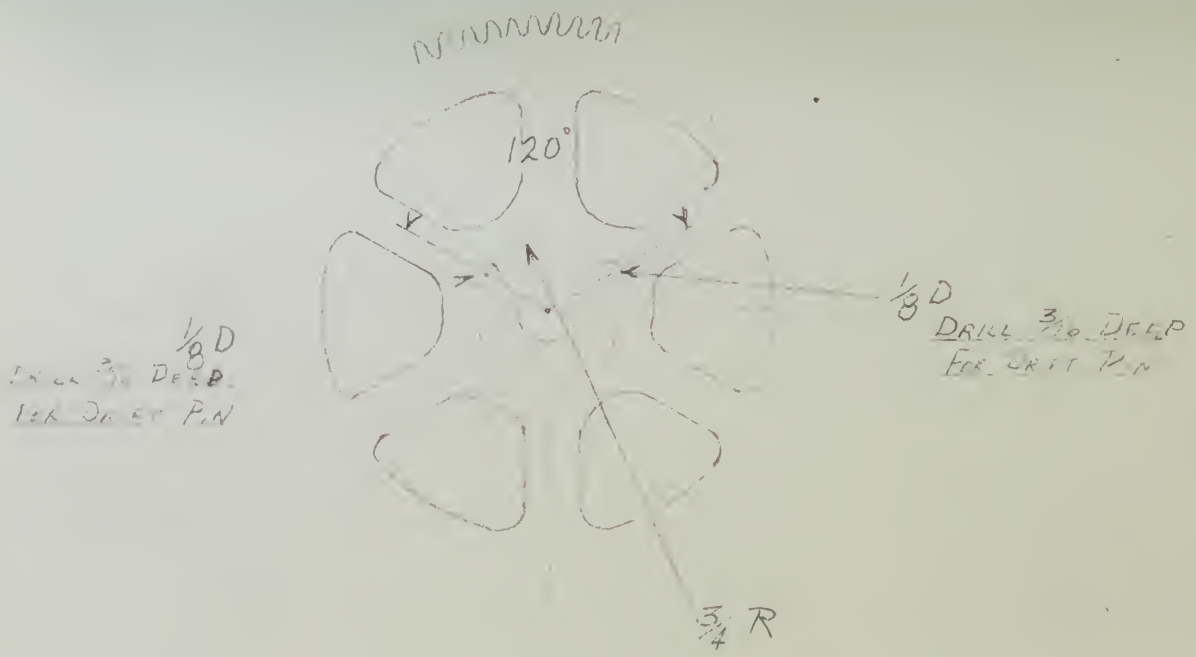

BOSTON GEAR CO WORM
GEAR G-1059

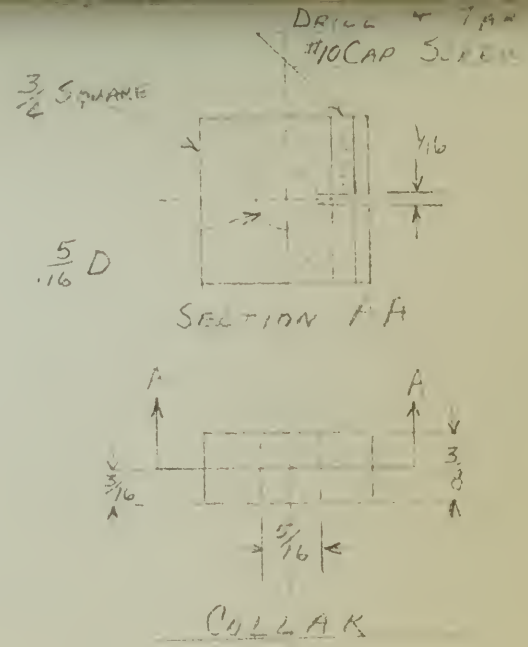

NOTE

SEE DRAWING No. N-1229
AND N-2226

NO.	MATERIAL	NO. REQ
MASSACHUSETTS INSTITUTE OF TECHNOLOGY		
CAMBRIDGE LABORATORY		
WORM GEAR + COLLAR TRAVERSING MECH.		
DRAWN BY LASTER	DATE 3-4-47	
CHECKED BY	SCALE FULL	
NEXT ASSEM. N-2226	N - 1232	

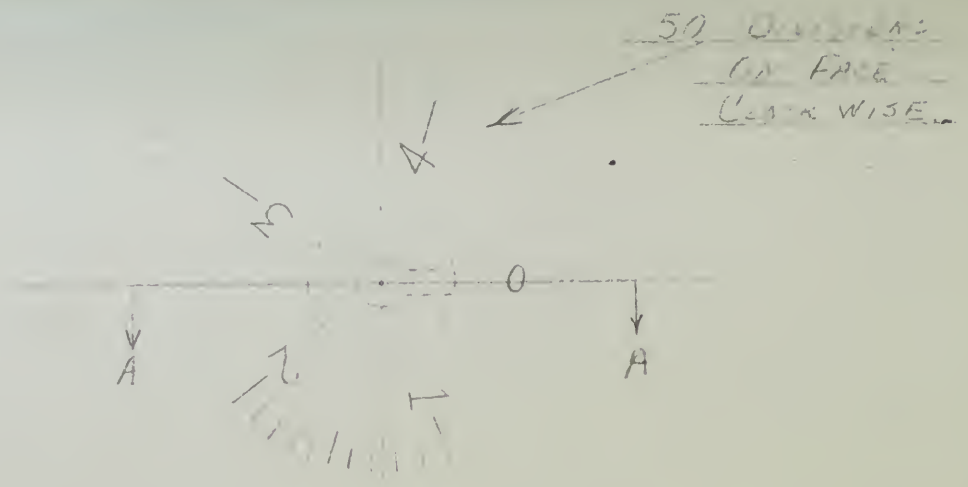

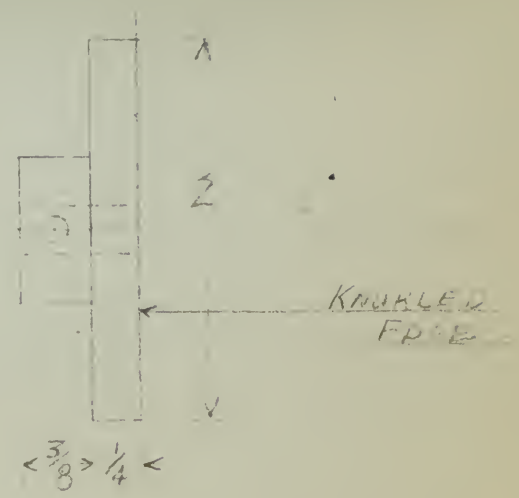

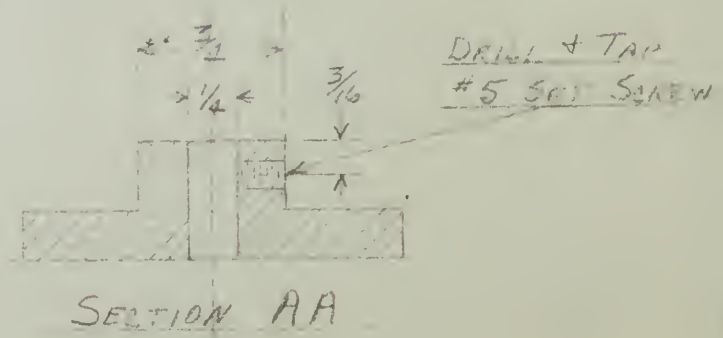

NO.	MATERIAL Brass	NO. REQ
MASSACHUSETTS INSTITUTE OF TECHNOLOGY GAS TURBINE LABORATORY		
Micrometer Head Traversing Mech		
DRAWN BY Laster	DATE 3-4-49	
CHECKED BY	SCALE Full	
NEXT ASSEM. N-2226	N - 1233	

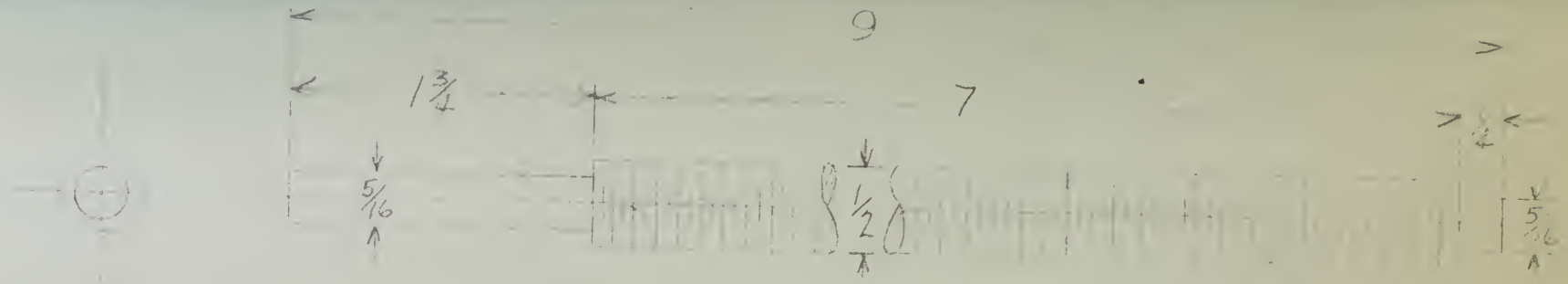

A.S.A. STANDARD FINE THREADS
20 THREADS PER INCH

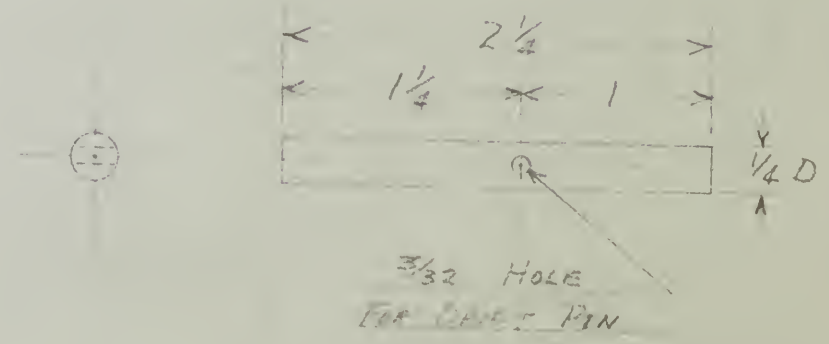

NO.	MATERIAL STEEL	NO. REQ.
MASSACHUSETTS INSTITUTE OF TECHNOLOGY		
GAS TURBINE LABORATORY		
TRAVERSING SCREW AND WORM SHAFT FOR TRAV MECH		
DRAWN BY LASTER	DATE 3-4-44	
CHECKED BY	SCALE FULL	
NEXT ASSEM. N-2226	N - 1234	

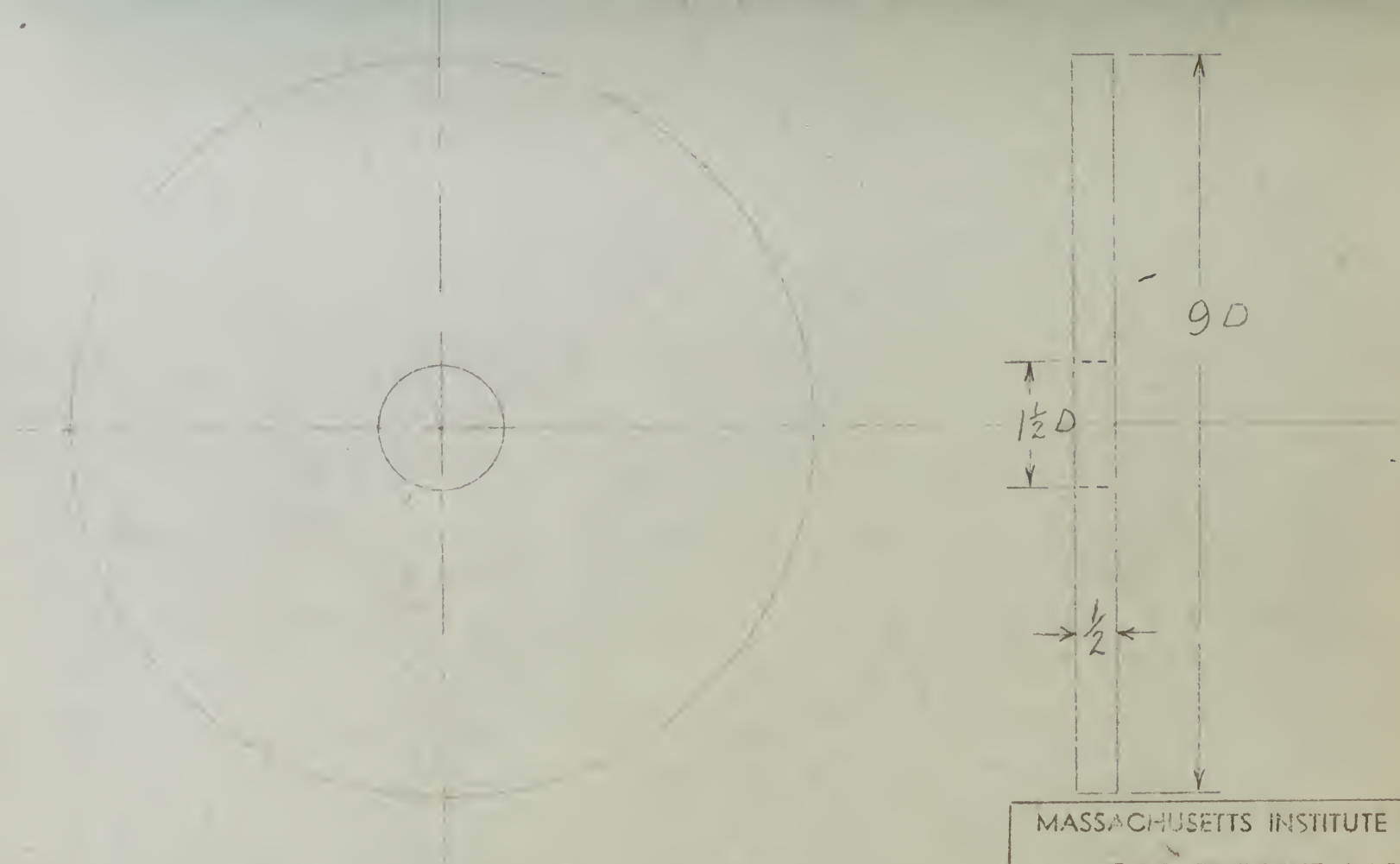

MATERIAL — WOOD

MASSACHUSETTS INSTITUTE OF TECHNOLOGY

GAS TURBINE LABORATORY

SPACER

INNER CASING AND SHAFT

DRAWN BY LARSTER	DATE 3-21-47
CHECKED BY	SCALE ½
NEXT ASSEM.	N - 1239

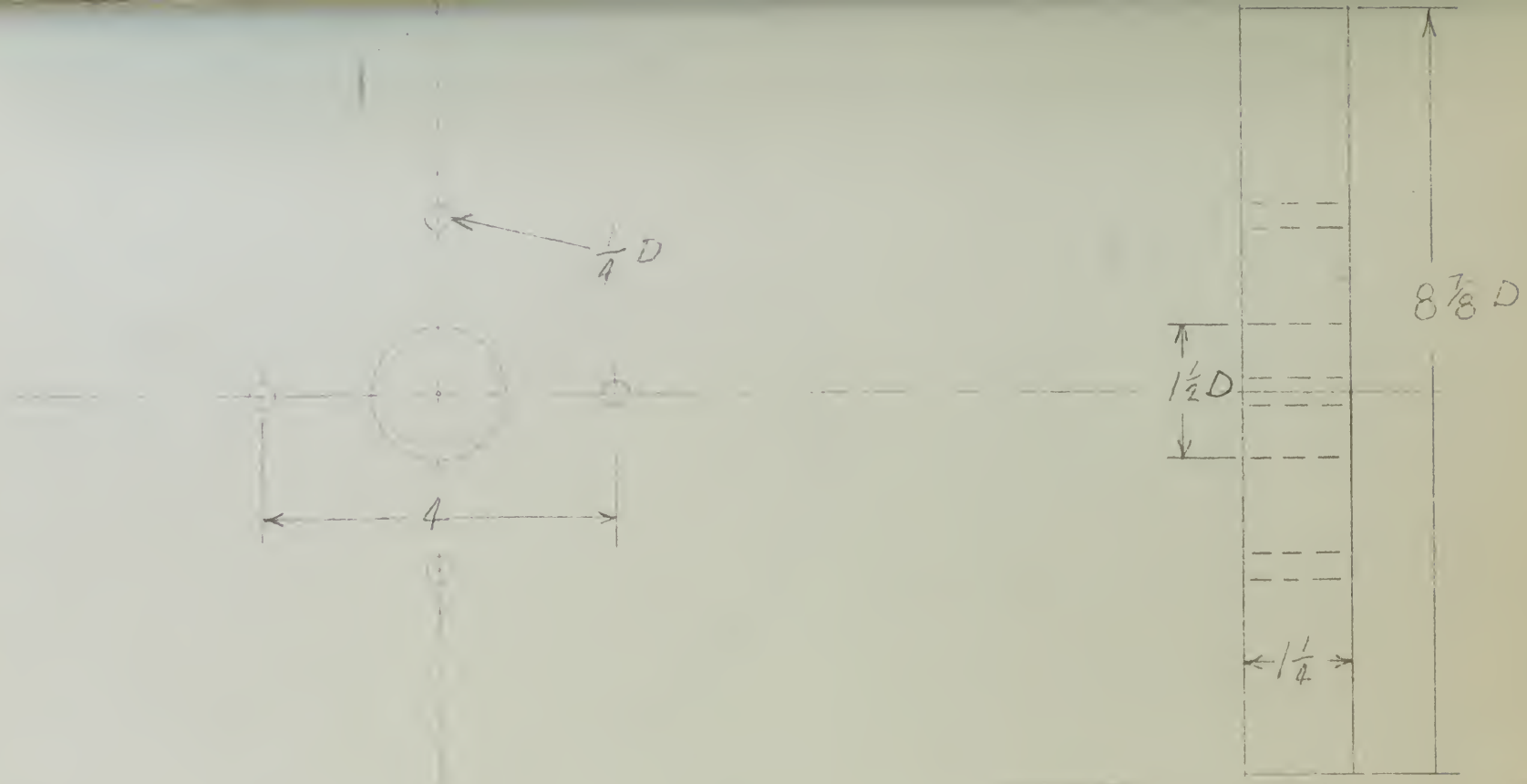

MATERIAL — WELD

MASSACHUSETTS INSTITUTE OF TECHNOLOGY

GAS TURBINE LABORATORY

SPACER

INNER CASING AND SHAFT

DRAWN BY LASTER	DATE 3-21-47
CHECKED BY	SCALE 1/1
NEXT ASSEM.	N 1240

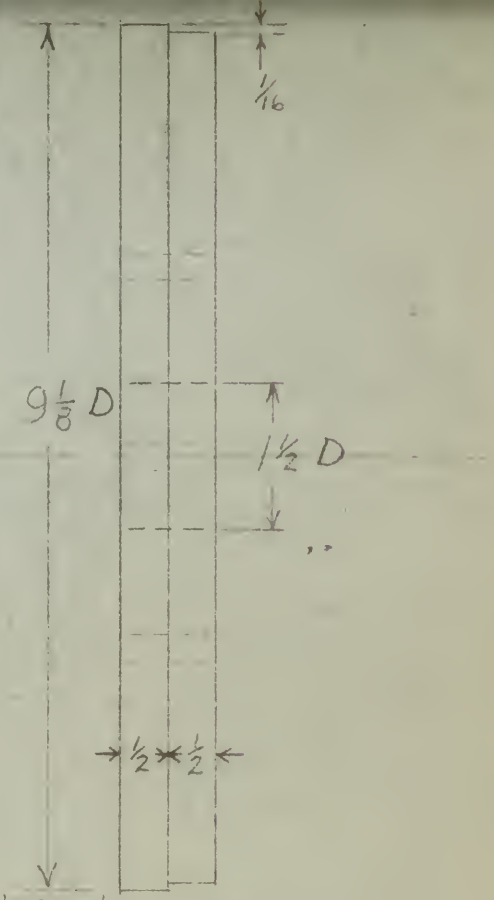

MATERIAL — WOOD

MASSACHUSETTS INSTITUTE OF TECHNOLOGY

GAS TURBINE LABORATORY

SPACER

INNER CASING AND SHAFT

DRAWN BY LASTER	DATE 5-21-40
CHECKED BY	SCALE 1/1
NEXT ASSEM.	N - 1241

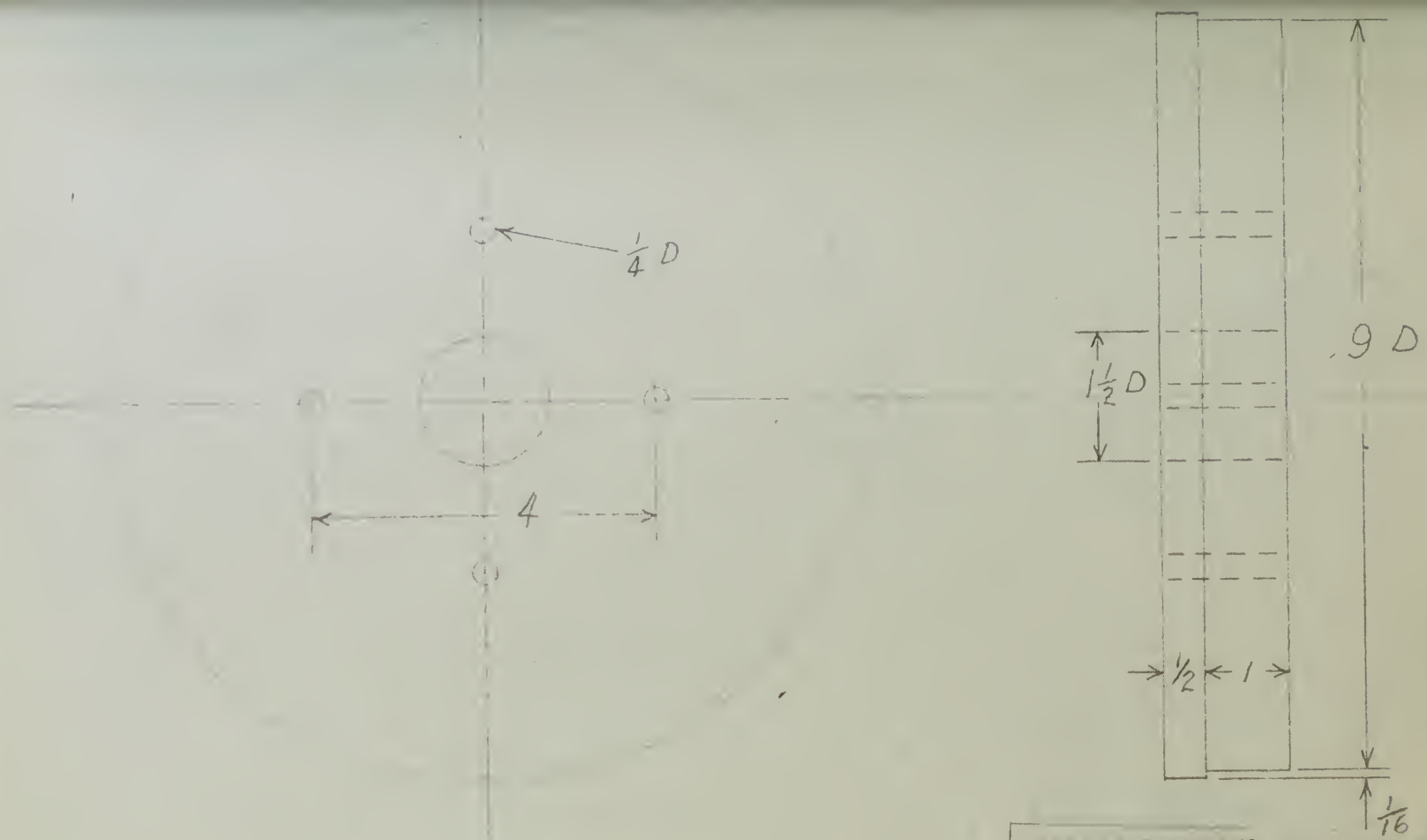

MATERIAL - WOOD

MASSACHUSETTS INSTITUTE OF TECHNOLOGY

GAS TURBINE LABORATORY

SPACER

INNER CASING AND SHAFT

DRAWN BY LASTER	DATE 3-21-49
CHECKED BY	SCALE 1/2
NEXT ASSEM.	N - 1242

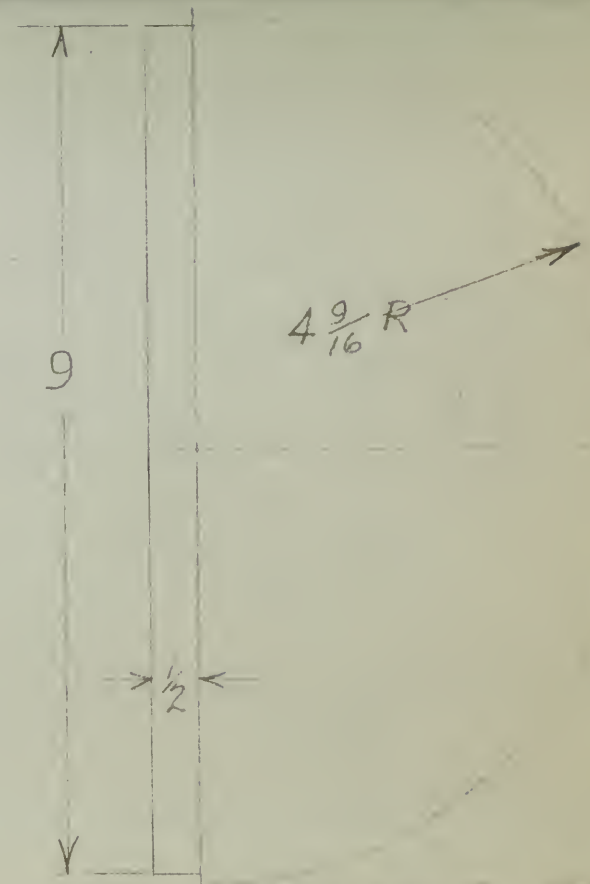

MATERIAL – BALSA

MASSACHUSETTS INSTITUTE OF TECHNOLOGY

GAS TURBINE LABORATORY

NOSE PIECE
INNER CASING

DRAWN BY LASTER	DATE 3-21-49
CHECKED BY	SCALE 1/2
NEXT ASSEM.	N – 1243

THIS DWG IN CUSTODY OF

PROF. W.R. HAWTHORNE

MIT GAS TURBINE LABORATORY

NO	MATERIAL	NO REQ.

MASSACHUSETTS INSTITUTE OF TECHNOLOGY

GAS TURBINE LABORATORY

INLET GUIDE VANE ASSEMBLY

DRAWN BY	DATE
CHECKED BY	SCALE
NEXT ASSEM.	N-5254

THIS DWG IN CUSTODY OF

PROF W R HAWTHORNE

MIT GAS TURBINE LABORATORY

NO	MATERIAL	NO. REQ

MASSACHUSETTS INSTITUTE OF TECHNOLOGY

GAS TURBINE LABORATORY

INLET GUIDE VANE

DR[illegible] BY	DATE
[illegible] BY	SCALE
[illegible] ASSEM.	N-5255

NO	MATERIAL	NO. REQ
A	STEEL FLANGE	1
B	STEEL FLANGE	1
C	STEEL SHAFT	1

MASSACHUSETTS INSTITUTE OF TECHNOLOGY
GAS TURBINE LABORATORY

SHAFT AND FLANGES

DRAWN BY LASTER
CHECKED BY
NEXT ASSEM.

N - 3-20

NO	MATERIAL	NO REQ.

MASSACHUSETTS INSTITUTE OF TECHNOLOGY

GAS TURBINE LABORATORY

AFTER SECTION
INNER CASING

DRAWN BY LASTER	DATE 2-11-49
CHECKED BY	SCALE ½
NEXT ASSEM.	No 2218

N-1225

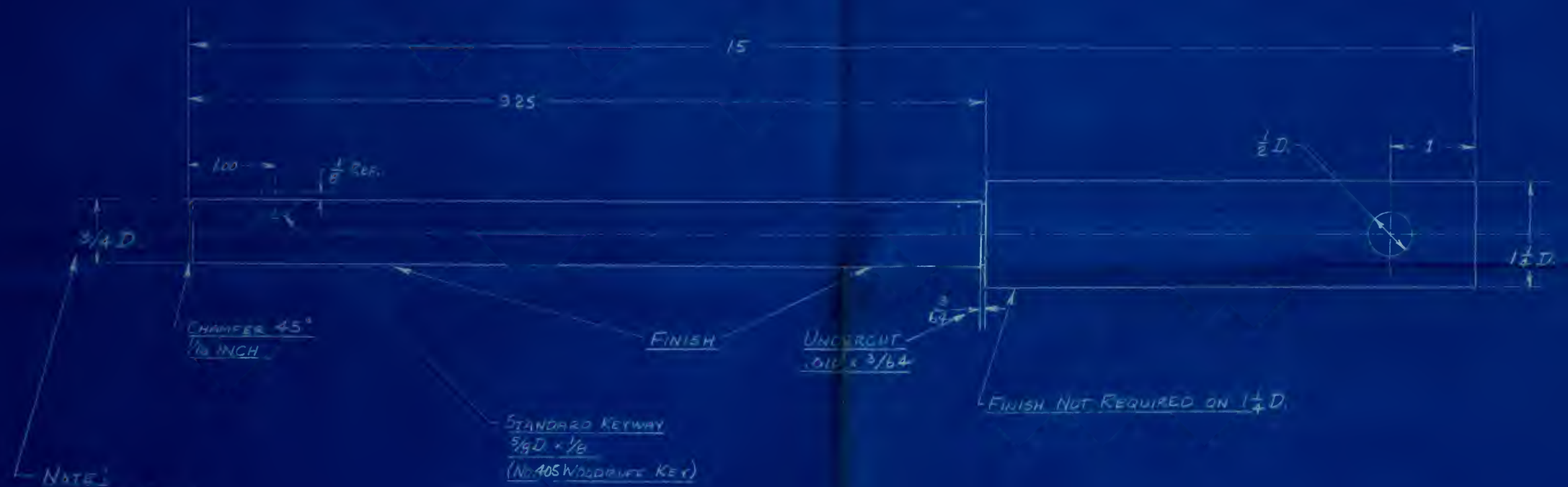

NO.	MATERIAL	STEEL	1
MASSACHUSETTS			
GAS TURBIN			
SHAFT			
DRAWN BY		DATE 2-16-49	
CHECKED BY		SCALE FULL	
NAVY ASSEM.		N 219	

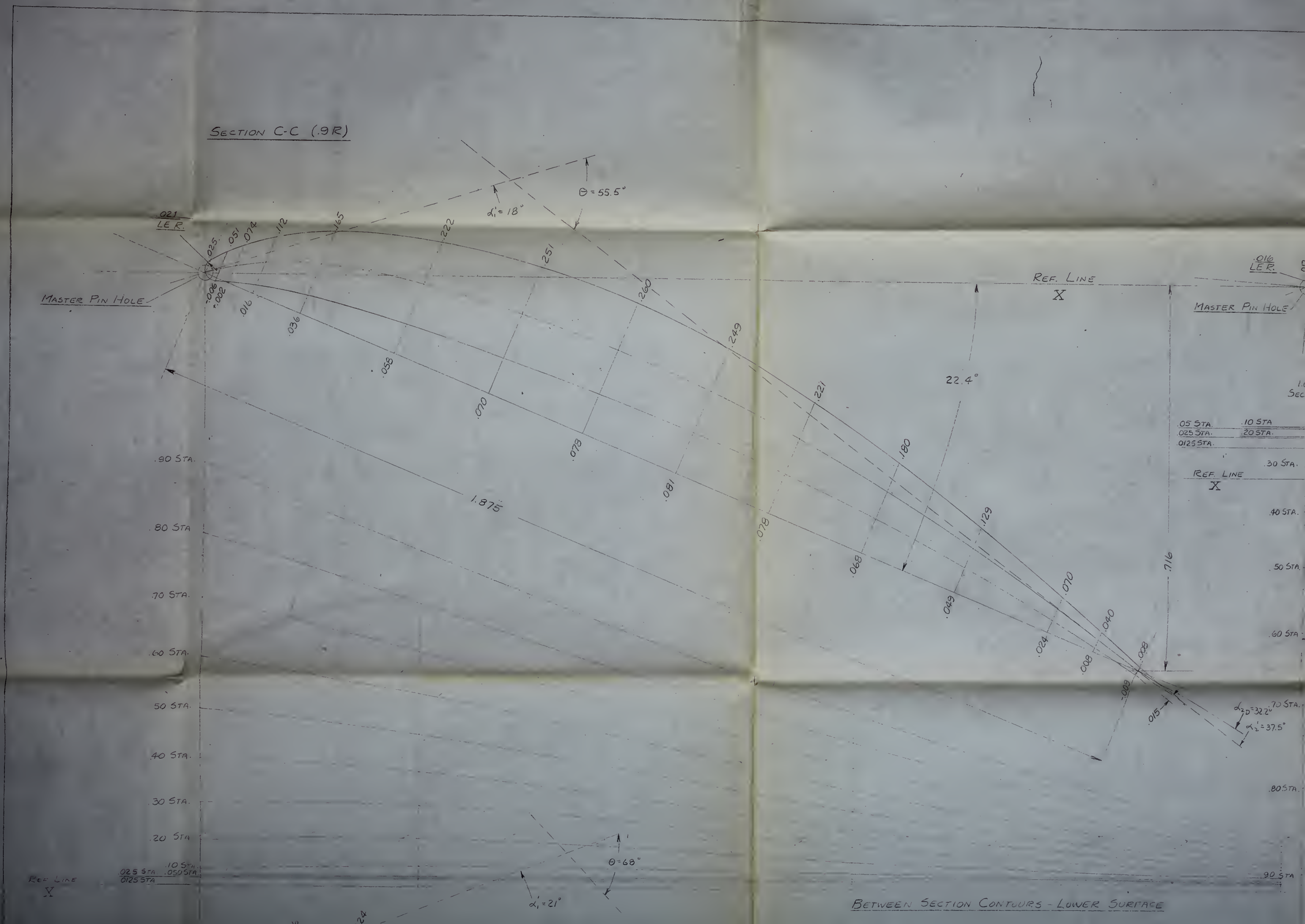
SECTION C-C (.9R)
.021 LE R.
MASTER PIN HOLE
.025
.051
.074
.112
.165
.222
.251
.260
.249
.221
.180
.129
.070
.040
.008
.009
.015
.016
.036
.058
.070
.078
.081
.078
.068
.049
.024
.008
.006
+.002
1.875
.716
22.4°
REF. LINE X
.016 LE R.
MASTER PIN HOLE
.05 STA.
.10 STA
.025 STA.
.20 STA.
.0125 STA.
.30 STA.
REF. LINE X
.40 STA.
.50 STA.
.60 STA
.70 STA.
.80 STA.
.90 STA
.90 STA.
.80 STA
.70 STA.
.60 STA.
.50 STA.
.40 STA.
.30 STA.
.20 STA
.10 STA.
.025 STA
.050 STA.
.0125 STA
REF. LINE X
θ = 55.5°
θ = 68°
α₁' = 18°
α₁' = 21°
α₂D = 32.2°
α₂' = 37.5°
BETWEEN SECTION CONTOURS - LOWER SURFACE

SECTION A-A (.5R)

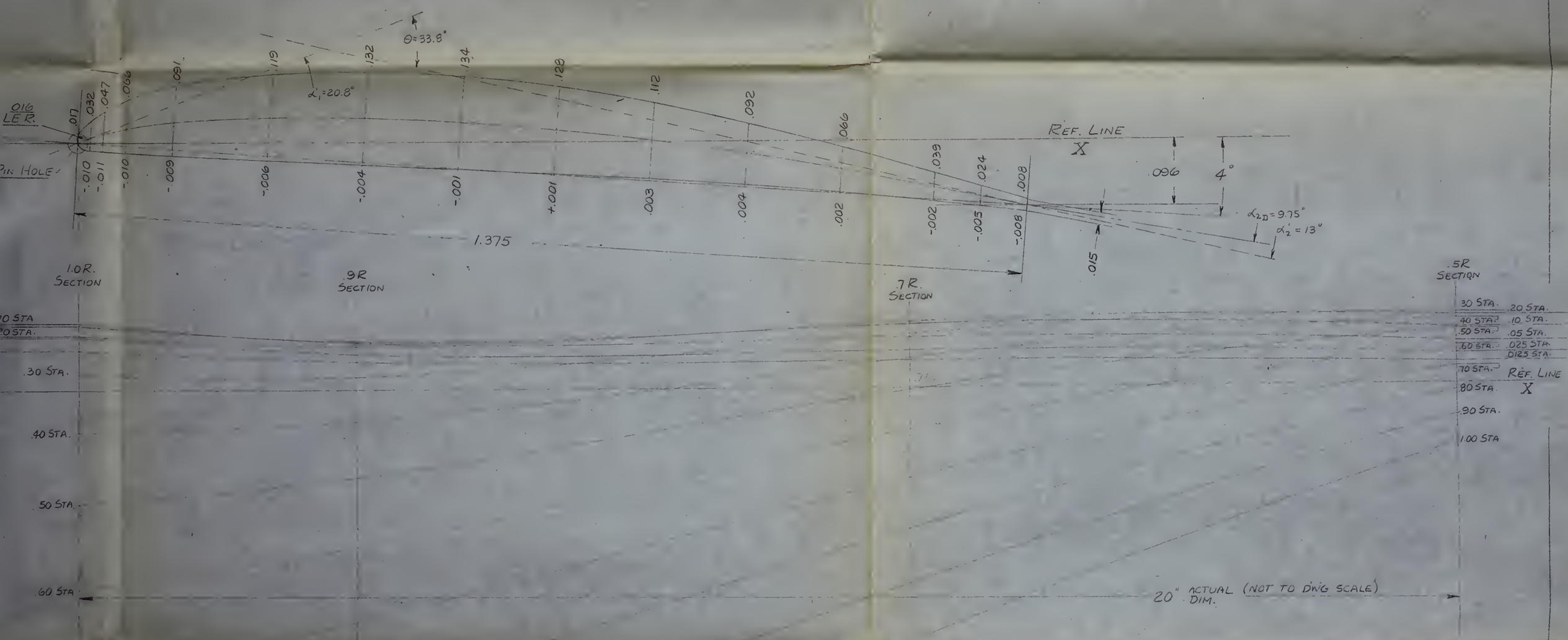

BETWEEN - SECTION CONTOURS - UPPER SURFACE

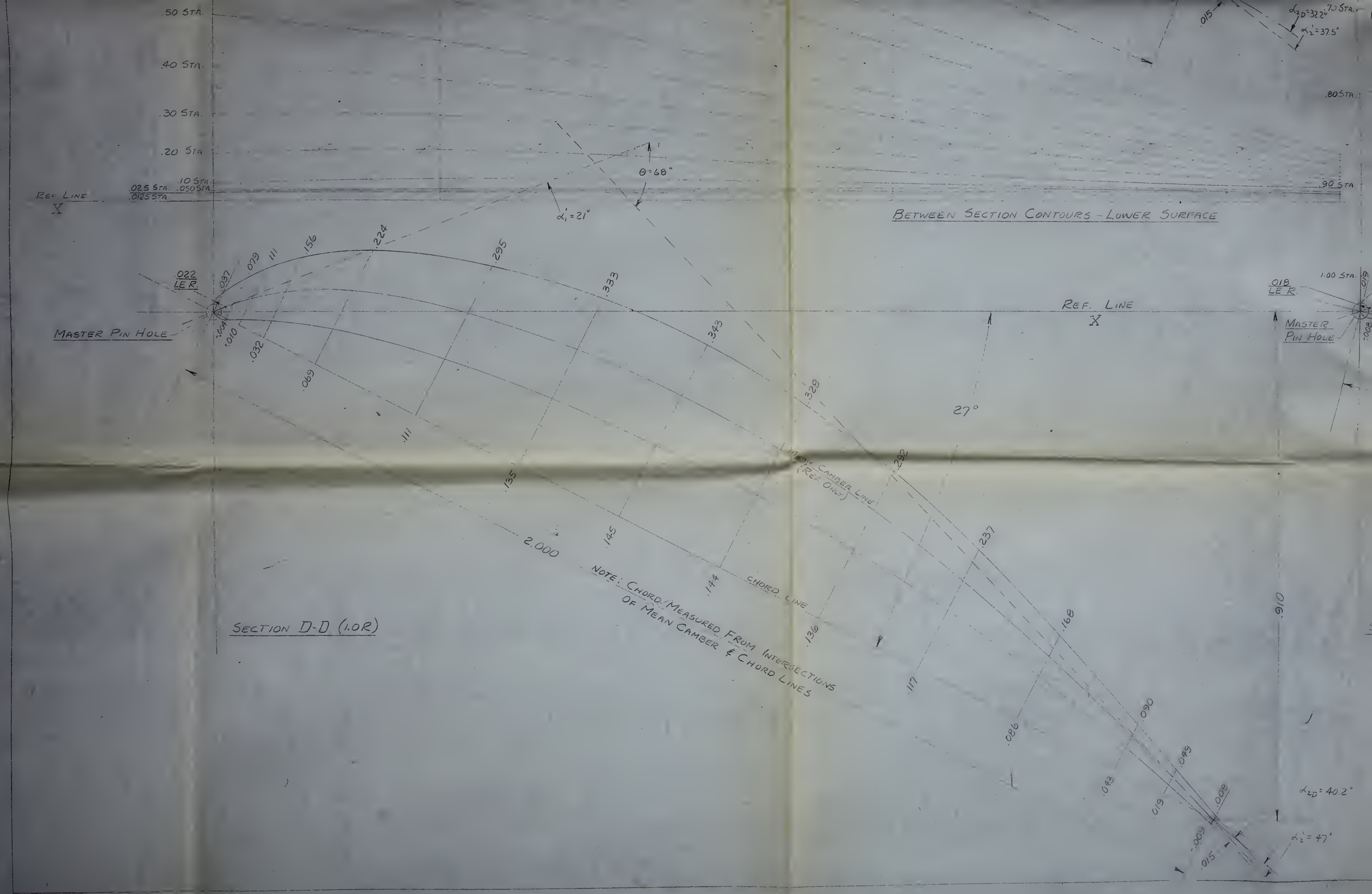

.50 STA.
.40 STA.
.30 STA.
.20 STA.
.10 STA.
.025 STA. .050 STA.
.0125 STA.
REF LINE X
θ=68°
α'₁=21°
BETWEEN SECTION CONTOURS - LOWER SURFACE
.70 STA.
.80 STA.
.90 STA.
1.00 STA.
.022 LE R.
.018 LE R.
MASTER PIN HOLE
REF. LINE X
MASTER PIN HOLE
27°
MEAN CAMBER LINE (REF. ONLY)
CHORD LINE
2.000
NOTE: CHORD MEASURED FROM INTERSECTIONS OF MEAN CAMBER & CHORD LINES
SECTION D-D (1.0R)
α₂D=32.2°
α'₂=37.5°
α₂D=40.2°
α'₂=47°

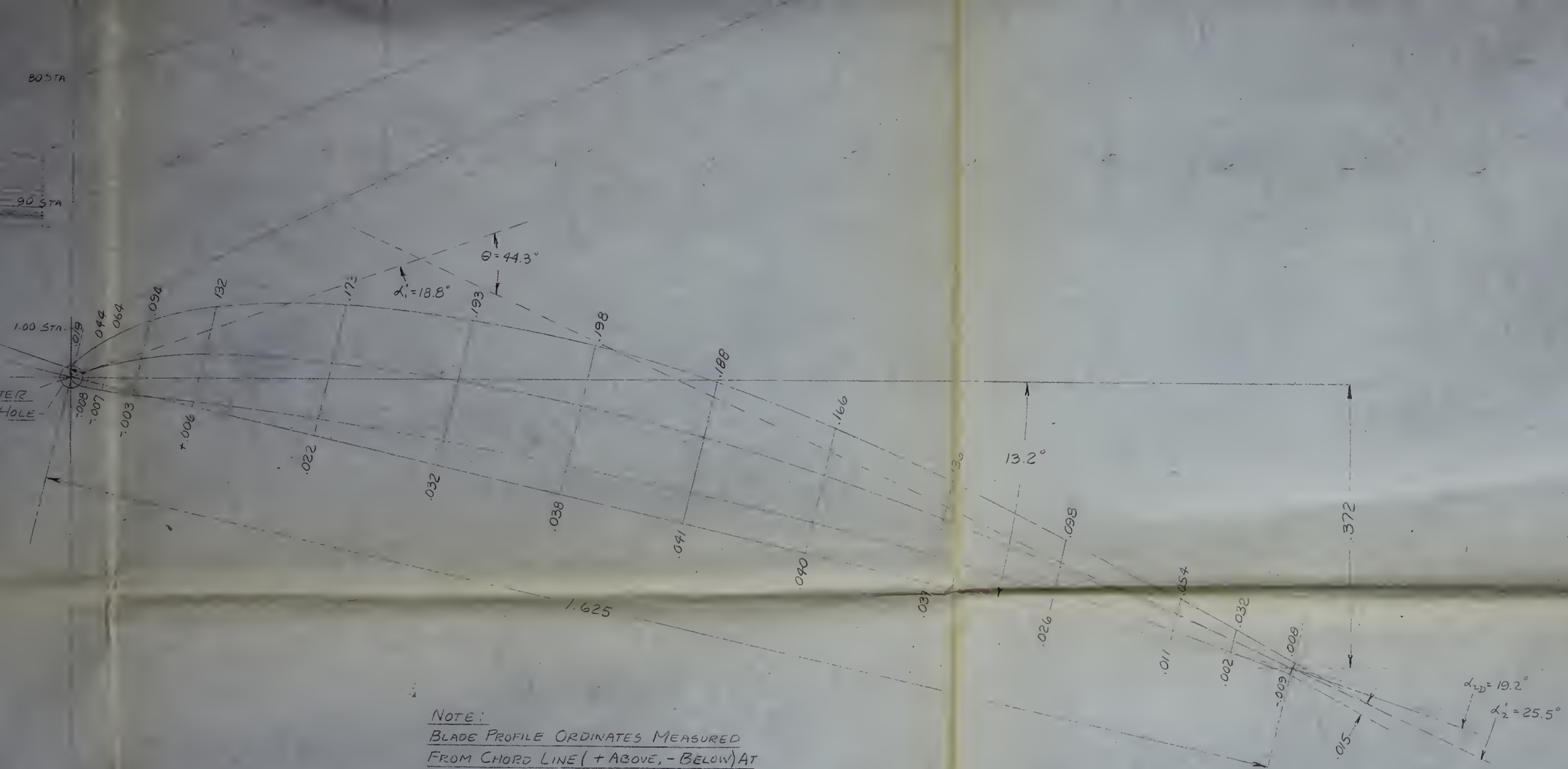

NOTE:
BLADE PROFILE ORDINATES MEASURED FROM CHORD LINE (+ ABOVE, − BELOW) AT BLADE STATIONS, FROM L.E. TO T.E IN PERCENT OF CHORD: 0, 1.25, 2.5, 5.0, 10, 20, 30, 40, 50, 60, 70, 80, 90, 95, 100.

SECTION B-B (.7R)

NOTE:
DESIGN ANGLES α_1', α_2', θ, α_{2D} FOR REFERENCE ONLY.
NOT TO BE USED FOR MANUFACTURE.

NO.	MATERIAL	NO. REQ.

MASSACHUSETTS INSTITUTE OF TECHNOLOGY
GAS TURBINE LABORATORY

INLET GUIDE VANE
BLADE SECTIONS

DRAWN BY Cq	DATE 3-17-49
CHECKED BY	SCALE 10 X
NEXT ASSY. N-4244	N - 5238

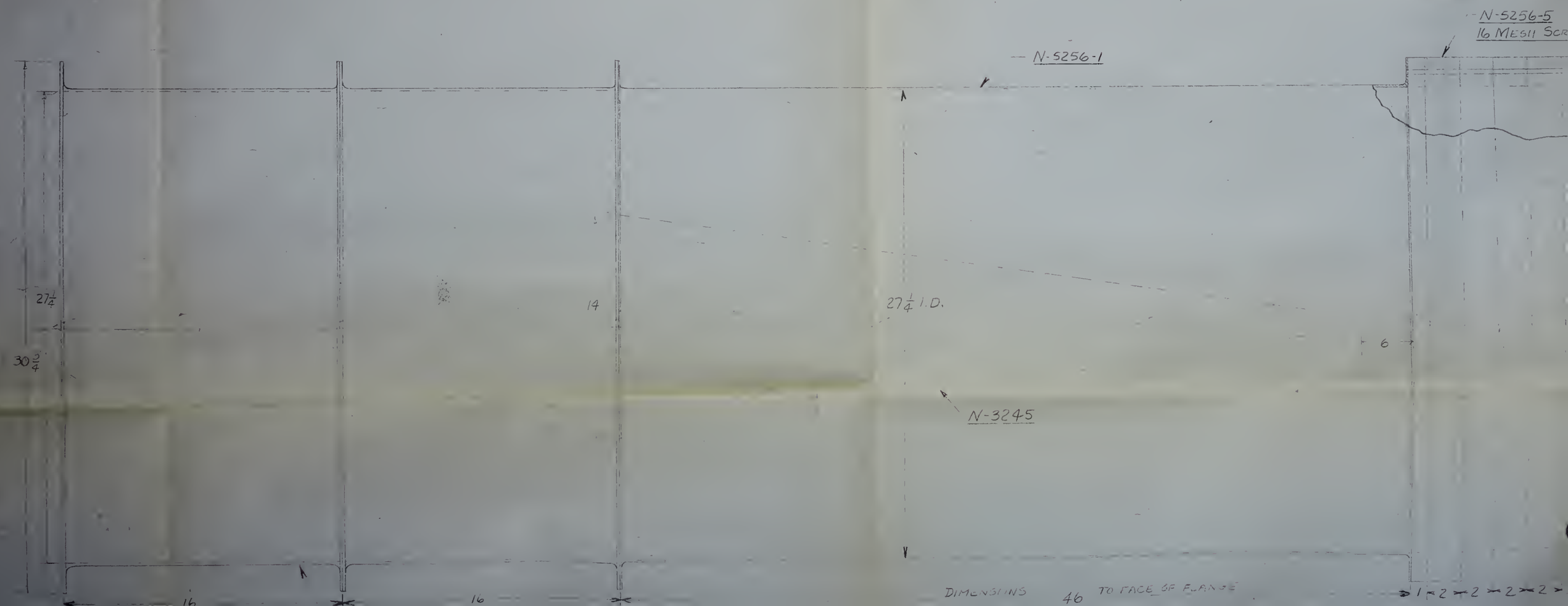
N-5256-5
16 MESH SCR
N-5256-1
27 1/4
30 3/4
14
27 1/4 I.D.
6
N-3245
16
16
DIMENSIONS
46
TO FACE OF FLANGE
1
2
2
2
2

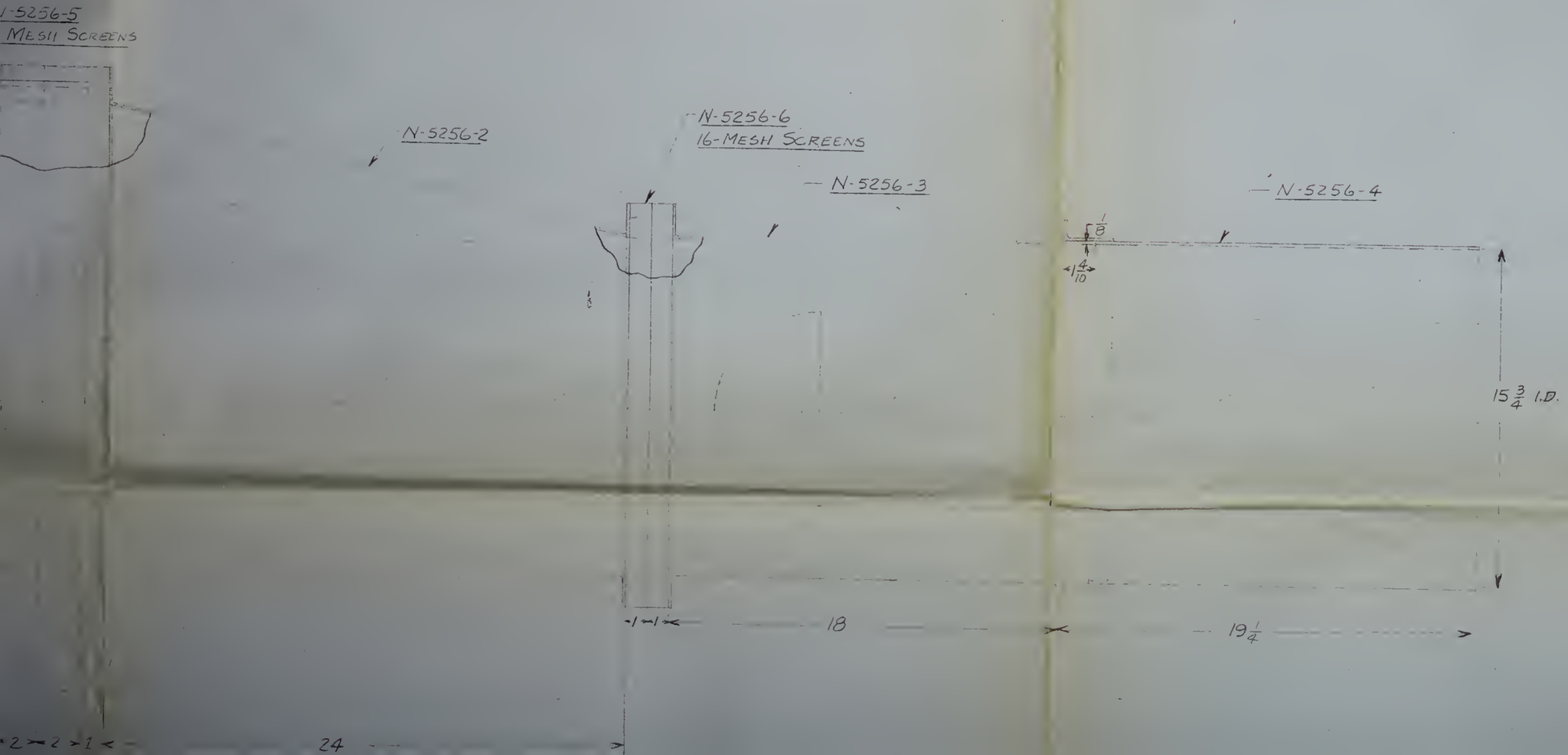
1-5256-5
MESH SCREENS
N-5256-2
N-5256-6
16-MESH SCREENS
N-5256-3
N-5256-4
1/8
4/10
15 3/4 I.D.
1
1
18
19 1/4
2
2
1
24

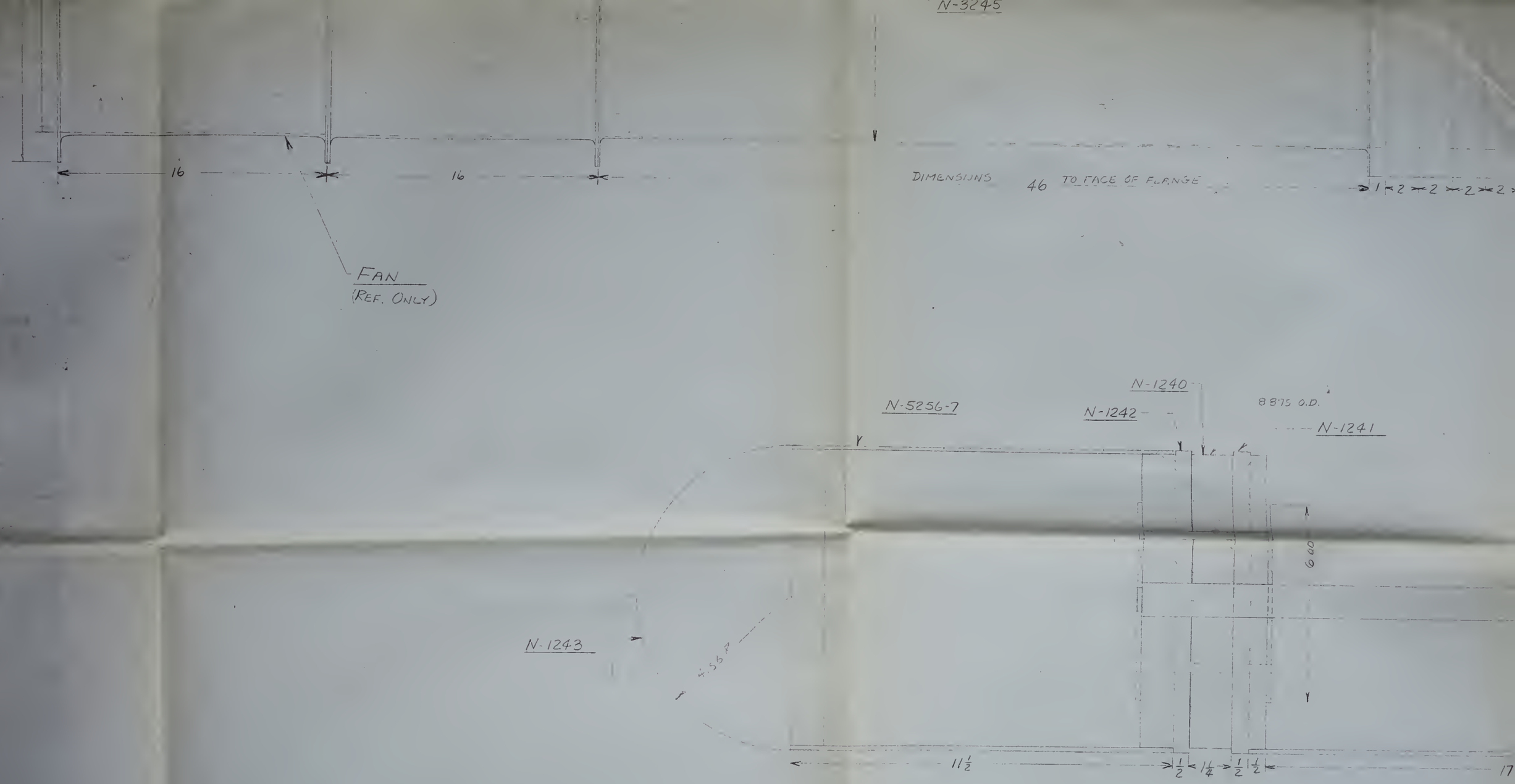
N-3245
16
16
DIMENSIONS
46
TO FACE OF FLANGE
1
2
2
2
2
FAN
(REF. ONLY)
N-1240
N-5256-7
N-1242
8.875 O.D.
N-1241
6.00
N-1243
4.56
11 1/2
1/2
1 1/4
1/2
1/2
17

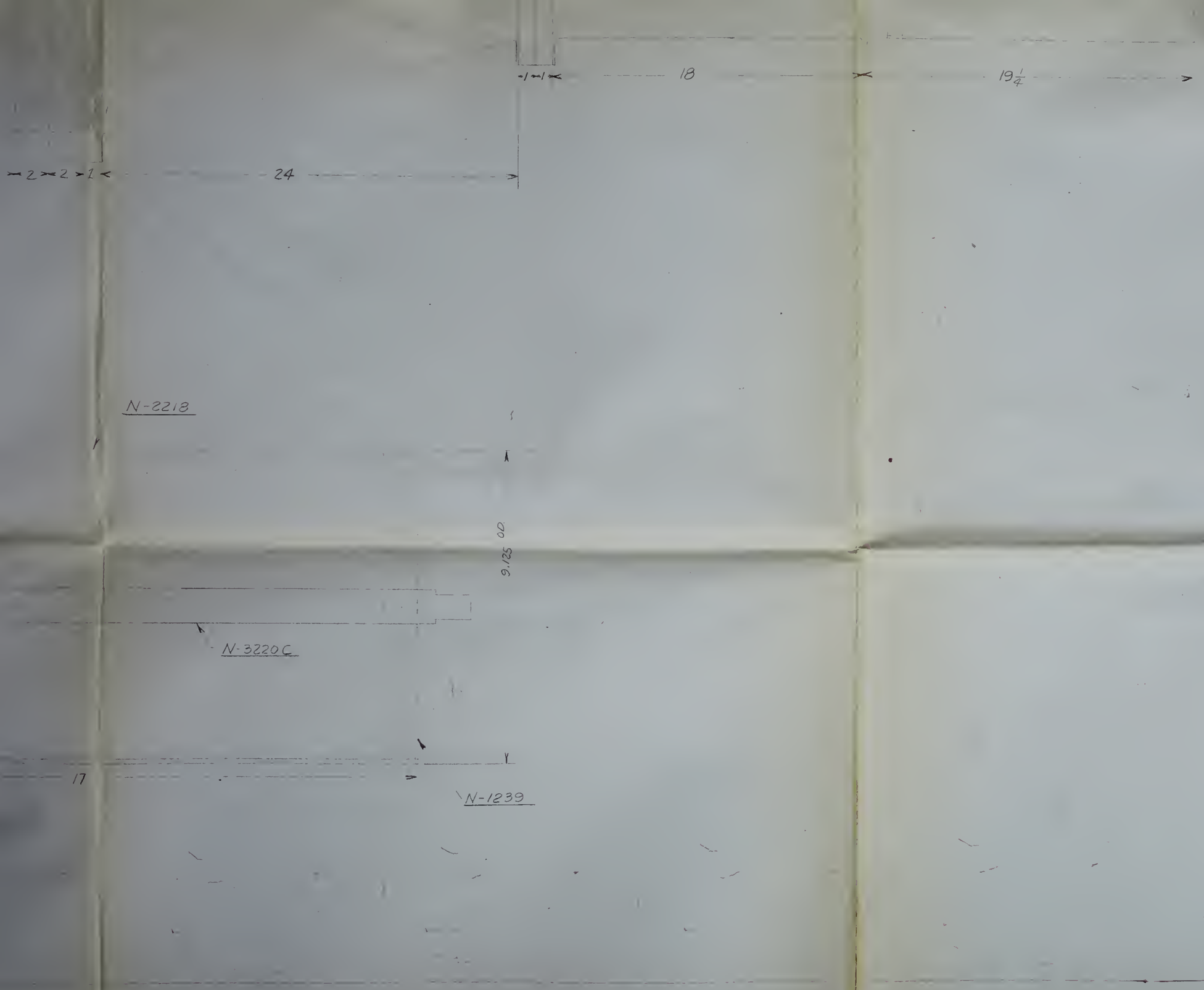

MATERIAL

MASSACHUSETTS INSTITUTE OF TECHNOLOGY

GAS TURBINE LABORATORY

ANNULAR-CASCADE TUNNEL

ASSEMBLY LAYOUT

DRAWN BY LASTER DATE 12-10-48

SCALE

N - 5256

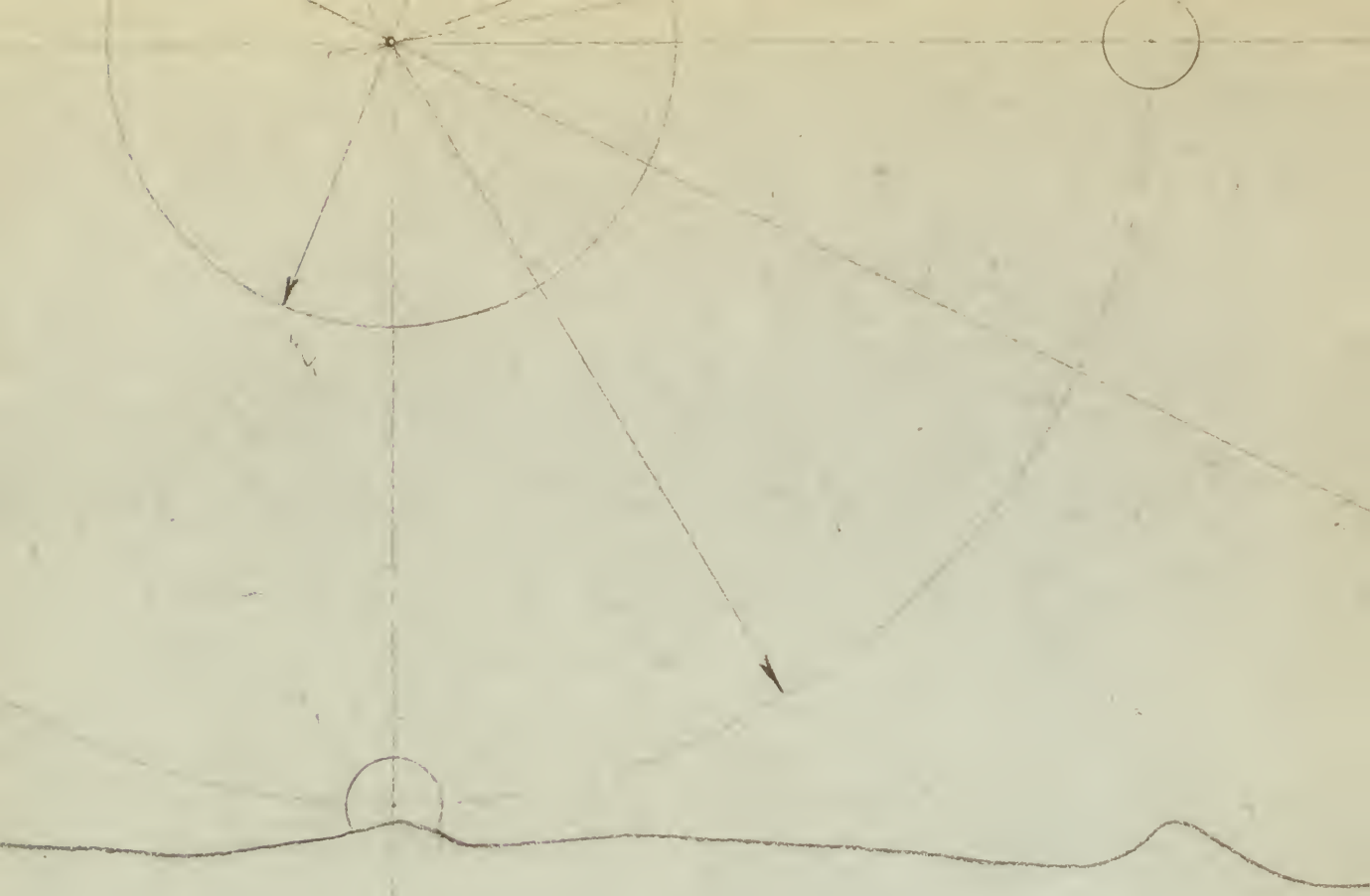

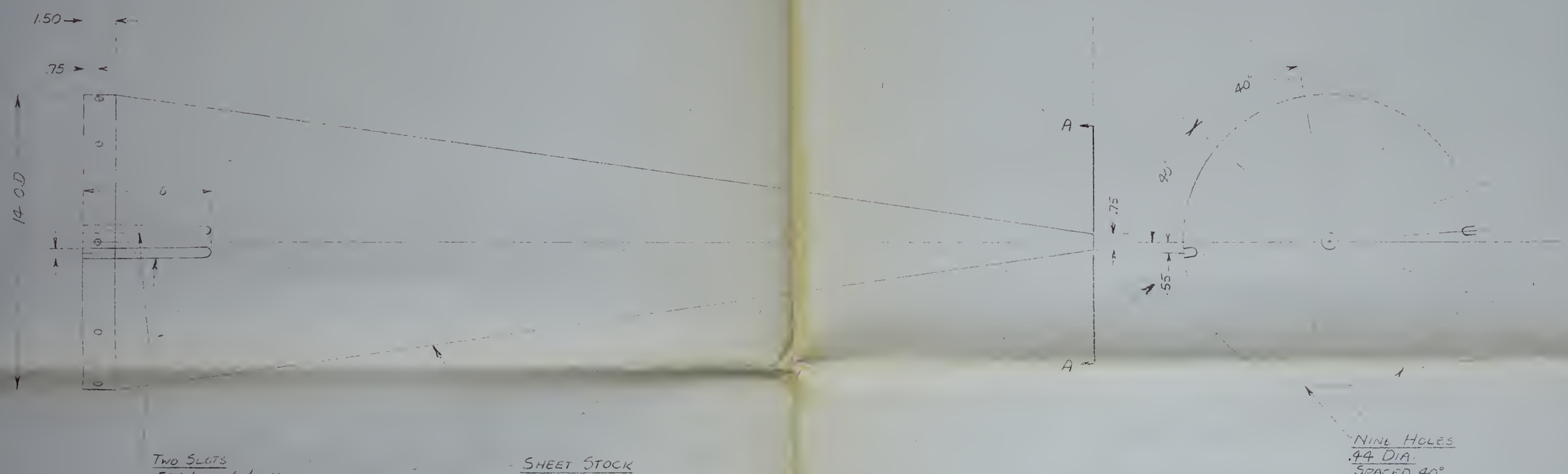

Two Slots
.50 Wide, 6 Long
Located Diametrically Opposite
Note Location of One Slot
with Respect To Hole

Sheet Stock
Max Thickness .047

NO.	MATERIAL	NO. REQ. 1
MASSACHUSETTS INSTITUTE OF TECHNOLOGY		
GAS TURBINE LABORATORY		
DIFFUSER CONE		
DRAWN BY Cen		DATE 12-14-48
CHECKED BY		SCALE 1/4
NEXT ASSEM.		N - 3245

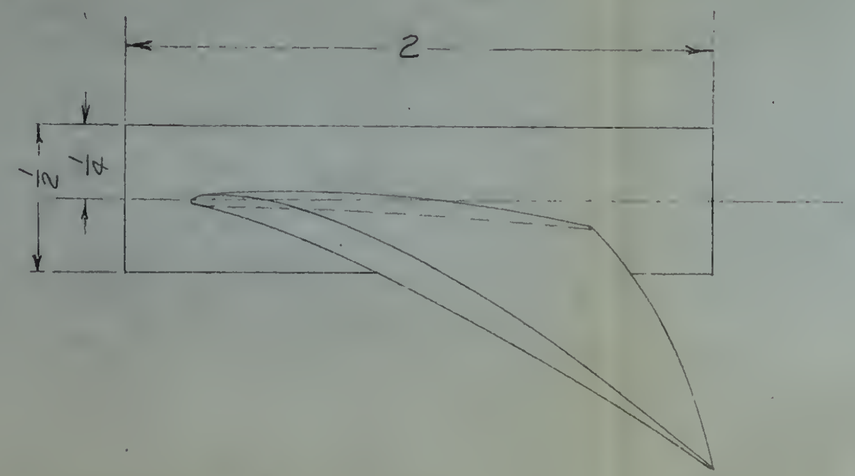

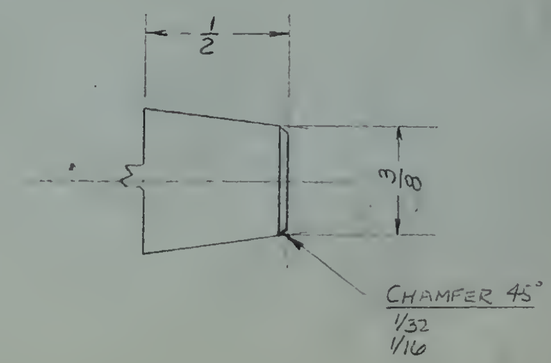

NOTE:
DIMENSIONS OF BLADE ROOT
ARE SUGGESTED DIM'S ONLY.

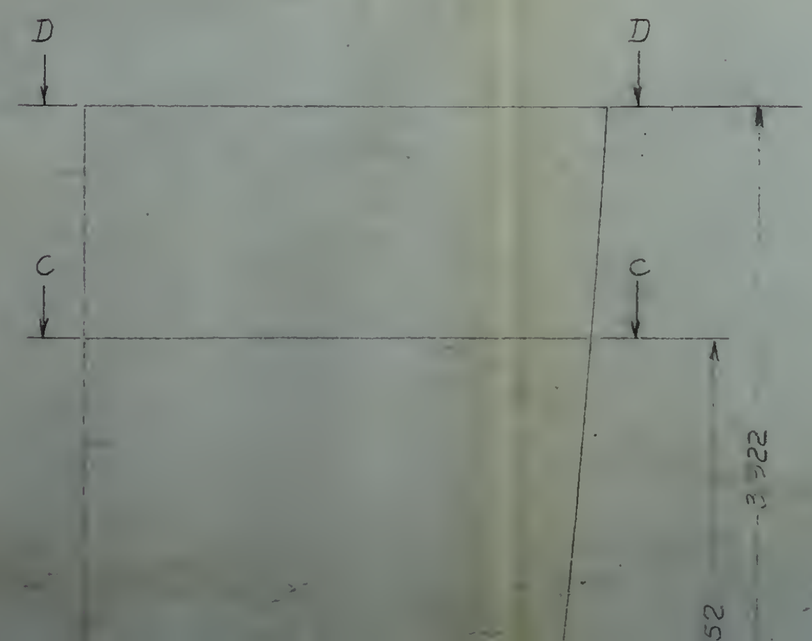

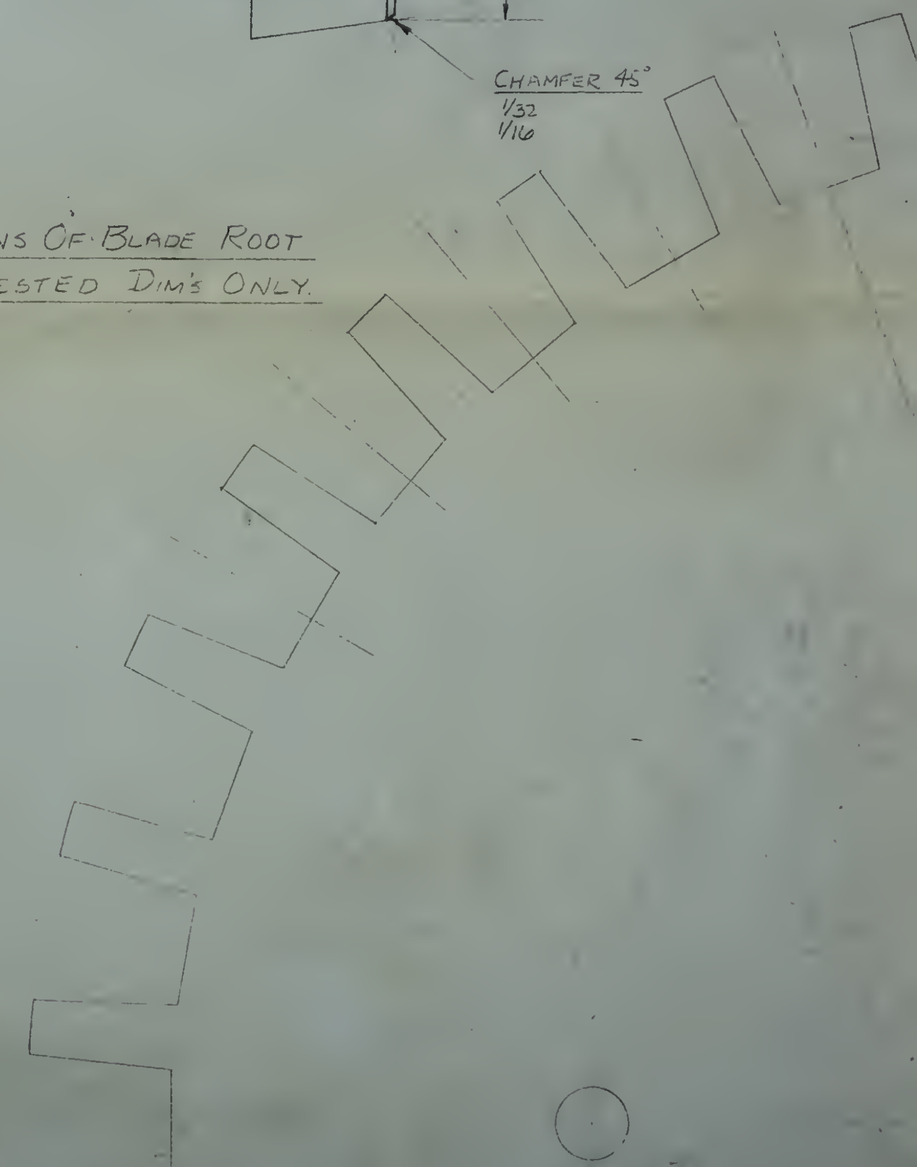

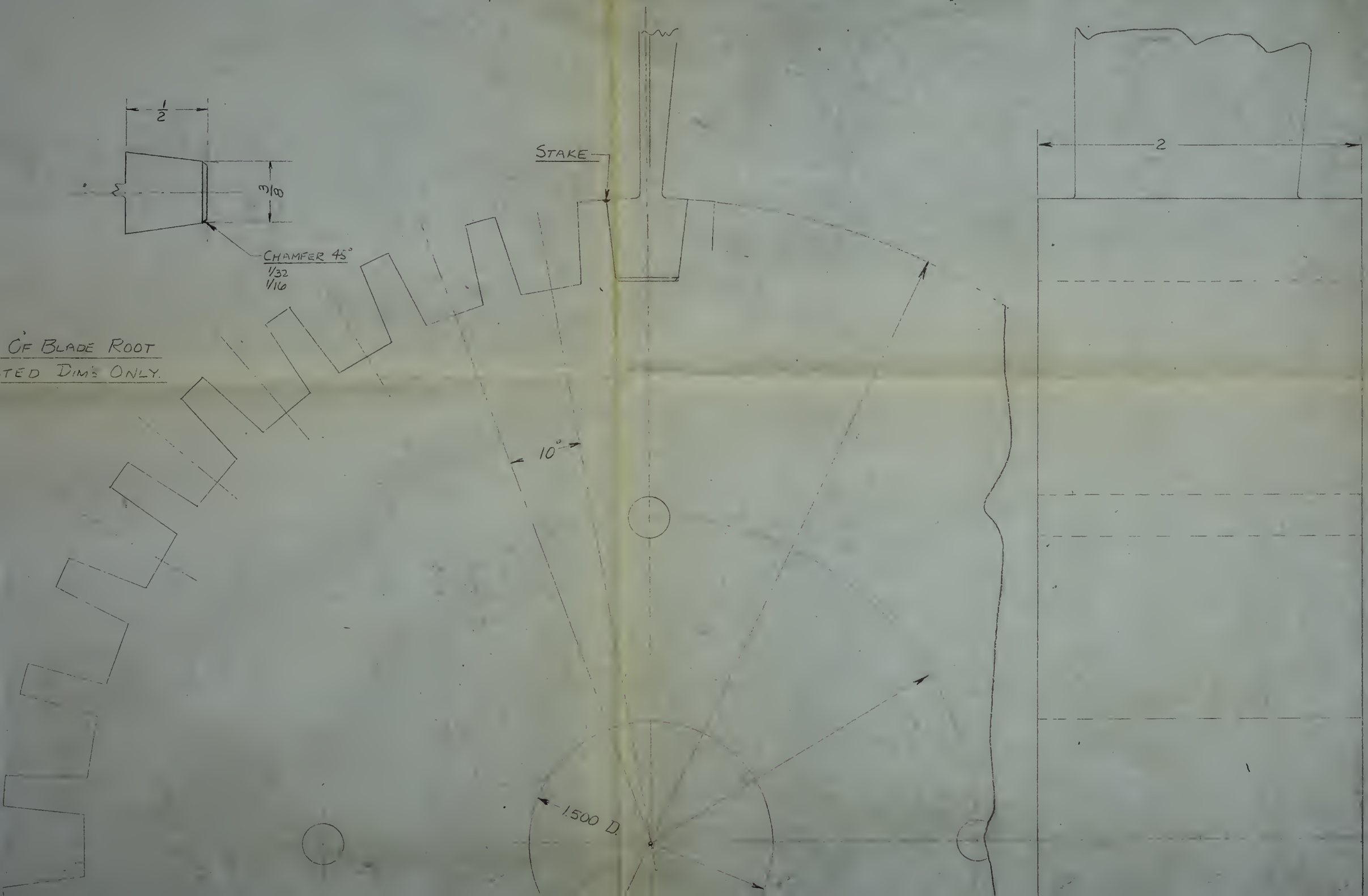
1/2
3/8
CHAMFER 45°
1/32
1/16
OF BLADE ROOT
TED DIM'S ONLY.
STAKE
10°
1.500 D.
2

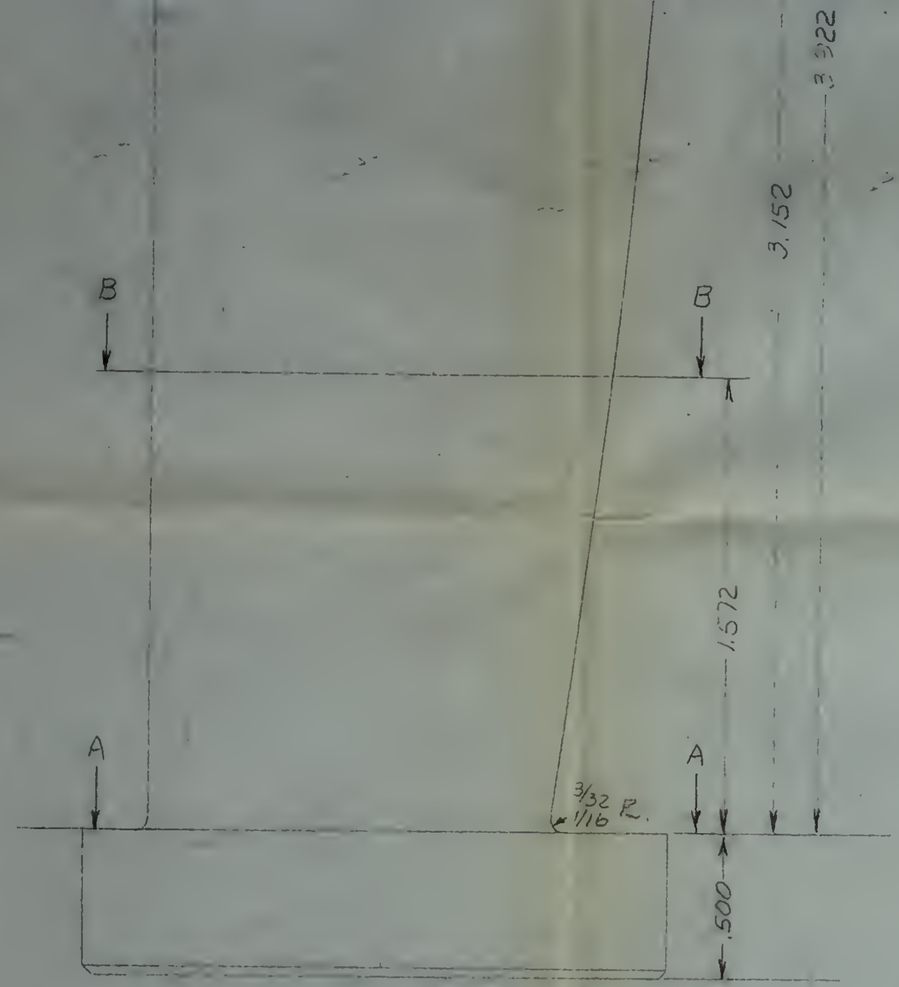

BLADE
36 REQ'D
SEE DWG. NO. N-5238

HUB
1 REQ'D.

NOTE:
OVERALL DIAMETER AFTER ASSEMBLING BLADES IN HUB TO BE $15\frac{11}{16}, \pm\frac{1}{32}$

HUB
1 REQ'D.

ETER AFTER ASSEMBLING BLADES
E $15\frac{11}{16}$, $\pm\frac{1}{32}$

MASSACHUSETTS INSTITUTE OF TECHNOLOGY
GAS TURBINE LABORATORY

TEST ASSEMBLY
INLET GUIDE VANES

DRAWN BY Cy	DATE 3-24-49
CHECKED BY	SCALE 2X
NEXT ASSEM.	N - 4244

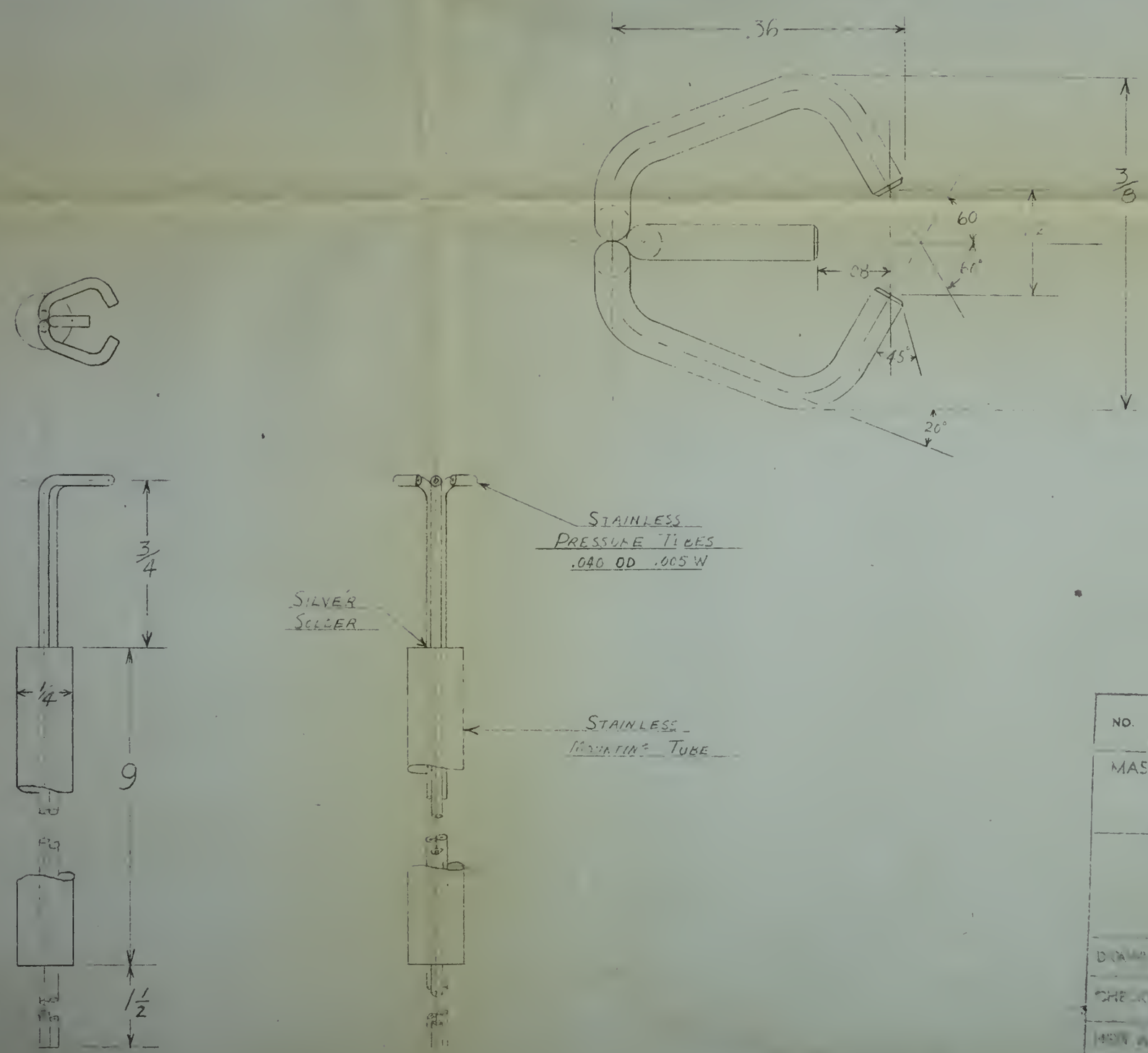

NO.	MATERIAL	NO REQ
MASSACHUSETTS INSTITUTE OF TECHNOLOGY GAS TURBINE LABORATORY		
YAW METER		
DRAWN BY LASTER	DATE 3-[illegible]	
CHECKED BY	SCALE 2/1 , 9/1	
NEW ASSEM. N-2226	N - 2237	

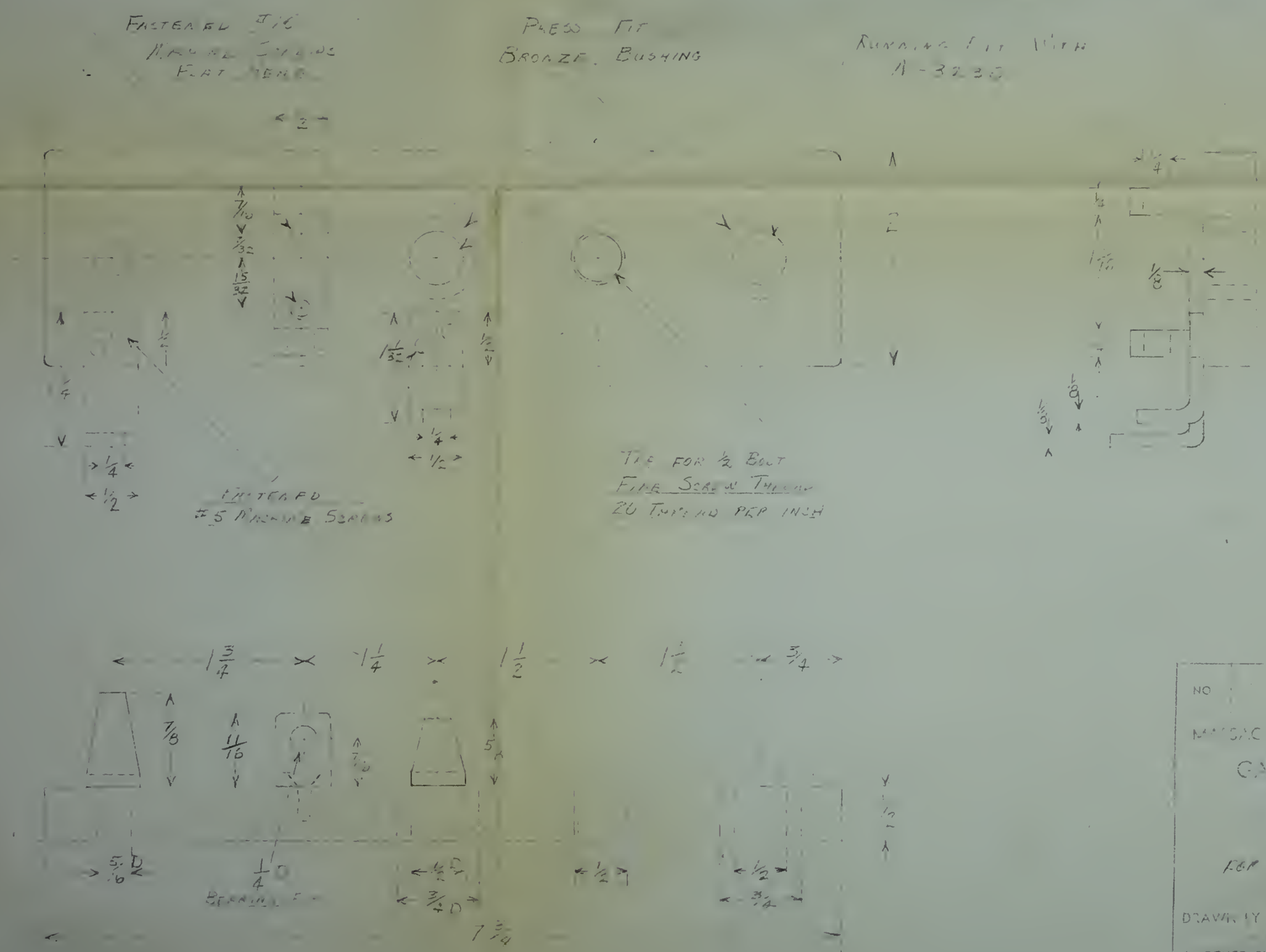

NO	MATERIAL STEEL	NO REQ
MASSACHUSETTS INSTITUTE OF TECHNOLOGY GAS TURBINE LABORATORY		
CARRIAGE FOR TRAVERSING MECH		
DRAWN BY LASTER	DATE 3-4-49	
CHECKED BY	SCALE FULL	
NEXT ASSEM. N-2226	N-2231	

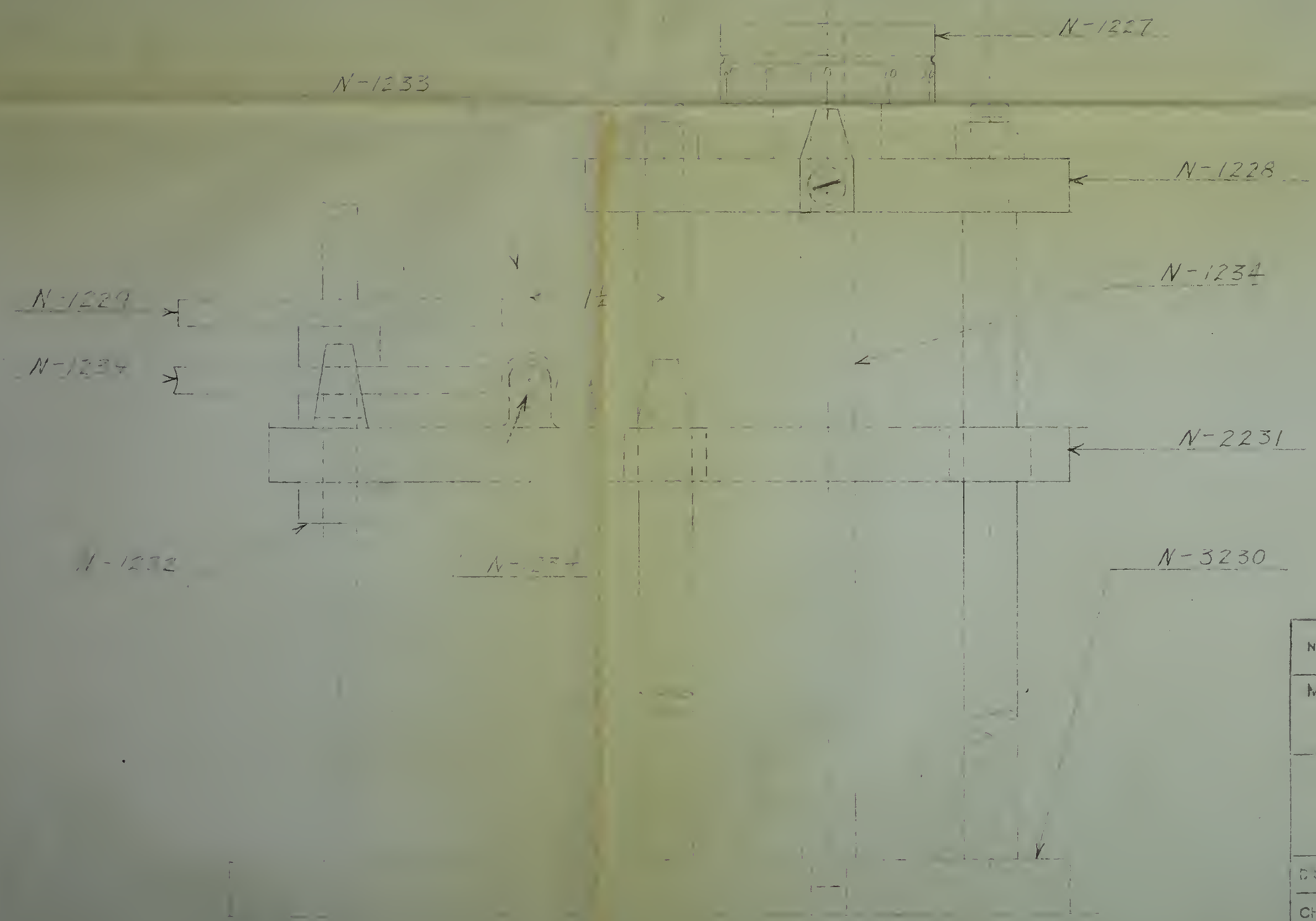

NO.	MATERIAL	NO. REQ.
MASSACHUSETTS INSTITUTE OF TECHNOLOGY GAS TURBINE LABORATORY		
TRUNNION MECHANISM		
DRAWN BY LASTAR	DATE 3-1-44	
CHECKED BY	SCALE Full	
NEXT ASSEM.	N-2226	

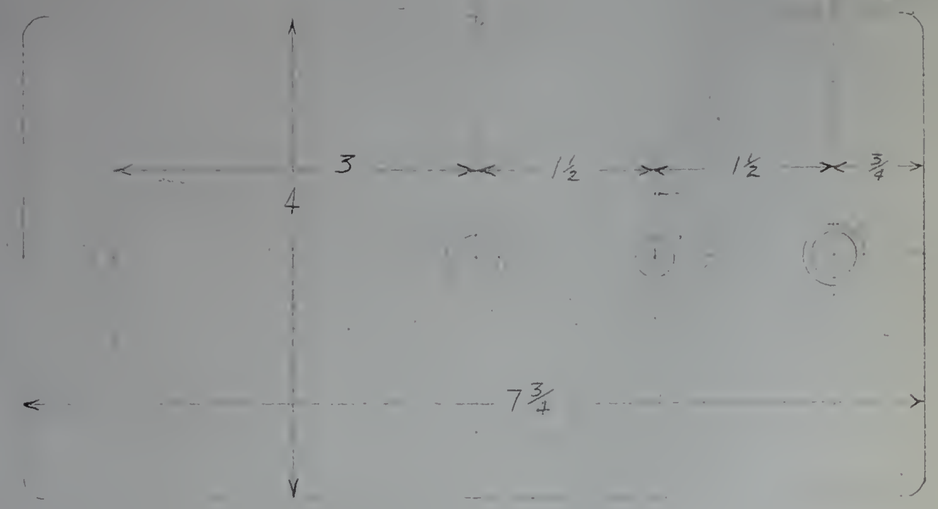

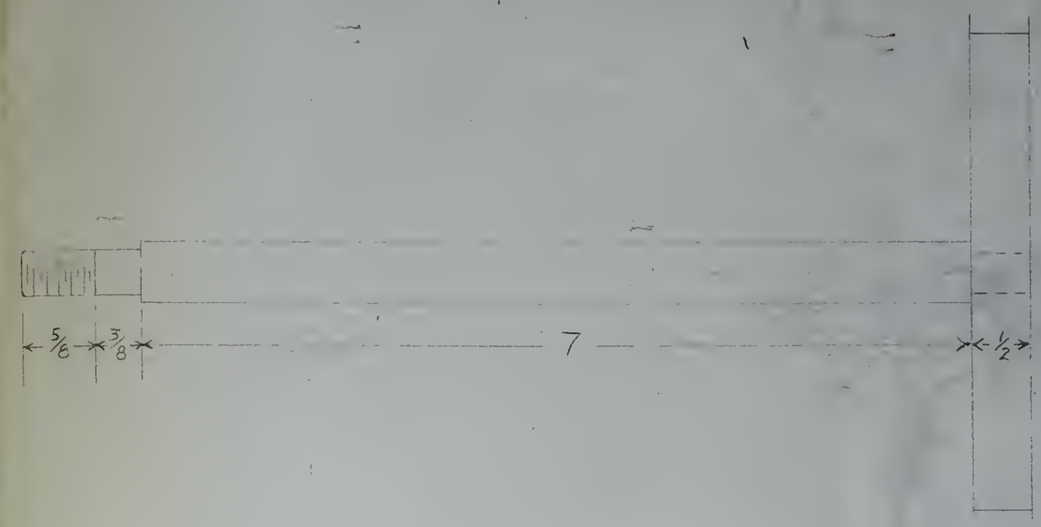

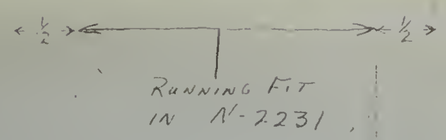

NO.	MATERIAL STEEL	NO. REQ.
MASSACHUSETTS INSTITUTE OF TECHNOLOGY GAS TURBINE LABORATORY		
BASE PLATE TRAVERSING MECHANISM		
DRAWN BY LASTER	DATE 3-2-49	
CHECKED BY	SCALE FULL	
NEXT ASSEM. N-2226	N - 3230	

1.875

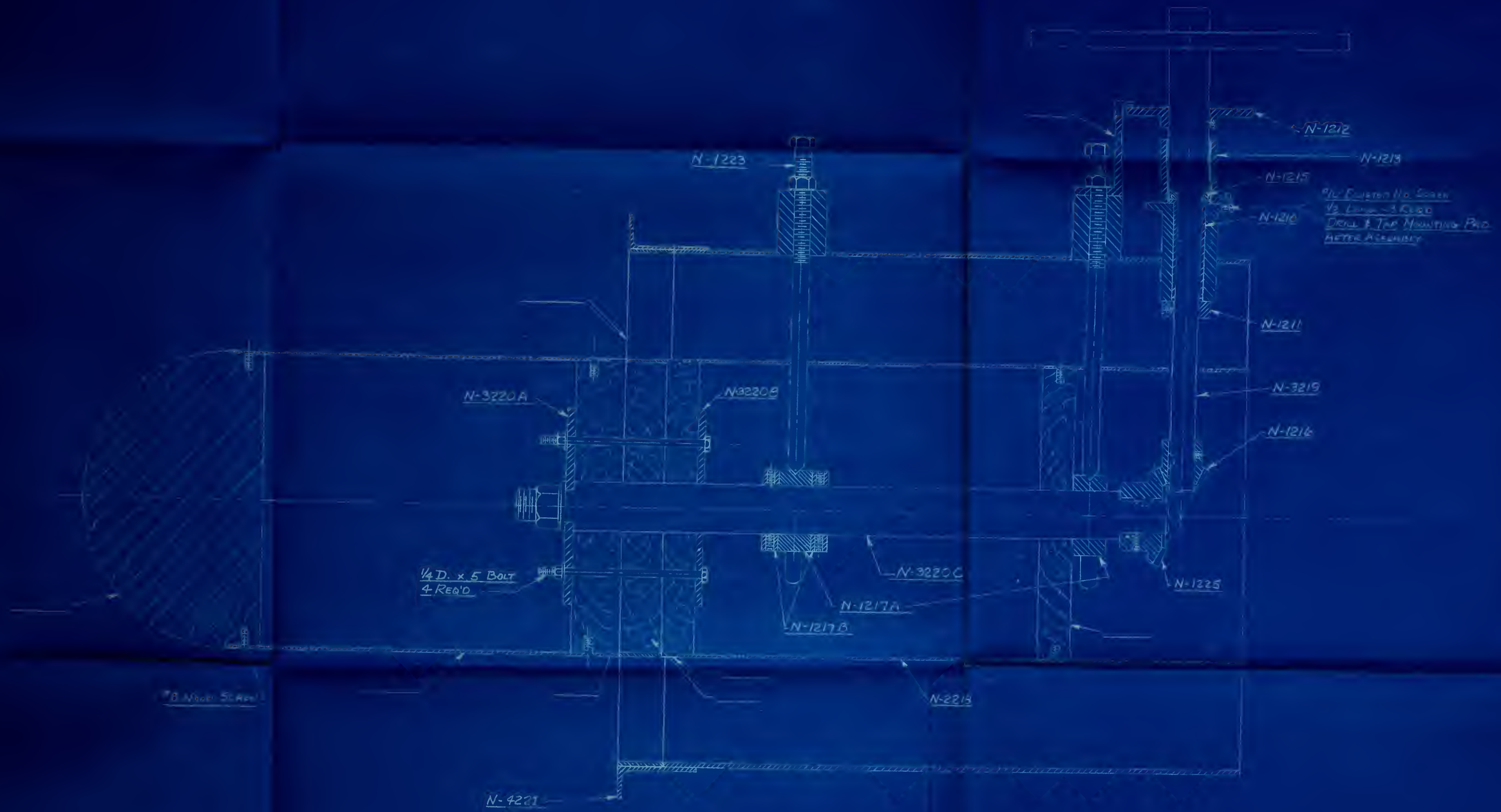

MATERIAL

MASSACHUSETTS INSTITUTE OF TECHNOLOGY

GAS TURBINE LABORATORY

AFTER SECTION ASSEMBLY

DRAWN BY

CHECKED BY

DATE 2-24-49

SCALE 1/2

N- 4221

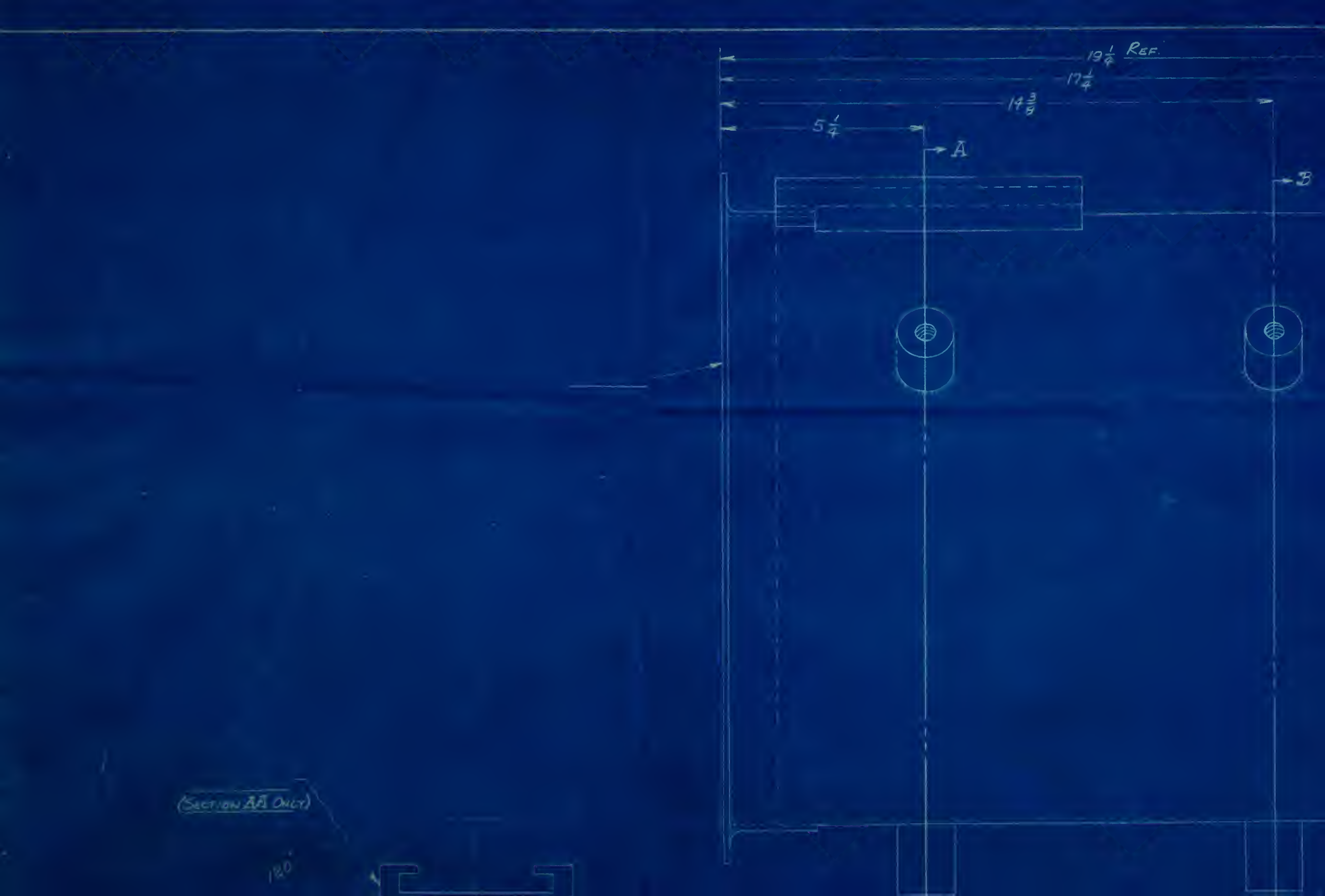
19 1/4 REF.
17 1/4
14 3/8
5 1/4
A
B
(SECTION AB ONLY)
180°

19 1/4 REF.
17 1/4
14 3/8
A
B
C
D

(SECTION AA ONLY)
120°
A
B
NOTE
GRIND FLUSH INSIDE
60°
N-1222
SECTION AA, BB
120°
120°
1/2" DRILL & TAP
AFTER WELDING IN POSITION

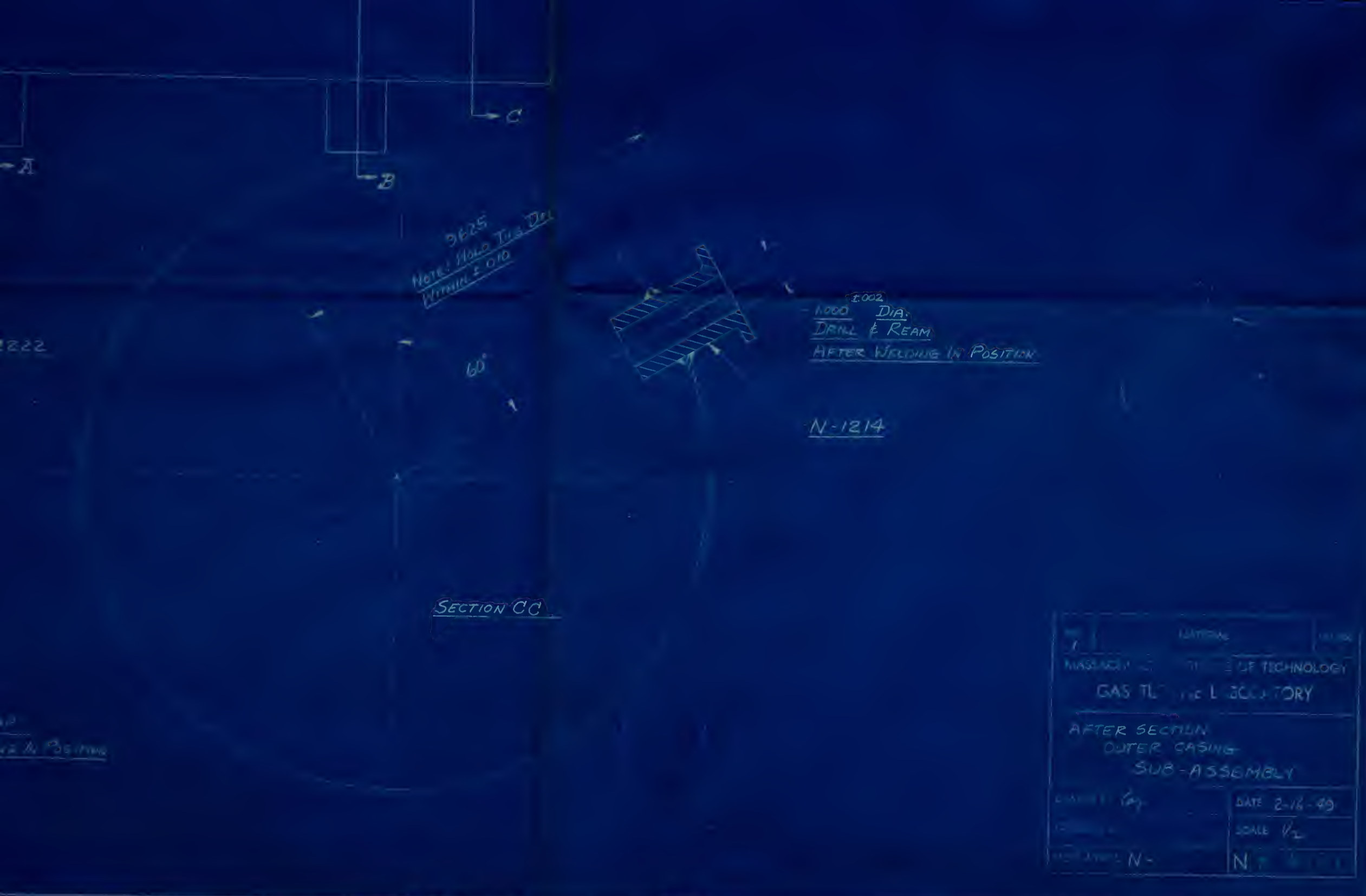

A
B
C
9625
NOTE: HOLD THIS DIA
WITHIN ±.010
60°
1.000 ±.002 DIA.
DRILL & REAM
AFTER WELDING IN POSITION
N-1214
SECTION CC
MATERIAL
MASSACHUSETTS INSTITUTE OF TECHNOLOGY
GAS TURBINE LABORATORY
AFTER SECTION
OUTER CASING
SUB-ASSEMBLY
DATE 2-16-49
SCALE 1/2
N-
N

1 1/2
1/4
16 7/8
C

AUG 31 BINDERY

Thesis 13676
L28 Laster
A design of an annular
cascade tunnel and a
cascade of airfoils.

Thesis 13676
L28 Laster
Design of an annular cascade
tunnel and a cascade of airfoils

Library
U. S. Naval Postgraduate School
Monterey, California

ARTISAN
GOLD LETTERING
AND
SMITH BINDERY
OAKLAND, CALIF

thesL28
A design of an annular cascade tunnel an
3 2768 002 12285 5
DUDLEY KNOX LIBRARY